Title
Investigating the Mechanism Underlying the Polled Phenotype in Cattle

Author
Hennig, Sadie

Publication Date
2021

Peer reviewed|Thesis/dissertation

Investigating the Mechanism Underlying the Polled Phenotype in Cattle

By

SADIE LYN HENNIG
DISSERTATION

Submitted in partial satisfaction of the requirements for the degree of

DOCTOR OF PHILOSOPHY

in

Animal Biology

in the

OFFICE OF GRADUATE STUDIES

of the

UNIVERSITY OF CALIFORNIA

DAVIS

Approved:

James Murray, Chair

Alison Van Eenennaam

Elizabeth Maga

Committee in Charge

2022

Table of Contents

Acknowledgements

There are countless people who have played so many important roles throughout my PhD journey that I would like to thank. First on the list is my family, who have been so supportive of me moving across the country to pursue this endeavor. Although they could not physically be here, they were always just a phone call away with encouraging words. I want to thank my mom for always being there for me, as well as my sister who would always listen to me vent about my struggles. Thank you to my grandparents, who always wanted to learn more about what I was doing, even if they didn't fully understand. I'd also like to thank all the individuals who have helped me here at UC-Davis. A special thanks goes to Dr. Joey Owen who was my partner in crime, going through the struggles of grad school with me, all while also being an amazing mentor and friend. I would like to thank Jason Lin, who started as my undergraduate research assistant and ended up becoming a graduate student working alongside me, helping me whenever I needed. I would also like to express my gratitude to Dr. Tom Bishop for providing me with all sorts of wisdom. I've made so many friends who helped me cope with the stresses of grad school life, and I'd like to thank Dr. Kazuki Takahashi, Dr. Ricardo and Sabrina Nociti, Dr. Rafael Sampaio, Dr. Lilli Fishman, Maci Mueller, Dr. Alba Ledesma, Bruna Miagawa and Ellie Harness to name a few. I also want to thank my good friend Theodore Hartin who helped me throughout this endeavor and provided me some much-needed support. I would like to thank Dr. Josephine Trott, Alma Islas-Trejo, Barbara Nitta, and Amy Young for helping me in troubleshooting so many experiments. Thank you to Dr. Elizabeth Maga for being a member of my PhD dissertation committee and being generous with offering lab space. I wish to thank Dr. Alison Van Eenennaam for being my "adoptive" PI, allowing me to conduct all my experiments in her lab, providing guidance and advice as a member of my PhD dissertation committee, and

treating me as an actual member of her lab. Finally, I would like to thank my PI, Dr. James Murray, who took me on as a graduate student at the last minute. Without him, none of this would have been possible. I am forever grateful.

Investigating the Mechanism Underlying the Polled Phenotype in Cattle

Abstract

The existence of horns in cattle is a safety concern for both handlers and animals, thus their physical removal via disbudding or dehorning must be done. This, however, raises animal welfare concerns. A naturally occurring hornless phenotype in cattle, referred to as the polled phenotype, has been observed, though its biological mechanism is still unknown. Four variants have been associated with the polled phenotype in cattle, two of which are dominant alleles at the *POLLED* locus (P_F and P_C) identified in Friesian dairy and Celtic beef breeds (e.g. Angus), respectively. In addition, a long intergenic non-coding RNA (*lincRNA#1*) has been found to be upregulated in the horn bud region of polled fetuses compared to horned fetuses, indicating a potential role in the development of horns. It has been demonstrated that introgression of the P_C allele, a 212 bp duplication that replaces 10 bp, into a pp horned cell line followed by somatic cell nuclear transfer (SCNT) results in the polled phenotype, however SCNT is inefficient, and is not practical for a production setting. Direct cytoplasmic injection (CPI) of gene editing reagents into one-cell zygotes would be a better alternative; however, this method first needs to be optimized to avoid potential off-target effects, reduce mosaicism, and increase biallelic editing efficiencies. In these studies, we created a CPI protocol to optimize CRISPR-Cas9 genome editing efficiencies in bovine embryos to investigate the underlying mechanism behind the polled phenotype in cattle. In the first experiment, gRNAs were designed targeting the *POLLED* locus (as well as two other loci for separate experiments) and mutation rates in embryos injected 18 hours post insemination (hpi) with Cas9 protein (84.2%) were significantly higher and mosaicism rates were lower (94.2%) than those injected with Cas9 mRNA (68.5%; 100%,

respectively), with off-target effects not cause for concern. After optimization of guide RNA (gRNA) design and discovering the most efficient type of Cas9 (mRNA or protein), we created a dual gRNA approach to induce deletions in the embryo genome and aimed to address two hypotheses: (1) the absence of the 10 bp sequence observed in the p allele at the *POLLED* locus, but absent in the P_C allele, is sufficient to result in the polled phenotype, and (2) the absence of *lincRNA#1* expression will result in horn development irrespective of the alleles present at the *POLLED* locus. To test the first hypothesis, we optimized the dual gRNA approach to delete a 133 bp region containing the 10 bp, testing timing of gRNA and Cas9 protein microinjection either 6, 8 or 18 hpi as well as comparing *in vitro* transcribed (IVT) verses synthetic gRNAs. We found that embryos injected 6 hpi had significantly higher rates of deletion (53%) in comparison to those injected 8 (12%) and 18 hpi (7%), and synthetic gRNAs performed significantly better than IVT gRNAs, with 84% deletion rates seen compared to 53%, respectively. Embryo transfers were performed, and fetuses were collected between three to five months of gestation. A total of seven fetuses were collected, two containing biallelic deletions; however, all exhibited horn bud development, indicating that the 10 bp deletion alone is insufficient to cause the polled phenotype. To address the second hypothesis, we utilized our optimized dual gRNA protocol to create a large (~3.7 kb) deletion in bovine embryos to knockout *lincRNA#1*. An 80% biallelic *lincRNA#1* knockout rate was achieved; however, the genotypically polled fetuses still presented as polled, indicating *lincRNA#1* does not play a role in inducing the polled phenotype. Overall, we optimized an efficient CPI system in embryos with high editing efficiency and no off-target effects and further optimized it to create a dual guide approach to create deletions in the bovine embryo genome. Utilizing the dual guide method resulted in high rates of deletion with lower

rates of mosaicism than previously seen, making it a promising approach to create genome edited livestock via CPI.

Chapter 1: Literature Review

Introduction

In cattle, the development of horns poses a risk to handlers and animals, making disbudding or dehorning (the physical removal of the horn buds/horns) a precautionary safety necessity[1,2]. This procedure, however, is extremely painful for the animal[1,3] and animal welfare concerns have been raised. The naturally occurring hornless phenotype (polled) exists in certain breeds of cattle, and has been linked to four specific variants, P_F[4-6], P_C[4,5], P_M[7] and P_G[8]. Additionally, a long intergenic non-coding RNA (*lincRNA#1*) has been found to be overexpressed in the horn bud region of polled fetuses compared to horned fetuses, indicating it also may play a role in horn bud development[4]. Several alternatives to disbudding/dehorning have been proposed, such as cryosurgery[9,10], the use of clove oil[9], and introgression of the dominant polled alleles at the *POLLED* locus in place of the recessive p allele associated with the horned phenotype into horned genetic lines using conventional breeding[11-14]; however, these approaches proved ineffective or impractical.

With the recent advances of site-directed nucleases, such as zinc finger nucleases (ZFNs)[15-18], transcription activator-like effector nucleases (TALENs)[19-21], and clustered regularly interspaced short palindromic repeats-CRISPR-associated protein 9 (CRISPR-Cas9)[22,23], introgression of the dominant P_C allele at the *POLLED* locus in a pp horned genetic line was accomplished in fibroblast cell culture using TALENs[24]. Somatic cell nuclear transfer (SCNT) was then used to clone the edited fibroblast cell line in enucleated oocytes that were activated and ultimately resulted in two genome edited homozygous P_CP_C polled Holstein bull calves[24]. SCNT is inefficient[25,26], however, and not a practical approach for large scale production[27] or for

introgression of an allele into multiple, different genetic lines. A better method would be to use direct cytoplasmic injection (CPI) of gene editing reagents into the one-cell embryo (zygote) for genome editing. A variety of studies across various livestock species have demonstrated the success of these site-directed nucleases, particularly the CRISPR-Cas9 system[28-33]; however, concerns such as potential off-target[34-39] effects and mosaicism[37,40-46] have been raised.

In this review, we examine the development of horns as well as the lack of horn growth in polled cattle. The disadvantages of horns are explained, and the disbudding and dehorning processes, as well as several alternatives, are discussed. The cons of introgressing dominant polled alleles at the *POLLED* locus into horned genetic lines via conventional breeding are laid out, and an alternative method using genome editing is proposed. The three most recent site-directed genome editing techniques, ZFNs, TALENs and CRISPR-Cas9, are discussed, along with possible hurdles that must be overcome before CPI may be used in embryos. Long non-coding RNAs (lncRNAs) are also explained, including their structure, classification and diverse, elusive regulatory functions.

Understanding Horns

Several genera within the family bovidae, including cattle, goats, sheep, bison and antelope, have cranial appendages, referred to as horns. Horns serve several functions including predator defense and mate and resource competition[47,48]. They may also play a role in thermoregulation[49]. Horn appearances vary greatly between species and breeds, each having their own distinct morphology[50,51]. Unlike antlers in deer and elk, which are shed annually and rapidly regenerate, horns are permanent and can only be removed if done by an external physical force[51]. True horns have a bony core fused to the fontal bone of the skull allowing the frontal sinus to

extend into the horn spike[51]. This horn interior contains blood vessels and nerves, making it an extremely sensitive region[52], with an outer "dead" keratin sheath covering the living tissue within[53].

It was initially believed that horns were direct outgrowths of the skull, forming horny spikes. A study involving horn bud tissue transplants in young cattle and goats disproved this and demonstrated that horn growth originated from the dermis and hypodermis rather than the frontal bone of the skull[54]. The horn bud in newborn calves is not directly linked to the skull and freely "floats" in the layer of tissue above the skull, making it easily moveable until it ultimately fuses to the skull at around two to three months of age[52]. At this point, the horn bud has differentiated into a bony cone, and by six to eight months of age, the bony cone completely fuses with the frontal sinus[52].

Although physical growth of horns occurs after birth, differentiation of the horn bud occurs during embryogenesis. The first sighting of horn bud development in bovine fetuses was observed at 60 days of gestation[55]. Wiener et al. performed extensive analysis of horn bud development in fetuses at various stages of gestational development, reporting horn bud detection between two to three months of gestation, with the horn bud presenting as a small yellowish spot on the fetal head[56]. The horn bud then appears to have a slight indentation at three to four months of gestation and is clearly visible at five to six months[56]. The horn bud is easily identifiable during late-term gestation (seven to eight months) with tightly packed hair follicles creating thick whorls of hair[56].

Histological investigation has been done in addition to the macroscopic identification of horn bud development[4,56]. In developing fetuses as young as 70 days of gestation, noticeable differences can be seen in the horn bud region compared to the frontal skin. Dense layering of

vacuolated keratinocytes in the epidermis of the horn bud region can be seen compared to the frontal skin[56]. Thick nerve bundles are also seen in the dermis of the horn bud region, but are absent in the frontal skin[4,56]. Hair follicle development occurs later in the horn bud region, with follicles not seen until five to six months of gestation, compared to three to four months of gestation in the frontal skin[56].

Horns in domestic cattle can endanger both handlers and other cattle[1,2]. Financial losses can also be incurred due to hide damage and bruising results in loss of meat during processing[57,58]. To prevent these horn-related issues, the horns are physically removed in procedures known as disbudding and dehorning. Disbudding is done when the calf is young and the horn bud has yet to fuse to the skull. This is typically performed by either scooping out the horn bud with a scoop dehorner, utilizing a caustic paste or by cauterizing the horn bud with a hot iron, damaging the cells, thus preventing horn growth[59,60]. The much more invasive method of removing horns after the horn has already fused to the frontal bone is referred to as dehorning[2,61].

Disbudding is typically performed over the more invasive dehorning method; however, both cause acute pain and stress to the animal[1,3]. Aside from suffering, the wound site has the possibility of getting infected, potentially affecting animal growth, further increasing producers' labor costs[3,62,63]. Since these procedures are so intrusive and cause the animals such pain and discomfort, they are cause for animal welfare concerns. Because of this concern, alternatives to disbudding have been explored. Clove oil injections under the skin in the horn bud region have been attempted, causing tissue necrosis, thus preventing horn bud development[9]. This method, however, simply delays the onset of horn growth rather than total prevention[9]. Cryosurgery is another novel method of disbudding involving the application of extremely cold temperatures to

the horn bud, triggering localized cell death by causing water within the cells to crystallize[9]. Although cryosurgery does not seem to produce less pain than disbudding by cauterization, it does not cause as much external tissue damage, therefore it was believed to be a more viable alternative if used in conjunction with proper pain management[10]. Cryosurgery, however, proved to be ineffective when compared to the standard cauterization method[9].

Understanding Polled

In cattle, there is a naturally occurring hornless phenotype, referred to as the polled phenotype. In comparison to horned cattle, polled cattle have no horns and a narrower, knob-like central prominence on the frontal bone, referred to as the poll[52]. In cattle, the polled phenotype is typically associated with beef production breeds, such as Angus, while the horned phenotype is typically found in dairy breeds, such as Holstein.

In 1993, linkage mapping originally pinpointed the *POLLED* (P) locus for cattle to bovine chromosome 1 (BTA1)[64], and further investigations narrowed the location to near the centromere[65-67]. To date, there are four known *POLLED* variants located on BTA1, all of which are dominant to the recessive wild type allele (p) associated with horns. The Friesian *POLLED* (P_F) variant, originally identified in Holstein-Friesian cattle, consists of an 80,128 bp duplication directly following the original sequence[4-6]. Common in beef breeds such as Angus, the Celtic *POLLED* (P_C) variant was initially discovered in European beef breeds of Celtic origin and corresponds to a 212 bp duplication that replaces a 10 bp sequence 6 bp downstream of the original sequence[4,5]. Mongolian *POLLED* (P_M) was identified in admixed Mongolian yaks and was found to be a 219 bp insertion 61 bp downstream from the original sequence and a 7 bp deletion - 6 bp insertion[7]. The last variant recently discovered in Brazilian *Bos indicus* Nellore

cattle, referred to as Guarani *POLLED* (P_G), corresponds to a 110 kb duplication, however the location of the duplicated sequences is not yet known[8]. Although these variants of *POLLED* are known, they do not code for any known transcript or protein, nor do they disrupt any known coding or regulatory region, so the causal mechanism behind polled remains unknown. There are several genes that have been shown to play important roles in the formation of horns[51,68], but will not be discussed in this review. For further information on these genes and their potential roles in horn bud development, the reader can refer to the review by Aldersey et al.[68].

In addition to the *POLLED* variants, Allais-Bonnet et al. discovered a long intergenic non-coding RNA, referred to as *lincRNA#1* (*LOC100848368*), that may play a role in the polled phenotype[4]. *lincRNA#1* was identified by reverse transcription quantitative polymerase chain reaction (RT-qPCR) to have slightly higher expression in the horn bud region of polled fetuses compared to the horn bud region of horned fetuses ($P = 0.052$)[4]. Long non-coding RNAs are difficult to detect since they are often present in very small quantities, so it is possible this difference is significant enough to have an impact on development[69]. Because of this difference in expression, it is possible that lincRNA#1 may play a role in horn bud differentiation and aid in the creation of the polled phenotype.

Due to the dominant nature of the *POLLED* alleles that result in the polled phenotype, initiatives to introgress these alleles into horned genetic lines have been undertaken as an alternative to disbudding and this is a highly recommended welfare guideline by various animal health organizations[11,12]. There are several limitations to this approach, however. First, crossing specialized breeds tailored for specific purposes, such as dairy and beef, results in a decrease in the genetic merit of those animals for their industry-specific breeding objective. To avoid crossing of breeds, polled Holstein bulls could be used to create polled lines, however the

dominant alleles at the *POLLED* locus that result in polled are still uncommon in dairy breeds[14]. In addition, polled Holstein sires have been found to have lower breeding values than horned Holstein bulls[70] and, on average, have a lifetime net merit of $100 less than their horned counterparts[14]. Simulation studies have even shown that a decreased rate of genetic gain and increased incidences of inbreeding would occur by conventional breeding of currently available polled dairy sires[13,14].

Due to the issues of introgressing the polled alleles at the *POLLED* locus into horned genetic lines via conventional breeding, it has been proposed to utilize genome editing to achieve this introgression. Utilizing this approach would mean the alleles could be introduced into elite genetic lines thereby avoiding the genetic drag that would be caused by introgression using conventional breeding, and it would also be a more rapid approach to achieve this outcome. Carlson et al. successfully achieved P_C allele introgression into a horned dairy cell line using TALENs[24]. SCNT of cells from the edited cell line was undertaken and resulted in two polled homozygous P_CP_C dairy bull calves[24]. Young et al. investigated the offspring of one of the genome edited bulls created by Carlson et al. and determined the introgression of the P_C allele is heritable[71], making genome editing a viable solution to introgress polled alleles into horned lines. Simulation studies have also shown that genome editing is an effective means of rapid introgression of polled alleles into horned breeds of cattle while preserving genetic merit and minimizing inbreeding, providing a feasible approach to address this escalating animal welfare issue[13,14] using genetics.

Site-Directed Nucleases: Keeping Genome Editing On-Target

Discoveries throughout the past few decades involving the use of site-directed nucleases have made targeted genome editing possible[15-23]. These programmable endonucleases target specific locations in the genome allowing for modifications such as the deletion of DNA segments or the substitution of undesirable alleles with desirable ones of the same species – comparable to crossbreeding, but allowing for faster and more efficient introgression of favorable traits[27,72]. This is all accomplished via targeted double-strand breaks (DSBs). Each genome editing system varies; however they all follow the same principle. The endonucleases are guided to specific DNA sites where they then induce a DSB, prompting DNA repair[27,72]. DNA is typically repaired using either the endogenous non-homologous end joining (NHEJ) or homology directed repair (HDR) pathways[27,72]. NHEJ DNA repair requires no DNA sequence homology and thus is prone to errors, resulting in small insertions or deletions (indels), allowing it to aid in the interference, or knocking out, of gene expression by generation of frameshift mutations[27,72]. The HDR repair pathway uses a repair template that shares a sequence identity with the area surrounding the DSB[27,72]. This repair mechanism can be used to alter an existing allele by making conversions (knock-ins) of genes of interest or substituting one allele for another[27,72].

Currently, there are three targeted genome editing techniques. These include ZFNs[15-18], TALENs[19-21], and CRISPR-Cas9[22,23]. ZFNs were the first genome editing system to be used and consist of two parts: an endonuclease cleavage domain (FokI) and a DNA binding domain consisting of an array of three to six zinc finger motifs[15,16]. These zinc finger motifs recognize specific DNA sequences flanking either side of the desired cleavage site, with 3 bp corresponding to one zinc finger motif[17]. Once the zinc fingers bind to their targets, FokI

dimerizes, cleaving the DNA[18,73]. ZFNs have been used to create a variety of genome edited livestock animals including α1,3-galactosyltransferase (GGTA1) knockout pigs to aid in xenotransplantation[74] and the substitution of the domestic swine wild type to warthog RELA ortholog to help fight African Swine Fever[75].

TALENs were the second site-directed nuclease system discovered. *Xanthomonas*, a bacterial species, produce TALE proteins as a means to infect plants. Using the type III secretion system, the bacteria inject TALE proteins into the plant where they are then transported to the nucleus and bind to DNA at specific promotor elements within the plant genome to aid in pathogen infection[19,20]. These DNA-binding motifs recognize specific nucleotides in the DNA and can direct the engineered nuclease to the appropriate cutting site[19-21]. TALE proteins are made up of 13 to 28 repeats, each repeat consisting of 34 amino acids, although 33 and 35 amino acid repeats have also been seen[19,20]. The amino acid sequence is conserved, however two adjacent amino acids at the 12th and 13th position can vary, determining the TALE's corresponding DNA target sequence within the genome[19]. Like ZFNs, the TALE proteins are bound to half of the FokI endonuclease. These proteins guide the FokI endonuclease to the target site, causing FokI to dimerize and create a DSB[19]. The success of TALENs has been seen in a wide variety of species including yeast[76], zebrafish[77], frogs[77] and rats[78]. In livestock, TALENs have been used to create numerous edits in pigs[79], goats[80], sheep[81] and cattle[24,81]. Although efficient, one major disadvantage of TALENs is their relatively high cost due to their complexity of design and synthesis[82].

The most recently discovered site-directed nuclease system is the CRISPR-Cas9 system, and its high efficiency and ease of use has made it a popular genome editing technique among scientists[72]. Initially observed in archaea and prokaryotes, this system aids in the defense against

invading viruses and plasmids via RNA-guided DNA cleavage[22]. These 21 to 37 bp CRISPR sequences were found to be surrounded by non-repeating DNA segments[83], discovered to be derived from bacteriophages[84]. Upstream of the repeat areas, researchers uncovered four CRISPR-Cas genes with motifs associated with endonuclease activity[83]. With these findings, it was believed this was a means of an adaptive immune system and was confirmed by studies done by Barrangou et al.[85].

Scientists have since been able to modify the CRISPR-Cas system as a means of site-directed cleavage for genome editing[22]. There are a variety of Cas proteins used to induce genetic changes in the mammalian genome, but the most commonly used protein is derived from *Streptococcus pyogenes* (Cas9)[23]. Similar to ZFNs and TALENs, the CRISPR-Cas9 system is made up of two components: a 20 bp guide RNA (gRNA) and an endonuclease (Cas9)[22,23]. The gRNA and Cas9 protein form a ribonucleoprotein (RNP) complex and the gRNA guides the Cas9 protein to the target site in the genome[22,23]. The Cas9 protein will recognized the target sequence utilizing the protospacer adjacent motif (PAM) site (NGG in the *S. pyogenes*-derived system), and will cleave the DNA, resulting in a DSB[22,23]. Since its discovery, the CRISPR-Cas9 system has allowed for the creation of a vast range of genome edited organisms including yeast[86], fruit flies[87], zebrafish[88], mice[89,90], rats[90], rabbits[91] and monkeys[92]. In livestock, genome edited animals such as CD163 knockout pigs resistant to porcine reproductive and respiratory syndrome (PRRS) virus[28,29], myostatin knockout pigs[30], sheep[31] and goats[32] with improved skeletal muscle development, and an SRY knock-in bull to increase male offspring for meat production[33] have all been generated using CRISPR-Cas9 technology.

ZFNs, TALENs and the CRISPR-Cas9 system are all useful tools for targeted genome editing, but deciding which to use requires an understanding of the advantages and disadvantages

of each system. There are four primary areas of comparison between ZFNs, TALENs and the CRISPR-Cas9 system: efficiency, ease of design and construction, size, and specificity. Efficiency amongst the systems vary greatly. ZFNs have been shown to have the lowest efficiency while TALENs and CRISPRs are much more efficient, with CRISPRs being superior to TALENs[93,94]. In addition to having higher efficiency, CRISPRs can cleave methylated DNA while ZFNs and TALENs cannot[95]. Regarding design and construction, ZFNs and TALENs require recoding of proteins using large (500 – 1,500 bp) DNA segments for each new target site[96]. CRISPRs, however, can be simply altered to target any genomic sequence by modifying the guide RNA's 20 bp protospacer while the Cas9 protein remains unaltered, making CRISPR design and construction much simpler and cheaper[96]. The versatility of the Cas9 protein allows it to utilize a variety of guide RNAs for site recognition, allowing the same Cas9 protein to edit the genome at several loci at the same time, a concept known as multiplex genome editing[97]. ZFNs and TALENs, however, are limited to a single locus[19,96]. One advantage ZFNs have is their small size. They are the smallest of the genome editing systems, with each monomer being ~ 1kb[94,96]. TALENs are larger, ~ 3 kb per monomer, and although the guide RNA in the CRISPR-Cas9 system is small, only 0.1 kb, the Cas9 protein itself is ~ 4.2 kb, making it a challenge to deliver via viral vectors[94,96]. Specificity and the possibility of off-target effects, that is the introduction of a DSB at a site other than the intended target site, also varies amongst the genome editing systems. ZFNs have been shown to have the highest incidences of off-target events, while those occurring for TALENs and CRISPRs are less common[96,98].

Focusing on the CRISPR-Cas9 system, the possibility of off-targets occurring at unintended loci is of utmost consideration when designing gRNAs, as unintended mutations potentially can have detrimental effects when creating genome edited embryos. Several studies

in humans[34,35], monkeys[36], cattle[37] and rodents[38,39,99] have concluded there is little concern from off-target effects and suggest that the rate of Cas9-mediated mutagenesis is comparable to *de novo* mutation rates. Several methods such as Sanger sequencing, mismatch cleavage assays (T7 endonuclease I and Surveyor nuclease), and next generation sequencing have been utilized for the detection of indels created by erroneous repair of off-target DSBs[100,101] in genome edited embryos. To utilize these methods, the probability of off-target locations is first calculated using online prediction tools. The top predicted sites are then PCR amplified and subject to next generation sequencing, TA cloning followed by Sanger sequencing, or the mismatch cleavage assay followed by Sanger sequencing[100]. Because online prediction algorithms may not be able to forecast all probable off-target sites, new detection approaches have been developed, such as high-throughput, genome-wide, translocation sequencing (HTGTS)[102] and unbiased, genome-wide profiling of DSBs assessed by sequencing (GUIDE-seq)[103].

It is thought that the 20-nt sequence of the gRNA as well as the presence of a PAM site next to the targeted sequence in the genome is precise in triggering Cas9 cleavage, however off-target cleavage can occur in the genome with three to five base pair mismatches in the PAM-distal sequence[95,104-106]. It also has been demonstrated that the seed region, or the 8 to 11 bp PAM-proximal sequence, determines Cas9 specificity, making it the most important region of the gRNA sequence[22,104]. The presence of off-target activity appears to be increased by higher concentrations of Cas9, as mismatches tend to be better tolerated[95,106]. Decreasing the concentration of Cas9 in an effort to minimize off-target activity has been done, but at the expense of on-target activity[95]. Some successful attempts to reduce off-target activity include creating truncated 17 to 18-nt gRNAs (tru-gRNAs)[107] or utilizing paired nickases to create two single-strand breaks, thus doubling the specificity[73,105,108,109]. It has also been demonstrated that

the delivery mechanism of Cas9 has an impact on off-target effects, with Cas9:gRNA RNP complex having significantly fewer off-target effects compared to plasmid DNA encoding Cas9 and gRNA or Cas9 mRNA co-delivered with gRNA[110].

Another difficulty associated with genome editing of livestock embryos is the level of mosaicism. Mosaicism is defined as the presence of more than two alleles observed when using the CRISPR/Cas9 system[40] as a result of editing occurring after the one-cell stage. When creating founder animals, the presence of mosaicism can be detrimental. Highly mosaic knockout animals can actually mask the impact of the knockout itself, rendering the edit meaningless[41]. Mosaic founders can be bred to acquire offspring containing solely the intended edit[42]. This approach is possible in mice, however due to the generation intervals of livestock, this is not feasible as it would be a time consuming and a financial burden[42].

Several methods can be utilized for mosaicism detection. One method is through target site PCR amplification, cloning amplicons into a plasmid vector followed by Sanger sequencing[111-114]. Although this method can accurately detect alleles present in each sample, it cannot discern the level of mosaicism within the samples themselves. Another quicker and more cost effective approach uses Sanger sequencing of PCR amplified target sites followed by the use of prediction software, such as CRISP-ID, Synthego's ICE tool or the TIDE bioinformatics package, to decompose the chromatogram data and calculate the number and types of alleles in each sample[115,116]. This method, however, heavily relies on the accuracy of the algorithms within the software. A better approach is next generation sequencing of the PCR products which provides a more precise identification of the alleles present, as well as their relative frequency[41]. Previous studies utilizing these methods have reported a vast range of mosaicism ranging from as low as 30% to as high as 100% in *in vitro* matured oocytes, parthenogenetically activated or *in*

vivo/vitro produced embryos[37,43-46]. When using the CRISPR-Cas9 system in embryos, it is thought that increased levels of mosaicism are not necessarily due to timing of injections, but rather due to inefficient gRNAs causing low Cas9 cleavage as well as the longevity of the Cas9 protein within the embryo, i.e. delivering a plasmid or mRNA compared to protein[37,41,117,118]. Utilization of a Cas9 plasmid or Cas9 mRNA allows for the cell's machinery to naturally replenish the Cas9 protein, allowing it to persist longer in the cell, thus making more DSBs and more mutations.

Due to issues resulting from mosaicism, SCNT is commonly utilized to create genome edited livestock. This technique allows for the creation of homozygous, non-mosaic cell lines that can then be cloned into an embryo and transferred into a synchronized recipient. SCNT, however, poses many issues itself[25,26]. Although cloning techniques have greatly improved over the years, the ability to produce animals via SCNT varies greatly, and is overall extremely inefficient[26], with only 0.5-5% of embryos developing to term[25]. In addition to the inefficiencies of SCNT, developmental abnormalities are also extremely common[25,26]. With these current issues, the ability to create SCNT genome edited animals on a larger scale is not feasible[27]. Direct cytoplasmic injection (CPI) of genome editing reagents into early stage *in vitro* fertilized (IVF) embryos could be an alternative, as IVF embryos have been shown to result in higher pregnancy rates, up to 51.8%[119]. CPI embryos would also maintain higher genetic diversity compared to SCNT produced animals[120]. Despite the advantages of CPI over SCNT, lower rates of mosaicism must first be achieved to make CPI a better alternative.

Long Non-Coding RNAs

With recent advances in sequencing technologies, it has been found that significantly more of the genome is transcribed than was previously thought. A vast variety of non-coding transcripts have been discovered, with the rate of discovery significantly surpassing scientists' abilities to be functionally annotated. These non-coding RNA transcripts have been classified into two distinct groups set by an arbitrary threshold of 200 bp. Non-coding RNAs under 200 bp in length consist of microRNAs (miRNAs)[121,122], small-interfering RNAs (siRNAs)[123], short hairpin RNAs (shRNAs)[123], and P-element-induced wimpy testis (PIWI)-interacting RNAs (piRNAs)[124], all of which typically negatively regulate gene expression. Long non-coding RNAs (lncRNAs), on the other hand, are a loosely classified category of long (greater than 200 bp) non-coding RNAs with mostly unknown function[125,126]. For this review, lncRNAs will be the sole focus.

LncRNAs are very similar to mRNAs in that they are transcribed by RNA polymerase II (Pol II), have a 5' cap, a poly A tail (though not present in all lncRNAs), and can undergo splicing[127]. LncRNA transcripts, however, are typically shorter than those of mRNA and contain fewer, but longer, exons[125,128]. Though structurally similar to mRNAs, lncRNAs differ from mRNAs in terms of primary sequence conservation, expression level, stability, subcellular localization and tissue specificity. LncRNAs have less primary sequence conservation compared to mRNAs[125,128] and tend to be expressed at much lower levels, often just a few molecules per cell, making them extremely difficult to detect[69,125,129]. Cytoplasmic mRNAs have been shown to be relatively stable compared to lncRNAs[130]. More recent studies, however, compared stability of mRNA with similar expression levels to those seen with lncRNAs and saw similar levels of instability[131], indicating the quantity of transcripts present affect stability rather than the differing

type of transcripts themselves. LncRNAs are also more enriched in the nucleus relative to the cytoplasm in comparison to mRNAs, with 17% of lncRNAs compared to 15% of mRNAs enriched in the nucleus and 4% compared to 26%, respectively, enriched in the cytoplasm[125]. In addition, lncRNAs are extremely tissue specific in expression, much more so than mRNAs[125,128,132]. One study demonstrated 78% of lncRNAs compared to only 19% of mRNAs were tissue specific[128]. LncRNAs have also been shown to have varying levels of expression regarding developmental stage or disease state[133,134].

Because the category of long non-coding RNAs is so broad, designating every non-coding transcript longer than 200 bp as a lncRNA, they can be further categorized based off their location in the genome. Long intronic RNAs are one type of lncRNA and are transcribed from introns of protein-coding genes, while long intergenic RNAs (lincRNAs) are located in between genes, not lying within coding regions[135]. There are also sense and anti-sense lncRNAs which originate from the sense and anti-sense strand of protein-coding genes[136,137]. In addition, some even act as pseudogenes, with transcripts similar to coding genes and differing only by a few mutations, thus rendering them non-coding[138].

LncRNAs have been shown to have both cis- and trans-regulatory roles, regulating genes in close genomic proximity as well as extremely distant genes. It has been demonstrated that transcriptional regulation is enriched for protein-coding genes located within 10 kb of a lncRNA[128]. Cis-lncRNAs can function in a variety of ways, including transcriptional interference or chromatin modifications. In regards to transcriptional interference, cis-lncRNAs can be transcribed from a gene's promoter region, tethering it that region, either blocking or recruiting transcription factors[139]. One study demonstrated how lncRNAs approximately 0.4 – 1.9 kb from *SER3* cause promotor interference, preventing transcription factor binding, thus repressing *SER3*

transcription[140,141]. Regarding chromatin modification, cis-lncRNAs can recruit chromatin modification complexes such as Rpd3 small histone deacetylase complexes (Rpd3S HDAC) or polycomb repressive complex (PRC)[142]. *Xist* is one of the most well-known lncRNA that utilizes this mode of regulation during X-inactivation, recruiting PRC2 to induce H3k27me3 modification, thus silencing genes on the X chromosome[143]. Another cis-lncRNA that functions by chromatin restructuring is *HOTTIP*[144]. *HOTTIP* initiates chromatin looping via recruitment of histone complexes, allowing for the transcription of the *HOXA* gene[144].

Although cis-acting lncRNAs are common, the existence of trans-acting lncRNAs also have been seen with a vast diversity in functionality including the recruitment of chromatin modification complexes[145,146] and binding to RNA polymerases in order to affect transcription[147]. In humans, *HOTAIR* is a trans-lncRNA transcribed from chromosome 12 and is transported by the Suz-Twelve protein to regulate the homologous target site at the *HOXD* locus on chromosome 2[148]. *HOTAIR* has also demonstrated abilities to modify gene expression by recruiting chromatin modification complexes[145,146]. Regarding trans-lncRNAs binding RNA polymerases, it has been shown that lncRNA *B2 RNA* stably binds to the polymerase II complex during the heat shock response, blocking its activity[147].

Trans-lncRNAs can also influence the activity or quantity of proteins and RNAs that they directly bind to by acting as decoys or "sponges". *NORAD* is a lncRNA that is activated by DNA damage and acts as a decoy for proteins involved in chromosomal instability and aberrant mitosis, thus negatively regulating those proteins and limiting their ability to repress DNA repair[149]. Trans-lncRNAs also have the ability to regulate gene expression by sequestering miRNAs, decreasing their concentration in the cell and, as a result, diminishing the overall accessible miRNA within the cell. This lncRNA mode of regulation, referred to as the competing

endogenous RNA (ceRNA) hypothesis, allows for the negative regulation of miRNAs, thus a positive regulation of gene expression[150]. One such example includes *lincRNA-ROR* which inhibits miR-145, thereby regulating Oct4, Nanog and Sox2 in pluripotent embryonic stem cells[151]. The ceRNA hypothesis is still heavily debated, with some researchers insisting that low lncRNA expression levels will merely have minimal influence on miRNA availability, and hence will be ineffective as a competitor[152].

Experimental Undertakings

In our studies, we aimed to test two hypotheses: (1) the absence of the 10 bp sequence that is observed in the p allele at the *POLLED* locus, but absent in the P_C allele, is sufficient to result in the polled phenotype and (2) the absence of *lincRNA#1* expression will result in horn development irrespective of the alleles present at the *POLLED* locus. We hypothesized that deleting the 10 bp sequence from both p alleles at the *POLLED* locus using genome editing would result in animals with a polled phenotype. Since it is believed that *lincRNA#1* suppresses horn bud development, we also hypothesized that knocking out both copies of *lincRNA#1* in both pp and P_Cp embryos using genome editing would always result in animals with a horned phenotype. To test these hypotheses, we performed CPI of bovine embryos to create knockouts of genomic regions containing either the 10 bp or *lincRNA#1*. Embryo transfers were performed, and the fetuses were analyzed to determine whether the missing 10 bp at the P_C locus and *lincRNA#1* are important components in the mechanism behind the polled phenotype.

To be able to investigate these hypotheses, we first needed to improve current CPI protocols to try to increase the efficiency and address mosaicism issues. To do this, a gRNA design protocol was established and form of Cas9 (mRNA or protein), form of gRNA (synthetic or *in vitro* transcribed) and timing of embryo injections post *in vitro* fertilization was optimized

to determine the most efficient approach to obtain biallelic knockouts with low levels of mosaicism.

References

1 Knierim, U., Irrgang, N. & Roth, B. A. To be or not to be horned—Consequences in cattle. *Livest. Sci.* **179**, 29-37, https://doi.org/10.1016/j.livsci.2015.05.014 (2015).

2 Cardoso, C. S., von Keyserlingk, M. A. G. & Hötzel, M. J. Trading off animal welfare and production goals: Brazilian dairy farmers' perspectives on calf dehorning. *Livest. Sci.* **187**, 102-108, https://doi.org/10.1016/j.livsci.2016.02.010 (2016).

3 Stafford, K. J. & Mellor, D. J. Dehorning and disbudding distress and its alleviation in calves. *Vet. J.* **169**, 337-349, https://doi.org/10.1016/j.tvjl.2004.02.005 (2005).

4 Allais-Bonnet, A. *et al.* Novel insights into the bovine polled phenotype and horn ontogenesis in Bovidae. *PLoS One* **8**, e63512, https://doi.org/10.1371/journal.pone.0063512 (2013).

5 Medugorac, I. *et al.* Bovine polledness--an autosomal dominant trait with allelic heterogeneity. *PLoS One* **7**, e39477, https://doi.org/10.1371/journal.pone.0039477 (2012).

6 Rothammer, S. *et al.* The 80-kb DNA duplication on BTA1 is the only remaining candidate mutation for the polled phenotype of Friesian origin. *Genet. Sel. Evol.* **46**, 1-5, https://doi.org/10.1186/1297-9686-46-44 (2014).

7 Medugorac, I. *et al.* Whole-genome analysis of introgressive hybridization and characterization of the bovine legacy of Mongolian yaks. *Nat. Genet.* **49**, 470-475, https://doi.org/10.1038/ng.3775 (2017).

8 Utsunomiya, Y. T. *et al.* Hornless Nellore cattle (Bos indicus) carrying a novel 110 kbp duplication variant of the polled locus. *Anim. Genet.* **50**, 187-188, https://doi.org/10.1111/age.12764 (2019).

9 Sutherland, M., Julian, A. & Huddart, F. Clove oil delays rather than prevents scur/horn growth in dairy cattle. *Vet. Sci.* **6**, https://doi.org/10.3390/vetsci6040102 (2019).

10 Sutherland, M. A. *et al.* Behavioral and physiological assessment of liquid nitrogen cryoablation to prevent horn development in dairy calves. *J. Vet. Behav.* **31**, 74-81, https://doi.org/10.1016/j.jveb.2019.03.007 (2019).

11 AVMA. Literature review on the welfare implications of the dehorning and disbudding of cattle. *American Veterinary Medical Association* (2014).

12 OIE. in *Terrestrial Animal Health Code* Vol. 1 (World Organization for Animal Health, 2018).

13 Mueller, M. L., Cole, J. B., Sonstegard, T. S. & Van Eenennaam, A. L. Simulation of introgression of the POLLED allele into the Jersey breed via conventional breeding vs. gene editing. *Transl. Anim. Sci.* **2**, S57-S60, https://doi.org/10.1093/tas/txy054 (2018).

14 Mueller, M. L., Cole, J. B., Sonstegard, T. S. & Van Eenennaam, A. L. Comparison of gene editing versus conventional breeding to introgress the POLLED allele into the US dairy cattle population. *J. Dairy Sci.* **102**, 4215-4226, https://doi.org/10.3168/jds.2018-15892 (2019).

15 Kim, Y. G., Cha, J. & Chandrasegaran, S. Hybrid restriction enzymes zinc finger fusions to Fok I cleavage domain. *Proc. Natl. Acad. Sci. USA* **93**, 1156-1160, https://doi.org/10.1073/pnas.93.3.1156 (1996).
16 Bibikova, M. *et al.* Stimulation of homologous recombination through targeted cleavage by chimeric nucleases. *Mol. Cell. Biol.* **21**, 289-297, https://doi.org/10.1128/MCB.21.1.289-297.2001 (2001).
17 Maeder, M. L. *et al.* Rapid "open-source" engineering of customized zinc-finger nucleases for highly efficient gene modification. *Mol. Cell.* **31**, 294-301, https://doi.org/10.1016/j.molcel.2008.06.016 (2008).
18 Mani, M., Smith, J., Kandavelou, K., Berg, J. M. & Chandrasegaran, S. Binding of two zinc finger nuclease monomers to two specific sites is required for effective double-strand DNA cleavage. *Biochem. Biophys. Res. Commun.* **334**, 1191-1197, https://doi.org/10.1016/j.bbrc.2005.07.021 (2005).
19 Boch, J. *et al.* Breaking the code of DNA binding specificity of TAL-Type III effectors. *Science* **326**, 1509-1512, https://doi.org/10.1126/science.1178811 (2009).
20 Moscou, M. J. & Bogdanove, A. J. A simple cipher governs DNA recognition by TAL effectors. *Science* **326**, 1501, https://doi.org/10.1126/science.1178817 (2009).
21 Bogdanove, A. J. & Voytas, D. F. TAL effectors: customizable proteins for DNA targeting. *Science* **333**, 1843-1846, https://doi.org/10.1126/science.1204094 (2011).
22 Jinek, M. *et al.* A programmable dual-RNA-guided DNA endonuclease in adaptive bacterial immunity. *Science* **337**, 816-821, https://doi.org/10.1126/science.1225829 (2012).
23 Ran, F. A. *et al.* Genome engineering using the CRISPR-Cas9 system. *Nat. Protoc.* **8**, 2281-2308, https://doi.org/10.1038/nprot.2013.143 (2013).
24 Carlson, D. F. *et al.* Production of hornless dairy cattle from genome-edited cell lines. *Nat. Biotechnol.* **34**, 479-481, https://doi.org/10.1038/nbt.3560 (2016).
25 Akagi, S., Geshi, M. & Nagai, T. Recent progress in bovine somatic cell nuclear transfer. *Anim. Sci. J.* **84**, 191-199, https://doi.org/10.1111/asj.12035 (2013).
26 Wang, Z. Genome engineering in cattle: recent technological advancements. *Chromosome Res.* **23**, 17-29, https://doi.org/10.1007/s10577-014-9452-6 (2015).
27 Petersen, B. Basics of genome editing technology and its application in livestock species. *Reprod. Domest. Anim.* **52 Suppl 3**, 4-13, https://doi.org/10.1111/rda.13012 (2017).
28 Burkard, C. *et al.* Precision engineering for PRRSV resistance in pigs: Macrophages from genome edited pigs lacking CD163 SRCR5 domain are fully resistant to both PRRSV genotypes while maintaining biological function. *PLoS Pathog.* **13**, e1006206, https://doi.org/10.1371/journal.ppat.1006206 (2017).
29 Whitworth, K. M. *et al.* Gene-edited pigs are protected from porcine reproductive and respiratory syndrome virus. *Nat. Biotechnol.* **34**, 20-22, https://doi.org/10.1038/nbt.3434 (2016).
30 Wang, K. *et al.* Efficient generation of myostatin mutations in pigs using the CRISPR/Cas9 system. *Sci. Rep.* **5**, 16623, https://doi.org/10.1038/srep16623 (2015).
31 Crispo, M. *et al.* Efficient generation of myostatin knock-out sheep using CRISPR/Cas9 technology and microinjection into zygotes. *PLoS One* **10**, e0136690, https://doi.org/10.1371/journal.pone.0136690 (2015).

32 Wang, X. *et al.* Generation of gene-modified goats targeting MSTN and FGF5 via zygote injection of CRISPR/Cas9 system. *Sci. Rep.* **5**, 13878, https://doi.org/10.1038/srep13878 (2015).
33 Owen, J. R. *et al.* One-step generation of a targeted knock-in calf using the CRISPR-Cas9 system in bovine zygotes. *BMC Genom.* **22**, 118, https://doi.org/10.1186/s12864-021-07418-3 (2021).
34 Veres, A. *et al.* Low incidence of off-target mutations in individual CRISPR-Cas9 and TALEN targeted human stem cell clones detected by whole-genome sequencing. *Cell Stem Cell* **15**, 27-30, https://doi.org/10.1016/j.stem.2014.04.020 (2014).
35 Yang, L. *et al.* Targeted and genome-wide sequencing reveal single nucleotide variations impacting specificity of Cas9 in human stem cells. *Nat. Commun.* **5**, 5507, https://doi.org/10.1038/ncomms6507 (2014).
36 Luo, X. *et al.* Trio deep-sequencing does not reveal unexpected off-target and on-target mutations in Cas9-edited rhesus monkeys. *Nat. Commun.* **10**, 5525, https://doi.org/10.1038/s41467-019-13481-y (2019).
37 Hennig, S. L. *et al.* Evaluation of mutation rates, mosaicism and off target mutations when injecting Cas9 mRNA or protein for genome editing of bovine embryos. *Sci. Rep.* **10**, 22309, https://doi.org/10.1038/s41598-020-78264-8 (2020).
38 Iyer, V. *et al.* Off-target mutations are rare in Cas9-modified mice. *Nat. Methods* **12**, 479, https://doi.org/10.1038/nmeth.3408 (2015).
39 Iyer, V. *et al.* No unexpected CRISPR-Cas9 off-target activity revealed by trio sequencing of gene-edited mice. *PLoS Genet.* **14**, e1007503, https://doi.org/10.1371/journal.pgen.1007503 (2018).
40 Teboul, L., Murray, S. A. & Nolan, P. M. Phenotyping first-generation genome editing mutants: a new standard? *Mamm. Genome* **28**, 377-382, https://doi.org/10.1007/s00335-017-9711-x (2017).
41 Vilarino, M. *et al.* CRISPR/Cas9 microinjection in oocytes disables pancreas development in sheep. *Sci. Rep.* **7**, 17472, https://doi.org/10.1038/s41598-017-17805-0 (2017).
42 Mehravar, M., Shirazi, A., Nazari, M. & Banan, M. Mosaicism in CRISPR/Cas9-mediated genome editing. *Dev. Biol.* **445**, 156-162, https://doi.org/10.1016/j.ydbio.2018.10.008 (2019).
43 Sato, M. *et al.* Direct injection of CRISPR/Cas9-related mRNA into cytoplasm of parthenogenetically activated porcine oocytes causes frequent mosaicism for indel mutations. *Int. J. Mol. Sci.* **16**, 17838-17856, https://doi.org/10.3390/ijms160817838 (2015).
44 Sato, M. *et al.* Timing of CRISPR/Cas9-related mRNA microinjection after activation as an important factor affecting genome editing efficiency in porcine oocytes. *Theriogenology* **108**, 29-38, https://doi.org/10.1016/j.theriogenology.2017.11.030 (2018).
45 Zhang, X. *et al.* Disruption of the sheep BMPR-IB gene by CRISPR/Cas9 in in vitro-produced embryos. *Theriogenology* **91**, 163-172 e162, https://doi.org/10.1016/j.theriogenology.2016.10.025 (2017).
46 Petersen, B. *et al.* Efficient production of biallelic GGTA1 knockout pigs by cytoplasmic microinjection of CRISPR/Cas9 into zygotes. *Xenotransplantation* **23**, 338-346, https://doi.org/10.1111/xen.12258 (2016).

47 Lundrigan, B. Morphology of horns and fighting behaviour in the family *bovidae*. *J. Mammol.* **77**, 462-475, https://doi.org/10.2307/1382822 (1996).
48 Stankowich, T. & Caro, T. Evolution of weaponry in female bovids. *Proc. Biol. Sci.* **276**, 4329-4334, https://doi.org/10.1098/rspb.2009.1256 (2009).
49 Pares-Cassanova, P. M. & Caballero, M. Possible tendency of polled cattle towards larger ears. *Revista Colombiana de Ciencias Pecuarias* **27**, 221-225 (2014).
50 Davis, E. B., Brakora, K. A. & Lee, A. H. Evolution of ruminant headgear: a review. *Proc. Biol. Sci.* **278**, 2857-2865, https://doi.org/10.1098/rspb.2011.0938 (2011).
51 Wang, Y. *et al.* Genetic basis of ruminant headgear and rapid antler regeneration. *Science* **364**, https://doi.org/10.1126/science.aav6335 (2019).
52 Grobler, R., van Marle-Köster, E. & Visser, C. Challenges in selection and breeding of polled and scur phenotypes in beef cattle. *Livest. Sci.* **247**, https://doi.org/10.1016/j.livsci.2021.104479 (2021).
53 Zhu, B., Zhang, M. & Zhao, J. Microstructure and mechanical properties of sheep horn. *Microsc. Res. Tech.* **79**, 664-674, https://doi.org/10.1002/jemt.22681 (2016).
54 Dove, F. W. The physiology of horn growth: A study of the morphogenesis, the interaction of tissues, and the evolutionary processes of a mendelian recessive character by means of transplantation of tissues. *J. Exp. Zool.* **69**, 347-405, https://doi.org/10.1002/JEZ.1400690302 (1935).
55 Evans, E. H. & Sack, W. O. Prenatal development of domestic and laboratory mammals: Growth curves, external features and selected references. *Anat., Histol., Embryol.* **2**, 11-45, https://doi.org/10.1111/j.1439-0264.1973.tb00253.x (1973).
56 Wiener, D. J., Wiedemar, N., Welle, M. M. & Drogemuller, C. Novel features of the prenatal horn bud development in cattle (Bos taurus). *PLoS One* **10**, e0127691, https://doi.org/10.1371/journal.pone.0127691 (2015).
57 Mendonça, F. S. *et al.* Genetic group and horns presence in injuries and economic losses of bovine carcasses. *Semina: Ciências Agrárias* **37**, https://doi.org/10.5433/1679-0359.2016v37n6p4265 (2016).
58 Youngers, M. E. *et al.* Prevalence of horns and bruising in feedlot cattle at slaughter. *Prof. Anim. Sci.* **33**, 135-139, https://doi.org/10.15232/pas.2016-01551 (2017).
59 Cozzi, G. *et al.* Dehorning of cattle in the EU Member States: A quantitative survey of the current practices. *Livest. Sci.* **179**, 4-11, https://doi.org/10.1016/j.livsci.2015.05.011 (2015).
60 Kling-Eveillard, F. *et al.* Attitudes of farmers towards cattle dehorning. *Livest. Sci.* **179**, 12-21, https://doi.org/10.1016/j.livsci.2015.05.012 (2015).
61 Robbins, J. A., Weary, D. M., Schuppli, C. A. & von Keyserlingk, M. A. G. Stakeholder views on treating pain due to dehorning dairy calves. *Anim. Welf.* **24**, 399-406, https://doi.org/10.7120/09627286.24.4.399 (2015).
62 Bates, A. J., Laven, R. A., Chapple, F. & Weeks, D. S. The effect of different combinations of local anaesthesia, sedative and non-steroidal anti-inflammatory drugs on daily growth rates of dairy calves after disbudding. *N. Z. Vet. J.* **64**, 282-287, https://doi.org/10.1080/00480169.2016.1196626 (2016).
63 Bates, A. J., Eder, P. & Laven, R. A. Effect of analgesia and anti-inflammatory treatment on weight gain and milk intake of dairy calves after disbudding. *N. Z. Vet. J.* **63**, 153-157, https://doi.org/10.1080/00480169.2014.982739 (2015).

64 Georges, M. *et al.* Microsatellite mapping of a gene affecting horn development in Bos taurus. *Nat. Genet.* **4**, 206-210, https://doi.org/10.1038/ng0693-206 (1993).
65 Schmutz, S. M., Marquess, F. L. S., Berryere, T. G. & Moker, J. S. DNA marker-assisted selection of the polled condition in Charolais cattle. *Mamm. Genome* **6**, 710-713, https://doi.org/10.1007/BF00354293 (1995).
66 Brenneman, R. A. *et al.* The polled locus maps to BTA1 in a Bos indicus x Bos taurus cross. *J. Hered.* **87**, 156-161, https://doi.org/10.1093/oxfordjournals.jhered.a022975 (1996).
67 Harlizius, B., Tammen, I., Eichler, K., Eggen, A. & Hetzel, D. J. S. New markers on bovine chromosome 1 are closely linked to the polled gene in Simmental and Pinzgauer cattle. *Mamm. Genome* **8**, 255-257, https://doi.org/10.1007/s003359900404 (1997).
68 Aldersey, J. E., Sonstegard, T. S., Williams, J. L. & Bottema, C. D. K. Understanding the effects of the bovine POLLED variants. *Anim. Genet.* **51**, 166-176, https://doi.org/10.1111/age.12915 (2020).
69 Pauli, A. *et al.* Systematic identification of long noncoding RNAs expressed during zebrafish embryogenesis. *Genome Res.* **22**, 577-591, https://doi.org/10.1101/gr.133009.111 (2012).
70 Windig, J. J., Hoving-Bolink, R. A. & Veerkamp, R. F. Breeding for polledness in Holstein cattle. *Livest. Sci.* **179**, 96-101, https://doi.org/10.1016/j.livsci.2015.05.021 (2015).
71 Young, A. E. *et al.* Genomic and phenotypic analyses of six offspring of a genome-edited hornless bull. *Nat. Biotechnol.* **38**, 225-232, https://doi.org/10.1038/s41587-019-0266-0 (2020).
72 Gaj, T., Gersbach, C. A. & Barbas, C. F., 3rd. ZFN, TALEN, and CRISPR/Cas-based methods for genome engineering. *Trends Biotechnol.* **31**, 397-405, https://doi.org/10.1016/j.tibtech.2013.04.004 (2013).
73 Kim, E. *et al.* Precision genome engineering with programmable DNA-nicking enzymes. *Genome. Res.* **22**, 1327-1333, https://doi.org/10.1101/gr.138792.112 (2012).
74 Hauschild, J. *et al.* Efficient generation of a biallelic knockout in pigs using zinc-finger nucleases. *Proc. Natl. Acad. Sci. USA* **108**, 12013-12017, https://doi.org/10.1073/pnas.1106422108 (2011).
75 Lillico, S. G. *et al.* Mammalian interspecies substitution of immune modulatory alleles by genome editing. *Sci. Rep.* **6**, 21645, https://doi.org/10.1038/srep21645 (2016).
76 Li, T. *et al.* Modularly assembled designer TAL effector nucleases for targeted gene knockout and gene replacement in eukaryotes. *Nucleic Acids Res.* **39**, 6315-6325, https://doi.org/10.1093/nar/gkr188 (2011).
77 Liu, Y. *et al.* A highly effective TALEN-mediated approach for targeted gene disruption in Xenopus tropicalis and zebrafish. *Methods* **69**, 58-66, https://doi.org/10.1016/j.ymeth.2014.02.011 (2014).
78 Tesson, L. *et al.* Knockout rats generated by embryo microinjection of TALENs. *Nat. Biotechnol.* **29**, 695-696, https://doi.org/10.1038/nbt.1940 (2011).
79 Carlson, D. F. *et al.* Efficient TALEN-mediated gene knockout in livestock. *Proc. Natl. Acad. Sci. USA* **109**, 17382-17387, https://doi.org/10.1073/pnas.1211446109 (2012).
80 Yu, B. *et al.* Efficient TALEN-mediated myostatin gene editing in goats. *BMC Dev. Biol.* **16**, 26, https://doi.org/10.1186/s12861-016-0126-9 (2016).

81 Proudfoot, C. *et al.* Genome edited sheep and cattle. *Transgenic Res.* **24**, 147-153, https://doi.org/10.1007/s11248-014-9832-x (2015).
82 Lee, J., Chung, J. H., Kim, H. M., Kim, D. W. & Kim, H. Designed nucleases for targeted genome editing. *Plant Biotechnol. J.* **14**, 448-462, https://doi.org/10.1111/pbi.12465 (2016).
83 Jansen, R., van Embden, D. A., Gaastra, W. & Schouls, L. M. Identification of genes that are associated with DNA repeats in prokaryotes. *Mol. Microbiol.* **43**, 1565-1575, https://doi.org/10.1046/j.1365-2958.2002.02839.x (2002).
84 Mojica, F. J., Diez-Villasenor, C., Garcia-Martinez, J. & Soria, E. Intervening sequences of regularly spaced prokaryotic repeats derive from foreign genetic elements. *J. Mol. Evol.* **60**, 174-182, https://doi.org/10.1007/s00239-004-0046-3 (2005).
85 Barrangou, R. *et al.* CRISPR provides acquired resistance against viruses in prokaryotes. *Science* **315**, 1709-1712, https://doi.org/10.1126/science.1138140 (2007).
86 DiCarlo, J. E. *et al.* Genome engineering in Saccharomyces cerevisiae using CRISPR-Cas systems. *Nucleic Acids Res.* **41**, 4336-4343, https://doi.org/10.1093/nar/gkt135 (2013).
87 Yu, Z. *et al.* Highly efficient genome modifications mediated by CRISPR/Cas9 in Drosophila. *Genetics* **195**, 289-291, https://doi.org/10.1534/genetics.113.153825 (2013).
88 Hwang, W. Y. *et al.* Efficient genome editing in zebrafish using a CRISPR-Cas system. *Nat. Biotechnol.* **31**, 227-229, https://doi.org/10.1038/nbt.2501 (2013).
89 Wang, H. *et al.* One-step generation of mice carrying mutations in multiple genes by CRISPR/Cas-mediated genome engineering. *Cell* **153**, 910-918, https://doi.org/10.1016/j.cell.2013.04.025 (2013).
90 Li, D. *et al.* Heritable gene targeting in the mouse and rat using a CRISPR-Cas system. *Nat. Biotechnol.* **31**, 681-683, https://doi.org/ (2013).
91 Yang, D. *et al.* Effective gene targeting in rabbits using RNA-guided Cas9 nucleases. *J. Mol. Cell. Biol.* **6**, 97-99, https://doi.org/10.1093/jmcb/mjt047 (2014).
92 Niu, Y. *et al.* Generation of gene-modified cynomolgus monkey via Cas9/RNA-mediated gene targeting in one-cell embryos. *Cell* **156**, 836-843, https://doi.org/10.1016/j.cell.2014.01.027 (2014).
93 Khan, S. H. Genome-editing technologies: Concept, pros, and cons of various genome-editing techniques and bioethical concerns for clinical application. *Mol. Ther. Nucleic Acids* **16**, 326-334, https://doi.org/10.1016/j.omtn.2019.02.027 (2019).
94 Kim, H. & Kim, J. S. A guide to genome engineering with programmable nucleases. *Nat. Rev. Genet.* **15**, 321-334, https://doi.org/10.1038/nrg3686 (2014).
95 Hsu, P. D. *et al.* DNA targeting specificity of RNA-guided Cas9 nucleases. *Nat. Biotechnol.* **31**, 827-832, https://doi.org/10.1038/nbt.2647 (2013).
96 Gupta, R. M. & Musunuru, K. Expanding the genetic editing tool kit: ZFNs, TALENs, and CRISPR-Cas9. *J. Clin. Invest.* **124**, 4154-4161, https://doi.org/10.1172/JCI72992 (2014).
97 Jao, L. E., Wente, S. R. & Chen, W. Efficient multiplex biallelic zebrafish genome editing using a CRISPR nuclease system. *Proc. Natl. Acad. Sci. USA* **110**, 13904-13909, https://doi.org/10.1073/pnas.1308335110 (2013).

98 Mussolino, C. *et al.* A novel TALE nuclease scaffold enables high genome editing activity in combination with low toxicity. *Nucleic Acids Res.* **39**, 9283-9293, https://doi.org/10.1093/nar/gkr597 (2011).
99 Willi, R., Smith, H. E., Wang, C., Liu, C. & Hennighausen, L. Mutation frequency is not increased in CRISPR–Cas9-edited mice. *Nat. Methods* **15**, 756-758, https://doi.org/10.1038/s41592-018-0148-2 (2018).
100 Jamal, M. *et al.* Keeping CRISPR/Cas on-target. *Curr. Issues Mol. Biol.* **20**, 1-12, https://doi.org/10.21775/cimb.020.001 (2016).
101 Koo, T., Lee, J. & Kim, J. S. Measuring and reducing off-target activities of programmable nucleases including CRISPR-Cas9. *Mol. Cells* **38**, 475-481, https://doi.org/10.14348/molcells.2015.0103 (2015).
102 Frock, R. L. *et al.* Genome-wide detection of DNA double-stranded breaks induced by engineered nucleases. *Nat. Biotechnol.* **33**, 179-186, https://doi.org/10.1038/nbt.3101 (2015).
103 Tsai, S. Q. *et al.* GUIDE-seq enables genome-wide profiling of off-target cleavage by CRISPR-Cas nucleases. *Nat. Biotechnol.* **33**, 187-197, https://doi.org/10.1038/nbt.3117 (2015).
104 Cong, L. *et al.* Multiplex genome engineering using CRISPR/Cas systems. *Science* **339**, 819-823, https://doi.org/10.1126/science.1231143 (2013).
105 Mali, P. *et al.* CAS9 transcriptional activators for target specificity screening and paired nickases for cooperative genome engineering. *Nat. Biotechnol.* **31**, 833-838, https://doi.org/10.1038/nbt.2675 (2013).
106 Pattanayak, V. *et al.* High-throughput profiling of off-target DNA cleavage reveals RNA-programmed Cas9 nuclease specificity. *Nat. Biotechnol.* **31**, 839-843, https://doi.org/10.1038/nbt.2673 (2013).
107 Fu, Y., Sander, J. D., Reyon, D., Cascio, V. M. & Joung, J. K. Improving CRISPR-Cas nuclease specificity using truncated guide RNAs. *Nat. Biotechnol.* **32**, 279-284, https://doi.org/10.1038/nbt.2808 (2014).
108 Cho, S. W. *et al.* Analysis of off-target effects of CRISPR/Cas-derived RNA-guided endonucleases and nickases. *Genome. Res.* **24**, 132-141, https://doi.org/10.1101/gr.162339.113 (2014).
109 Ran, F. A. *et al.* Double nicking by RNA-guided CRISPR Cas9 for enhanced genome editing specificity. *Cell* **154**, 1380-1389, https://doi.org/10.1016/j.cell.2013.08.021 (2013).
110 Liang, X. *et al.* Rapid and highly efficient mammalian cell engineering via Cas9 protein transfection. *J. Biotechnol.* **208**, 44-53, https://doi.org/10.1016/j.jbiotec.2015.04.024 (2015).
111 Tao, L. *et al.* Efficient biallelic mutation in porcine parthenotes using a CRISPR-Cas9 system. *Biochem. Biophys. Res. Commun.* **476**, 225-229, https://doi.org/10.1016/j.bbrc.2016.05.100 (2016).
112 Bevacqua, R. J. *et al.* Efficient edition of the bovine PRNP prion gene in somatic cells and IVF embryos using the CRISPR/Cas9 system. *Theriogenology* **86**, 1886-1896 e1881, https://doi.org/10.1016/j.theriogenology.2016.06.010 (2016).

113 Zhou, X. *et al.* Efficient generation of gene-modified pigs harboring precise orthologous human mutation via CRISPR/Cas9-induced homology-directed repair in zygotes. *Hum. Mutat.* **37**, 110-118, https://doi.org/10.1002/humu.22913 (2016).
114 Whitworth, K. M. *et al.* Zygote injection of CRISPR/Cas9 RNA successfully modifies the target gene without delaying blastocyst development or altering the sex ratio in pigs. *Transgenic Res.* **26**, 97-107, https://doi.org/10.1007/s11248-016-9989-6 (2017).
115 Brinkman, E. K., Chen, T., Amendola, M. & van Steensel, B. Easy quantitative assessment of genome editing by sequence trace decomposition. *Nucleic Acids Res.* **42**, e168-e168, https://doi.org/10.1093/nar/gku936 (2014).
116 Dehairs, J., Talebi, A., Cherifi, Y. & Swinnen, J. V. CRISP-ID: decoding CRISPR mediated indels by Sanger sequencing. *Sci. Rep.* **6**, 28973, https://doi.org/10.1038/srep28973 (2016).
117 Tan, W., Proudfoot, C., Lillico, S. G. & Whitelaw, C. B. Gene targeting, genome editing: from Dolly to editors. *Transgenic Res.* **25**, 273-287, https://doi.org/10.1007/s11248-016-9932-x (2016).
118 Tanihara, F. *et al.* Effects of concentration of CRISPR/Cas9 components on genetic mosaicism in cytoplasmic microinjected porcine embryos. *J. Reprod. Dev.* **65**, 209-214, https://doi.org/10.1262/jrd.2018-116 (2019).
119 Munoz, M. *et al.* Prediction of pregnancy viability in bovine in vitro-produced embryos and recipient plasma with Fourier transform infrared spectroscopy. *J. Dairy Sci.* **97**, 5497-5507, https://doi.org/10.3168/jds.2014-8067 (2014).
120 Bishop, T. F. & Van Eenennaam, A. L. Genome editing approaches to augment livestock breeding programs. *J. Exp. Biol.* **223**, https://doi.org/10.1242/jeb.207159 (2020).
121 Bartel, D. P. MicroRNAs: Genomics, biogenesis, mechanism, and function. *Cell* **116**, 281-297, https://doi.org/10.1016/s0092-8674(04)00045-5 (2004).
122 Winter, J., Jung, S., Keller, S., Gregory, R. I. & Diederichs, S. Many roads to maturity: microRNA biogenesis pathways and their regulation. *Nat. Cell Biol.* **11**, 228-234, https://doi.org/10.1038/ncb0309-228 (2009).
123 Rao, D. D., Vorhies, J. S., Senzer, N. & Nemunaitis, J. siRNA vs. shRNA: similarities and differences. *Adv. Drug Deliv. Rev.* **61**, 746-759, https://doi.org/10.1016/j.addr.2009.04.004 (2009).
124 Siomi, M. C., Sato, K., Pezic, D. & Aravin, A. A. PIWI-interacting small RNAs: the vanguard of genome defence. *Nat. Rev. Mol. Cell. Biol.* **12**, 246-258, https://doi.org/10.1038/nrm3089 (2011).
125 Derrien, T. *et al.* The GENCODE v7 catalog of human long noncoding RNAs: analysis of their gene structure, evolution, and expression. *Genome Res.* **22**, 1775-1789, https://doi.org/10.1101/gr.132159.111 (2012).
126 Carninci, P. *et al.* The transcriptional landscape of the mammalian genome. *Science* **309**, 1559-1563, https://doi.org/10.1126/science.1112014 (2005).
127 Quinn, J. J. & Chang, H. Y. Unique features of long non-coding RNA biogenesis and function. *Nat. Rev. Genet.* **17**, 47-62, https://doi.org/10.1038/nrg.2015.10 (2016).
128 Cabili, M. N. *et al.* Integrative annotation of human large intergenic noncoding RNAs reveals global properties and specific subclasses. *Genes. Dev.* **25**, 1915-1927, https://doi.org/10.1101/gad.17446611 (2011).

129 Hezroni, H. *et al.* Principles of long noncoding RNA evolution derived from direct comparison of transcriptomes in 17 species. *Cell Rep.* **11**, 1110-1122, https://doi.org/10.1016/j.celrep.2015.04.023 (2015).
130 Clark, M. B. *et al.* Genome-wide analysis of long noncoding RNA stability. *Genome. Res.* **22**, 885-898, https://doi.org/10.1101/gr.131037.111 (2012).
131 Mele, M. *et al.* Chromatin environment, transcriptional regulation, and splicing distinguish lincRNAs and mRNAs. *Genome. Res.* **27**, 27-37, https://doi.org/10.1101/gr.214205.116 (2017).
132 Guttman, M. *et al.* Ab initio reconstruction of cell type-specific transcriptomes in mouse reveals the conserved multi-exonic structure of lincRNAs. *Nat. Biotechnol.* **28**, 503-510, https://doi.org/10.1038/nbt.1633 (2010).
133 Flynn, R. A. & Chang, H. Y. Long noncoding RNAs in cell-fate programming and reprogramming. *Cell Stem Cell* **14**, 752-761, https://doi.org/10.1016/j.stem.2014.05.014 (2014).
134 Batista, P. J. & Chang, H. Y. Long noncoding RNAs: cellular address codes in development and disease. *Cell* **152**, 1298-1307, https://doi.org/10.1016/j.cell.2013.02.012 (2013).
135 Hangauer, M. J., Vaughn, I. W. & McManus, M. T. Pervasive transcription of the human genome produces thousands of previously unidentified long intergenic noncoding RNAs. *PLoS Genet.* **9**, e1003569, https://doi.org/10.1371/journal.pgen.1003569 (2013).
136 Pandey, R. R. *et al.* Kcnq1ot1 antisense noncoding RNA mediates lineage-specific transcriptional silencing through chromatin-level regulation. *Mol. Cell.* **32**, 232-246, https://doi.org/10.1016/j.molcel.2008.08.022 (2008).
137 Pastori, C. *et al.* Comprehensive analysis of the transcriptional landscape of the human FMR1 gene reveals two new long noncoding RNAs differentially expressed in Fragile X syndrome and Fragile X-associated tremor/ataxia syndrome. *Hum. Genet.* **133**, 59-67, https://doi.org/10.1007/s00439-013-1356-6 (2014).
138 Milligan, M. J. & Lipovich, L. Pseudogene-derived lncRNAs: emerging regulators of gene expression. *Front. Genet.* **5**, 476, https://doi.org/10.3389/fgene.2014.00476 (2014).
139 Wang, K. C. & Chang, H. Y. Molecular mechanisms of long noncoding RNAs. *Mol. Cell.* **43**, 904-914, https://doi.org/10.1016/j.molcel.2011.08.018 (2011).
140 Martens, J. A., Laprade, L. & Winston, F. Intergenic transcription is required to repress the *Saccharomyces cerevisiae SER3* gene. *Nature* **429**, 571-574, https://doi.org/10.1038/nature02538 (2004).
141 Thompson, D. M. & Parker, R. Cytoplasmic decay of intergenic transcripts in Saccharomyces cerevisiae. *Mol. Cell. Biol.* **27**, 92-101, https://doi.org/10.1128/MCB.01023-06 (2007).
142 Ma, L., Bajic, V. B. & Zhang, Z. On the classification of long non-coding RNAs. *RNA Biol.* **10**, 925-933, https://doi.org/10.4161/rna.24604 (2013).
143 Maenner, S. *et al.* 2-D structure of the A region of Xist RNA and its implication for PRC2 association. *PLoS Biol.* **8**, e1000276, https://doi.org/10.1371/journal.pbio.1000276 (2010).
144 Wang, K. C. *et al.* A long noncoding RNA maintains active chromatin to coordinate homeotic gene expression. *Nature* **472**, 120-124, https://doi.org/10.1038/nature09819 (2011).

145 Tsai, M. C. *et al.* Long noncoding RNA as modular scaffold of histone modification complexes. *Science* **329**, 689-693, https://doi.org/10.1126/science.1192002 (2010).
146 Chu, C., Qu, K., Zhong, F. L., Artandi, S. E. & Chang, H. Y. Genomic maps of long noncoding RNA occupancy reveal principles of RNA-chromatin interactions. *Mol. Cell.* **44**, 667-678, https://doi.org/10.1016/j.molcel.2011.08.027 (2011).
147 Espinoza, C. A., Allen, T. A., Hieb, A. R., Kugel, J. F. & Goodrich, J. A. B2 RNA binds directly to RNA polymerase II to repress transcript synthesis. *Nat. Struct. Mol. Biol.* **11**, 822-829, https://doi.org/10.1038/nsmb812 (2004).
148 Rinn, J. L. *et al.* Functional demarcation of active and silent chromatin domains in human *HOX* loci by noncoding RNAs. *Cell* **129**, 1311-1323, https://doi.org/10.1016/j.cell.2007.05.022 (2007).
149 Lee, S. *et al.* Noncoding RNA NORAD regulates genomic stability by sequestering PUMILIO proteins. *Cell* **164**, 69-80, https://doi.org/10.1016/j.cell.2015.12.017 (2016).
150 Salmena, L., Poliseno, L., Tay, Y., Kats, L. & Pandolfi, P. P. A ceRNA hypothesis: the Rosetta Stone of a hidden RNA language? *Cell* **146**, 353-358, https://doi.org/10.1016/j.cell.2011.07.014 (2011).
151 Wang, Y. *et al.* Endogenous miRNA sponge lincRNA-RoR regulates Oct4, Nanog, and Sox2 in human embryonic stem cell self-renewal. *Dev. Cell.* **25**, 69-80, https://doi.org/10.1016/j.devcel.2013.03.002 (2013).
152 Thomson, D. W. & Dinger, M. E. Endogenous microRNA sponges: evidence and controversy. *Nat Rev Genet* **17**, 272-283, https://doi.org/10.1038/nrg.2016.20 (2016).

Chapter 2: Evaluation of mutation rates, mosaicism and off target mutations when injecting Cas9 mRNA or protein for genome editing of bovine embryos

Sadie L. Hennig[1], Joseph R. Owen[1], Jason C. Lin[1], Amy E. Young[1], Pablo J. Ross[1], Alison L. Van Eenennaam[1] and James D. Murray[1,2].

[1]Department of Animal Science, University of California – Davis, Davis, CA
[2]Department of Population Health and Reproduction, School of Veterinary Medicine, University of California – Davis, Davis, CA

[Published in Scientific Reports (2020) 10:22309]

This chapter was performed in collaboration with a fellow PhD student, Joseph Owen, and was published in Scientific Reports in 2020 (volume 10, article number 22309). It is the culmination of experiments completed during my Master's degree (gRNA design, testing, and blastocyst development and mutation efficiency) as well as experiments completed during my PhD (allelic variation and off-target analysis).

ABSTRACT

The CRISPR/Cas9 genome editing tool has the potential to improve the livestock breeding industry by allowing for the introduction of desirable traits. Although an efficient and targeted tool, the CRISPR/Cas9 system can have some drawbacks, including off-target mutations and mosaicism, particularly when used in developing embryos. Here, we introduced genome editing reagents into single-cell bovine embryos to compare the effect of Cas9 mRNA and protein on the mutation efficiency, level of mosaicism, and evaluate potential off-target mutations utilizing next generation sequencing. We designed guide-RNAs targeting three loci (POLLED, H11, and ZFX) in the bovine genome and saw a significantly higher rate of mutation in embryos injected with Cas9 protein (84.2%) vs. Cas9 mRNA (68.5%). In addition, the level of mosaicism was higher in embryos injected with Cas9 mRNA (100%) compared to those injected with Cas9 protein (94.2%), with little to no unintended off-target mutations detected. This study demonstrated that the use of gRNA/Cas9 ribonucleoprotein complex resulted in a high editing efficiency at three different loci in bovine embryos and decreased levels of mosaicism relative to Cas9 mRNA. Additional optimization will be required to further reduce mosaicism to levels that make single-step embryo editing in cattle commercially feasible.

INTRODUCTION

CRISPR-mediated genome editing in livestock zygotes offers an attractive approach to introduce useful genetic variation into the next generation of cattle breeding programs. However, genetic mosaicism is particularly problematic for CRISPR-mediated genome editing in developing zygotes[1,2]. Genetic mosaicism complicates phenotypic analysis of F0 animals and may complicate screening multiple founders and breeding mosaic founders to produce an F1

generation. While this is routine in plant and mouse research, such approaches are time-consuming and essentially cost-prohibitive in uniparous large food animal species with long generation intervals like cattle.

A limited number of genome editing studies have been reported in bovine zygotes[3], and indicate the frequent production of mosaic embryos. The frequency of mosaicism varies depending upon the type of site-directed nuclease used, the timing of editing relative to embryonic development, the form and efficiency of the targeting regents, the intrinsic properties of the target locus, and the method of delivery[1].

Correspondingly, there are a number of experimental variables that need to be optimized to improve the efficiency of obtaining non-mosaic, homozygous genome edited founder cattle. In this study, we focused on the type of CRISPR/Cas9 system delivered (i.e. mRNA or protein) and report the impact on mutation efficiency, levels of mosaicism, and off-target mutations based on next generation sequencing when using CRISPR-mediated genome editing of bovine zygotes.

RESULTS

Guide Construction and Testing

To determine the optimal parameters for CRISPR/Cas9-mediated genome editing in bovine zygotes, efficiency following microinjection was investigated for three gRNA per locus on three different chromosomes. Three gRNAs were designed targeting the POLLED locus on chromosome 1, a safe harbor locus (H11) on chromosome 17 and a locus (ZFX) on the X chromosome downstream of the Zinc Finger, X-linked gene (Supplementary Table S1). Three gRNAs per locus were independently injected alongside Cas9 protein in groups of 30 zygotes, 18 h post insemination (hpi). Groups of 50 non-injected embryos were cultured as controls. The

highest mutation rates were 76.9% for gRNA2 targeting the POLLED locus, 83.3% for gRNA1 targeting the H11 locus, and 77.8% for gRNA3 targeting the ZFX locus (Supplementary Table S2; $\chi 2$ test, $P < 0.05$). Overall, there was a decrease in the number of embryos that reached the blastocyst stage as the rate of mutation for a given gRNA increased. For each locus, the gRNA with the highest mutation rate was associated with the lowest developmental rate (Supplementary Table S2). gRNAs with the highest mutation rate were selected for further analysis.

Guides targeting the POLLED locus, the H11 locus and the ZFX locus were then injected in groups of 30 in vitro fertilized embryos 18hpi alongside either Cas9 mRNA or protein (Table 1). The blastocyst rate of uninjected controls (30.7%) was significantly higher than embryos that were microinjected with gRNA and Cas9 editing reagents (Fig. 1a; $P < 0.001$). The overall mutation rate did not differ among the three loci for a given form of Cas9 (Fig. 1b; $P = 0.45$;); however the probability of a mutation was higher ($P = 0.002$) when Cas9 protein was microinjected as compared to Cas9 mRNA (Fig. 1c).

Evaluation of Mosaicism and Off-Target Insertions and Deletions

To evaluate the level of mosaicism, 69 blastocysts (19 gRNA2 targeting the POLLED locus (10 Cas9 mRNA, 9 Cas9 protein), 26 gRNA1 targeting the H11 locus (11 Cas9 mRNA, 15 Cas9 protein), and 24 targeting the ZFX locus (13 Cas9 mRNA, 11 Cas9 protein)) were collected, barcoded by PCR amplification and sequenced on a PacBio sequencer (Supplementary Table S3). Consensus sequences were called from raw reads using circular consensus sequencing (ccs) with a minimum of 3 passes, a minimum predicted accuracy of 99% and a maximum length of 700 bp (Supplementary Table S4). Unsorted ccs reads were aligned to each of the target sequences to analyze the types of insertions/deletions (indels) surrounding the predicted cut site with 26,460 reads aligned to the POLLED target site; 78,305 reads aligned to the H11 target site;

and 66,780 reads aligned to ZFX target site (Supplementary Table S5). About half of the aligned sequences for the POLLED locus were wild type sequences (47.8%), while almost three quarters of the H11 and ZFX reads were wild type sequences (75.7% and 71.3%, respectively). The primary indels for reads aligned to the POLLED locus were 7 bp deletion (1672 reads), 11 bp deletion (1751), 4 bp deletion (6356 reads) and 1 bp insertion (2250 reads); aligned to the H11 locus were 11 bp deletion (3246 reads), 6 bp deletion (3813 reads), 3 bp deletion (4091 reads), and 1 bp deletion (7853 reads); and aligned to the ZFX locus were 14 bp deletion (4222 reads), 9 bp deletion (2998 reads), 3 bp deletion (3198 reads), 1 bp deletion (2194 reads) and 1 bp insertion (6532 reads) (Supplementary Table S5).

Ccs reads were then sorted by barcode and analyzed by individual embryos (Fig. 2). Seven samples were discarded from further analysis due to a lack of reads following the quality filtering step (Supplemental Table S3). A total of 10 samples contained only wild type sequence (7 Cas9 mRNA and 3 Cas9 protein), resulting in an overall mutation rate of ~ 84% (Table 2). Of the 62 samples injected 18hpi, four contained only mutated alleles, without evidence for any wild type sequence. All four samples were from embryos injected with Cas9 protein (Supplementary Table S6). Three of these samples contained only one allele and were presumably non-mosaic homozygous, although our analyses could not rule out an unmappable mutation (e.g. large insertion) at the second allele. Each of the mutated embryos containing more than a single allele had at least three individual alleles or a disproportion of reads for each allele, for example 75% wildtype and 25% mutant (Supplementary Fig. S1), suggesting these embryos were mosaic rather than heterozygous. This translates to 94.2% mosaicism when injecting Cas9 protein compared to 100% mosaicism when injecting Cas9 mRNA.

There was a decreased average number of alleles (3.0 ± 0.4) when targeting the POLLED locus using Cas9 protein (Fig. 1d; Table 2), as compared to Cas9 mRNA. There was no significant difference in the number of alleles for the other loci when comparing Cas9 mRNA or protein. However, there was a significant increase in the number of alleles when comparing pooled samples of embryos injected 18hpi with guides alongside Cas9 mRNA (5.23 ± 0.268), as compared to protein (4.23 ± 0.268) (ANOVA, $P < 0.05$). In addition, there was a significant increase in the percentage of wild type alleles present when injecting Cas9 mRNA compared to Cas9 protein for each of the three loci (42.5% vs. 9.1%, 70.9% vs. 33.7% and 79.7% vs. 43.5%, for POLLED, H11 and ZFX, respectively; $P < 0.05$).

A total of 24 potential off-target sites were predicted across 11 bovine chromosomes (1, 4, 7, 8, 10, 12, 14, 18, 21, 27 and X) (Supplementary Table S7) for the three loci. The 24 predicted off-target sites were PCR amplified, barcoded and sequenced using an Illumina MiSeq sequencer for each of the 69 samples (Supplementary Table S3). HTStream processed reads were aligned to the 24 predicted sites with 10,399,614 reads mapped with coverage ranging from 1X to 112X per sample per site (Supplementary Table S7). Genetic variation was found throughout the samples in each of the 24 predicted off-target sites with almost no indels present at the predicted off-target cut site with the exception of two targets. A 12 bp deletion 26 bp downstream from a predicted off-target cut site for the H11 gRNA targeting chr1: 7454978 was detected in 69,434 reads (6.8%) (Supplemental Table S7). Additionally, 2397 reads (0.51%) contained a 3 bp deletion 11 bp downstream from the predicted off-target cut site of the ZFX gRNA target chr21: 28506796 (Supplemental Table S7).

DISCUSSION

The ability to efficiently generate non-mosaic, homozygous founder animals is important for the production of genome edited livestock. The use of the CRISPR/Cas9 system has been reported across many livestock species[3], but few reports have characterized its use in bovine embryos. In this study, using the CRISPR/Cas9 system, we identified gRNAs that resulted in high rates of mutation at target locations in two autosomes and the X chromosome in bovine embryos with an overall high efficiency (81–90%; Table 1). Significant differences were observed in gRNA efficiency within a locus, but not between loci. It has been demonstrated that microinjection itself does not have a significant impact on the development of bovine embryos[4], but we found that microinjection of editing reagents in zygotes reduced development to the blastocyst stage compared to non-injected controls as the mutation efficiency of a given gRNA increased (Supplementary Table S2). However, no difference was observed in the number of embryos that reached the blastocyst stage when comparing embryos injected with Cas9 mRNA or protein (16.2% vs. 16.4%; Fig. 1a). This finding was important because we observed a significantly higher mutation rate in blastocysts when injecting Cas9 protein compared to Cas9 mRNA (84.2% and 68.5%, respectively; Fig. 1b). This difference is likely due to the immediate availability of the gRNA/Cas9 ribonucleoprotein (RNP) complex to induce mutation in the embryo. When Cas9 mRNA is injected, there is a delay in genome editing as Cas9 mRNA must be translated into protein before it can combine with the gRNA to induce a DSB[5].

Mosaicism, the presence of more than two alleles in an individual, is a common problem in livestock genome editing[6], with a high rate of embryos resulting in multiple alleles (Table 3). Studies utilizing transcription activator-like effector nucleases (TALENs) have demonstrated lower mosaicism rates than we observed here; however, the proportion of edited embryos tends

to be lower as well[7,8]. A study employing a zinc finger nuclease (ZFN) in bovine embryos demonstrated both high embryo editing efficiency and mosaicism rates as compared to those found in TALEN edited embryos[9]. However, the prevalence of mosaicism was reduced when injecting embryos at 8hpi compared to 18hpi, before S-phase had occurred[9]. While we were able to induce mutations in embryos at a high rate, we also observed a high level of mosaicism when injecting 18hpi. Many studies of editing in livestock zygotes similarly report high levels of mosaicism when utilizing CRISPR/Cas9 (Table 3). Many of these studies characterized mosaicism by sequencing the PCR amplicon of the genomic regions flanking the gRNA target sequence and then decomposing the resulting chromatogram data with the TIDE bioinformatics package[10]. Although this approach is cost-effective and rapid, next generation sequencing of the PCR products allows for a more accurate characterization of the different alleles that are present in a mosaic individual, and their relative abundance[11]. However, this approach does present some concern with PacBio sequencing being highly error prone in regards to indels and SNPs. However, given the short sequences of the target amplicons, we were able to generate circular consensus sequencing (CCS) reads, increasing the confidence in the accuracy of the alleles that were being called[12].

In bovine embryos, DNA replication occurs approximately 12–14 h after fertilization[13]. When injecting at 18hpi, as is often done when using traditional *in-vitro* fertilization (IVF) protocols, most zygotes would be expected to have completed DNA replication[14] and there would likely be more than two copies of each chromosome, thus more opportunities for multiple genomic edits to occur, resulting in mosaicism. Additionally, following cytoplasmic injection, the gRNA/Cas9 ribonucleoprotein (RNP) complex needs time to enter the nucleus, find its target and cleave the DNA. Furthermore, if injecting Cas9 mRNA, translation to Cas9 protein must

also occur, further delaying the editing process, thus resulting in a higher rate of mosaicism. It has been suggested that injection of the CRISPR/Cas9 RNP prior to the S-phase of DNA replication could reduce mosaicism[1].

One recent study with bovine embryos reported low rates (~30%) of mosaicism when introducing Cas9 RNA or protein into early stage zygotes (0 or 10hpi) prior to the S-phase of DNA replication[14]. In that study, the authors were targeting two genes simultaneously via microinjection of two gRNAs into either matured oocytes before IVF or into zygotes at various time points post IVF. Allele identification was first made by Sanger sequencing of an amplicon of the targeted region, and then by clonal sequencing of 10 colonies derived from the PCR product per embryo. PCR and cloning-based approaches can identify that a range of alleles exist but cannot accurately quantitate the abundance of each allelic species. The authors went on to employ next generation sequencing on 20 embryos per group to characterize the alleles in non-mosaic embryos. The authors considered embryos that contained biallelic mutations resulting in frame-disrupting alleles to be non-mosaic, regardless of the number of alleles.

In the current study, we employed next generation sequencing to quantitate the abundance of each allele. The fact that we observed multiple alleles occurring in only a small percentage of reads (< 25%) in many samples analyzed in this study (Fig. 2) suggests that editing continued in some subset of cells after the first cleavage division. Further, we considered an embryo containing more than one population of genetically distinct cells to be mosaic irrespective of whether the edit resulted in a missense or nonsense mutation. It is important to determine if founder animals are mosaic because mosaicism complicates the interpretation of the effect of a given genome alteration[6], and subsequent breeding of mosaic founder animals to

achieve non-mosaic animals can take years[15]. Additionally, mosaics do not fit easily into the proposed regulatory framework for genome edited food animals[16].

Along with the level of mosaicism, one of the concerns raised with the generation of genome edited animals is the potential for off-target mutation events. Typically, online prediction tools are used to calculate the likelihood of off-target sites[17-19]. The top predicted sites can then be PCR amplified and the presence of a mutation determined by either next generation sequencing, TA cloning followed by Sanger sequencing, or mismatch cleavage assays followed by Sanger sequencing[20]. In this study, we used the targeted approach using online predictive tools to identify off-target sites rather than a genome-wide approach. Off-target cleavage can occur in the genome with three to five base pair mismatches in the PAM-distal sequence[17,21-23]. Cas9 specificity is determined by the seed region, or the 8 to 11-nt PAM-proximal sequence, making it the most vital part of the gRNA sequence[21,24]. In our gRNA design, we excluded all gRNAs with less than three mismatches across the off-target sequence. We determined this threshold based on previous studies showing reduced Cas9 activity in regions with at least three mismatches[25].

In the 69 samples analyzed, there were two potential off-target mutations detected. One of these (H11) was in a region that had known annotated wild type 12 bp deletions (rs876383581 and rs521367917) around the potential cut-site. Additionally, 0.51% of total reads contained a 3 bp deletion 11 bp downstream from the predicted off-target cut site for the ZFX gRNA target chr21: 28,506,796 (Supplemental Table S7). This predicted site does not have any annotated variation. It is important to note that although this off-target location had three mismatches to the gRNA sequence, all three of the mismatches were located outside the seed region (8–11 bp upstream of the PAM sequence). This guide was designed using off-target prediction software

and the Btau 4.6.1 bovine reference genome[26], which was the only *Bos taurus* reference genome available with the online tool at the time. When the off-target prediction software was re-run for the off-target analysis, the most recent reference genome available was UMD 3.1.1[26]. Using the new reference genome, this locus on chromosome 21 was identified as having the requisite three mismatches, but there were no mismatches in the seed region, as specified by our guide design criteria. More recently, an improved reference bovine genome ARS-UCD1.2 was published[27]. Using the online tool with the updated reference genome resulted in the same predicted off-target sites as UMD 3.1.1.

One of the stated concerns with off-target mutation events is that if they occur in functional regions, such as coding sequences or regulatory regions, they could potentially be detrimental to the health or development of the resulting animal. Neither of these two off-target deletions were in a region of annotated function. As there were approximately 20 individual blastocysts included in these analyses, these deletions may also have been the result of naturally occurring polymorphic variation. A detailed sequence analysis of 2703 individuals from different breeds of cattle revealed a high level of genetic diversity including 84 million single-nucleotide polymorphisms (SNPs) and 2.5 million small insertion deletions[28]. Data like these are essential to put naturally occurring variation, like that seen at the H11 locus, in context. Various studies in humans[29,30], monkeys[31], and rodents[32,33] suggest that the off-target frequency of Cas9-mediated mutagenesis does not differ from the de novo mutation rate.

Overall, we demonstrated efficient CRISPR/Cas9 genome editing across three different loci on three different chromosomes. We found that injecting zygotes with Cas9 protein results in a significantly higher mutation rate compared to Cas9 mRNA (82.2% vs 65.4%). In addition, zygotes injected with Cas9 protein displayed a significantly lower number of alleles compared to

those injected with Cas9 mRNA (4.2 vs 5.2). Although off-target events did not appear to be an issue, the rate of mosaicism was still high, and further optimization needs to be done before this technique is feasible in a livestock production setting.

MATERIALS AND METHODS

Guide Construction

Guides sequences were designed using the online tools sgRNA Scorer 2.0[34,35] and Cas-OFFinder[36] and targeting the POLLED locus on chromosome 1, a safe harbor locus (H11) on chromosome 17 and in the 3′ UTR of the Zinc-finger X-linked (*ZFX*) gene (ZFX) on the X chromosome. Guides were selected with no less than three mismatches in the guide sequence for off-target sites using the UMD3.1.1 bovine reference genome[26], and at least one mismatch in the seed region (8–11 bp upstream of the PAM sequence). Oligonucleotides were ordered from Eurofins USA (Louisville, KY) for the top four guides for construction of the gRNA and were used for in vitro transcription using the AmpliScribe T7-Flash Transcription kit (Lucigen, Palo Alto, CA) and purified using the MEGAclear Transcription Clean-Up kit (Thermo Fisher, Chicago, IL) as described by Vilarino et al[11]. Cleavage efficiency was tested using an in vitro cleavage assay by combining 60 ng of PCR amplified product, 100 ng of gRNA, 150 ng of Cas9 protein (PNA Bio, Inc., Newbury Park, CA), 1 μL of 10X BSA, 1 μL of NEB Buffer 3.1 and water bringing the total volume to 10 μL in a 0.2 μL tube and incubating at 37 °C for 1 h. The incubated product was then run on a 2% agarose gel with 5 μL of Sybr Gold at 100 V for 1 h and visualized using a ChemiDoc-ItTS2 Imager (UVP, LLC, Upland, CA).

Embryo Production

Bovine ovaries were collected from a local processing plant and transported to the laboratory at 35–37 °C in sterile saline. Cumulus-oocyte complexes (COCs) were aspirated from follicles and groups of 50 COCs were transferred to 4-well dishes containing 400 μL of maturation media[37]. COCs were incubated for 21–24 hr at 38.5 °C in a humidified 5% CO_2 incubator. Approximately 25 oocytes per drop were fertilized in 60 μL drops of SOF-IVF[37] with 1×10^6 sperm per mL and incubated for 18 hr at 38.5 °C in a humidified 5% CO_2 incubator. Presumptive zygotes were denuded by light vortex in SOF-HEPES medium[37] for 5 min. 25 zygotes per drop were incubated in 50 μL drops of KSOM culture media (Zenith Biotech, Glendale, CA, USA) at 38.5°C in a humidified atmosphere of 5% CO_2, 5% O_2, and 90% N_2 for 7–8 days.

Guide Testing

Mutation rate for each guide was determined by laser-assisted cytoplasmic injection[4] of in vitro fertilized embryos with 6pL of a solution containing 67 ng/μL of in vitro transcribed gRNA alongside 133 ng/μL of Cas9 mRNA or 167 ng/μL of Cas9 protein (PNA Bio, Inc., Newbury Park, CA) incubated at room temperature for 30 min prior to injection. Injected embryos were incubated for 7–8 days. Embryos that reached blastocyst stage were lysed in 10 μL of Epicenter DNA extraction buffer (Lucigen, Palo Alto, CA) using a Simpli-Amp Thermal Cycler (Applied Biosystems, Foster City, California) at 65 °C for 6 min, 98 °C for 2 min and held at 4 °C. The target region was amplified by two rounds of the polymerase chain reaction (PCR) using primers developed using Primer3 (Supplementary Table S1)[38,39]. The first round of PCR was performed on a SimpliAmp Thermal Cycler (Applied Biosystems, Foster City, California) with 10 μL GoTAQ Green Master Mix (Promega Biosciences LLC, San Luis Obispo,

CA), 0.4 μL of each primer at 10 mM and 9.2 μL of DNA in lysis buffer for 5 min at 95 °C, 35 cycles of 30 s at 95 °C, 30 s at anneal temp (Supplementary Table S1), and 30 s at 72 °C, followed by 5 min at 72 °C. The second round of PCR was run with 10 μL GoTAQ Green Master Mix (Promega Biosciences LLC, San Luis Obispo, CA), 4.2 μL of water, 0.4 μL of each primer at 10 mM and 5 μL of first round PCR for 3 min at 95 °C, 35 cycles of 30 s at 95 °C, 30 s at anneal temp (Supplementary Table S1), and 30 s at 72 °C, followed by 5 min at 72 °C. Products were visualized on a 1% agarose gel using a ChemiDoc-ItTS2 Imager (UVP, LLC, Upland, CA), purified using the QIAquick Gel Extraction Kit (Qiagen, Inc., Valencia, CA) and Sanger sequenced (GeneWiz, South Plainfield, NJ).

Allelic Variation and Off-Target Analysis

Embryos that reached the blastocyst stage were lysed and underwent whole-genome amplification using the Repli-G Mini kit (Qiagen, Inc., Valencia, CA). To determine presumptive off-target sites, guide sequences were mapped against the bosTau8 bovine reference genome using the online tool Cas-OFFinder [36]. A total of 24 off-target sites were predicted using the online tool: eight off-target sites for the POLLED gRNA, eleven off-target sites for the H11 gRNA and five off-target sites for the ZFX gRNA (Supplementary Table S7). Whole-genome amplified samples were used for PCR amplification of cut-sites and presumptive off-target sites using a dual round PCR approach described above to barcode each sample with a reduction from 35 to 5 cycles in the first round of PCR. Primers were designed to amplify each region using Primer3[38,39] with a 15 bp adapter sequence attached to the forward (AGA TCT CTC GAG GTT) and reverse (GTA GTC GAA TTC GTT) (Supplementary Information S1). The second round of PCR amplified off the adapters adding an independent barcode for each sample to identify reads for pooled sequencing (Supplementary Table S1).

PCR samples targeting the gRNA cut site underwent SMRTbell library preparation and were sequenced on a PacBio Sequel II sequencer by GENEWIZ, LLC (South Plainfield, NJ, USA). Consensus sequences were called, reads sorted by barcode and BAM converted to individual FASTQ files using SMRT Link v8.0.0.80529 (https://www.pacb.com/support/software-downloads/). Reads were aligned to each target site using BWA v0.7.16a[40]. SAM files were converted to BAM files, sorted and indexed using SAMtools v1.9[41]. Number and types of alleles were determined for each sample using CrispRVariants v1.12.0[42].

Off-target PCR samples underwent library preparation using the Illumina TruSeq library kit and were sequenced (300 bp paired-end) on an Illumina MiSeq Next Generation Sequencer by the DNA Technologies and Expression Analysis Cores at the UC Davis Genome Center. Paired-end reads were processed and overlapped to form high quality single-end reads using HTStream Overlapper v1.1.0 (https://github.com/ibest/HTStream). Processed reads were aligned to each target site using BWA v0.7.16a[40]. SAM files were converted to BAM files, sorted and indexed using SAMtools v1.9[41]. Insertions and deletions were called using CrispRVariants v1.12.0[42].

Statistical Analysis

Comparison between blastocyst development and mutation rates were evaluated using a logistic regression model with Cas9 form and gRNA modeled as fixed effects. To analyze the level of mosaicism, an ANOVA test was used to determine significance between number of alleles per sample and percent wild type when injecting alongside Cas9 mRNA or protein. Samples with only wild type alleles were removed from analysis. Differences were considered significant when $P < 0.05$.

ACKNOWLEDGEMENTS

The authors would sincerely like to thank Ashley Young and Rebecca Ozeran for diligent collection and transport of ovaries from the processing plant to UC Davis. The library preparation and sequencing for off-target analysis were carried out at the DNA Technologies and Expression Analysis Cores at the UC Davis Genome Center, supported by NIH Shared Instrumentation Grant 1S10OD010786-01. The authors would like to thank the University of California Davis Bioinformatics Core Facility for assistance with data analysis. This project was supported by Biotechnology Risk Assessment Grant Program competitive grant no. 2015-33522-24106 from the U.S. Department of Agriculture, the Academic Federation Innovation Development Award at UC Davis, the Russell L. Rustici Rangeland and Cattle Research Endowment in the College of Agricultural and Environmental Science at UC Davis, the California Agricultural Experiment Station of the University of California, Davis, the Henry A. Jastro Research Fellowship in the College of Agricultural and Environmental Science at UC Davis and the National Institute for Food and Agriculture National Needs Graduate and Postgraduate Fellowship no. 2017-38420-26790 from the U.S. Department of Agriculture.

AUTHOR'S CONTRIBUTIONS

SLH and JRO performed the experiments with additional input from PJR, ALV and JDM. SLH, JRO, JCL and AEY participated in sample processing and data analysis. SLH, JRO, ALV and JDM wrote the manuscript with suggestions from all the co-authors. All authors read and approved the final version.

COMPETING INTERESTS

The authors declare no competing interests.

DATA AVAILABILITY

Raw sequence reads from PacBio Sequel II and Illumina MiSeq sequencing are available in the NCBI Sequence Read Archive as BioProject PRJNA623431 and SRA accession number SRR11850065. Individual results for the blastocyst development and mutation rate from each replicate (~ 30 embryos) of control and microinjected embryos are available in Supplementary Table S8.

REFERENCES

1 Mehravar, M., Shirazi, A., Nazari, M. & Banan, M. Mosaicism in CRISPR/Cas9-mediated genome editing. *Dev. Biol.* **445**, 156-162. https://doi.org/10.1016/j.ydbio.2018.10.008 (2019).

2 Vilarino, M. *et al.* Mosaicism diminishes the value of pre-implantation embryo biopsies for detecting CRISPR/Cas9 induced mutations in sheep. *Transgenic Res.* **27**, 525-537. https://doi.org/10.1007/s11248-018-0094-x (2018).

3 Mclean, Z., Oback, B. & Laible, G. Embryo-mediated genome editing for accelerated genetic improvement of livestock. *Front. Agric. Sci. Eng.* https://doi.org/10.15302/J-FASE-2019305 (2020).

4 Bogliotti, Y. S., Vilarino, M. & Ross, P. J. Laser-assisted cytoplasmic microinjection in livestock zygotes. *J. Vis. Exp.* https://doi.org/10.3791/54465 (2016).

5 Glass, Z., Lee, M., Li, Y. & Xu, Q. Engineering the delivery system for CRISPR-based genome editing. *Trends Biotechnol.* **36**, 173-185. https://doi.org/10.1016/j.tibtech.2017.11.006 (2018).

6 Teboul, L., Murray, S. A. & Nolan, P. M. Phenotyping first-generation genome editing mutants: a new standard? *Mamm. Genome* **28**, 377-382. https://doi.org/10.1007/s00335-017-9711-x (2017).

7 Carlson, D. F. *et al.* Efficient TALEN-mediated gene knockout in livestock. *Proc. Natl. Acad. Sci. USA* **109**, 17382-17387. https://doi.org/10.1073/pnas.1211446109 (2012).

8 Proudfoot, C. *et al.* Genome edited sheep and cattle. *Transgenic Res.* **24**, 147-153. https://doi.org/10.1007/s11248-014-9832-x (2015).

9 Wei, J. *et al.* Efficient introgression of allelic variants by embryo-mediated editing of the bovine genome. *Sci. Rep.* **5**, 11735. https://doi.org/10.1038/srep11735 (2015).

10 Brinkman, E. K., Chen, T., Amendola, M. & van Steensel, B. Easy quantitative assessment of genome editing by sequence trace decomposition. *Nucleic Acids Res.* **42**, e168-e168 (2014).

11 Vilarino, M. *et al.* CRISPR/Cas9 microinjection in oocytes disables pancreas development in sheep. *Sci. Rep.* **7**, 17472. https://doi.org/10.1038/s41598-017-17805-0 (2017).

12 Wenger, A. M. *et al.* Accurate circular consensus long-read sequencing improves variant detection and assembly of a human genome. *Nat. Biotechnol.* **37**, 1155-1162. https://doi.org/10.1038/s41587-019-0217-9 (2019).
13 Comizzoli, P., Marquant-Le Guienne, B., Heyman, Y. & Renard, J. P. Onset of the first S-phase is determined by a paternal effect during the G1-phase in bovine zygotes. *Biol. Reprod.* **62**, 1677-1684. https://doi.org/10.1095/biolreprod62.6.1677 (2000).
14 Lamas-Toranzo, I. *et al.* Strategies to reduce genetic mosaicism following CRISPR-mediated genome edition in bovine embryos. *Sci. Rep.* **9**, 14900. https://doi.org/10.1038/s41598-019-51366-8 (2019).
15 Bishop, T. F. & Van Eenennaam, A. L. Genome editing approaches to augment livestock breeding programs. *J. Exp. Biol.* https://doi.org/10.1242/jeb.207159 (2020).
16 Van Eenennaam, A. L., Wells, K. D. & Murray, J. D. Proposed U.S. regulation of gene-edited food animals is not fit for purpose. *NPJ Sci. Food* **3**, 3. https://doi.org/10.1038/s41538-019-0035-y (2019).
17 Hsu, P. D. *et al.* DNA targeting specificity of RNA-guided Cas9 nucleases. *Nat. Biotechnol.* **31**, 827-832. https://doi.org/10.1038/nbt.2647 (2013).
18 Doench, J. G. *et al.* Optimized sgRNA design to maximize activity and minimize off-target effects of CRISPR-Cas9. *Nat. Biotechnol.* **34**, 184-191. https://doi.org/10.1038/nbt.3437 (2016).
19 Haeussler, M. *et al.* Evaluation of off-target and on-target scoring algorithms and integration into the guide RNA selection tool CRISPOR. *Genome Biol.* **17**, 148. https://doi.org/10.1186/s13059-016-1012-2 (2016).
20 Jamal, M. *et al.* Keeping CRISPR/Cas on-Target. *Curr. Issues Mol. Biol.* **20**, 1-12. https://doi.org/10.21775/cimb.020.001 (2016).
21 Cong, L. *et al.* Multiplex genome engineering using CRISPR/Cas systems. *Science* **339**, 819-823. https://doi.org/10.1126/science.1231143 (2013).
22 Mali, P. *et al.* RNA-guided human genome engineering via Cas9. *Science* **339**, 823-826. https://doi.org/10.1126/science.1232033 (2013).
23 Pattanayak, V. *et al.* High-throughput profiling of off-target DNA cleavage reveals RNA-programmed Cas9 nuclease specificity. *Nat. Biotechnol.* **31**, 839-843. https://doi.org/10.1038/nbt.2673 (2013).
24 Jinek, M. *et al.* A programmable dual-RNA-guided DNA endonuclease in adaptive bacterial immunity. *Science* **337**, 816-821 (2012).
25 Anderson, E. M. *et al.* Systematic analysis of CRISPR-Cas9 mismatch tolerance reveals low levels of off-target activity. *J. Biotechnol.* **211**, 56-65. https://doi.org/10.1016/j.jbiotec.2015.06.427 (2015).
26 Elsik, C. G. *et al.* The genome sequence of taurine cattle: A window to ruminant biology and evolution. *Science* **324**, 522-528. https://doi.org/10.1126/science.1169588 (2009).
27 Rosen, B. D. *et al.* De novo assembly of the cattle reference genome with single-molecule sequencing. *Gigascience* https://doi.org/10.1093/gigascience/giaa021 (2020).
28 Hayes, B. J. & Daetwyler, H. D. 1000 bull genomes project to map simple and complex genetic traits in cattle: Applications and outcomes. *Annu. Rev. Anim. Biosci.* **7**, 89-102. https://doi.org/10.1146/annurev-animal-020518-115024 (2019).

29 Veres, A. *et al.* Low incidence of off-target mutations in individual CRISPR-Cas9 and TALEN targeted human stem cell clones detected by whole-genome sequencing. *Cell Stem Cell* **15**, 27-30. https://doi.org/10.1016/j.stem.2014.04.020 (2014).
30 Yang, L. *et al.* Targeted and genome-wide sequencing reveal single nucleotide variations impacting specificity of Cas9 in human stem cells. *Nat. Commun.* **5**, 5507. https://doi.org/10.1038/ncomms6507 (2014).
31 Luo, X. *et al.* Trio deep-sequencing does not reveal unexpected off-target and on-target mutations in Cas9-edited rhesus monkeys. *Nat. Commun.* **10**, 5525. https://doi.org/10.1038/s41467-019-13481-y (2019).
32 Iyer, V. *et al.* Off-target mutations are rare in Cas9-modified mice. *Nat. Methods* **12**, 479. https://doi.org/10.1038/nmeth.3408 (2015).
33 Willi, R., Smith, H. E., Wang, C., Liu, C. & Hennighausen, L. Mutation frequency is not increased in CRISPR–Cas9-edited mice. *Nat. Methods* **15**, 756-758 (2018).
34 Aach, J., Mali, P. & Church, G. M. CasFinder: Flexible algorithm for identifying specific Cas9 targets in genomes. *bioRxiv.* https://doi.org/10.1101/005074 (2014).
35 Chari, R., Yeo, N. C., Chavez, A. & Church, G. M. sgRNA Scorer 2.0: A species-independent model to predict CRISPR/Cas9 activity. *ACS Synth. Biol.* **6**, 902-904. https://doi.org/10.1021/acssynbio.6b00343 (2017).
36 Bae, S., Park, J. & Kim, J. S. Cas-OFFinder: A fast and versatile algorithm that searches for potential off-target sites of Cas9 RNA-guided endonucleases. *Bioinformatics* **30**, 1473-1475. https://doi.org/10.1093/bioinformatics/btu048 (2014).
37 Bakhtari, A. & Ross, P. J. DPPA3 prevents cytosine hydroxymethylation of the maternal pronucleus and is required for normal development in bovine embryos. *Epigenetics* **9**, 1271-1279. https://doi.org/10.4161/epi.32087 (2014).
38 Koressaar, T. & Remm, M. Enhancements and modifications of primer design program Primer3. *Bioinformatics* **23**, 1289-1291. https://doi.org/10.1093/bioinformatics/btm091 (2007).
39 Untergasser, A. *et al.* Primer3--new capabilities and interfaces. *Nucleic Acids Res.* **40**, e115. https://doi.org/10.1093/nar/gks596 (2012).
40 Li, H. Aligning sequence reads, clone sequences and assembly contigs with BWA-MEM. arXiv:1303.3997v (2013).
41 Li, H. *et al.* The Sequence Alignment/Map format and SAMtools. *Bioinformatics* **25**, 2078-2079. https://doi.org/10.1093/bioinformatics/btp352 (2009).
42 Lindsay, H. *et al.* CrispRVariants charts the mutation spectrum of genome engineering experiments. *Nat. Biotechnol.* **34**, 701-702. https://doi.org/10.1038/nbt.3628 (2016).
43 Petersen, B. *et al.* Efficient production of biallelic GGTA1 knockout pigs by cytoplasmic microinjection of CRISPR/Cas9 into zygotes. *Xenotransplantation* **23**, 338-346. https://doi.org/10.1111/xen.12258 (2016).
44 Zhang, X. *et al.* Disruption of the sheep BMPR-IB gene by CRISPR/Cas9 in in vitro-produced embryos. *Theriogenology* **91**, 163-172 e162. https://doi.org/10.1016/j.theriogenology.2016.10.025 (2017).
45 Crispo, M. *et al.* Efficient generation of Myostatin knock-out sheep using CRISPR/Cas9 Technology and microinjection into zygotes. *PLoS One* **10**, e0136690. https://doi.org/10.1371/journal.pone.0136690 (2015).

46 Tao, L. *et al.* Efficient biallelic mutation in porcine parthenotes using a CRISPR-Cas9 system. *Biochem. Biophys. Res. Commun.* **476**, 225-229 (2016).
47 Wang, Y. *et al.* Efficient generation of gene-modified pigs via injection of zygote with Cas9/sgRNA. *Sci. Rep.* **5**, 8256. https://doi.org/10.1038/srep08256 (2015).
48 Daigneault, B. W., Rajput, S., Smith, G. W. & Ross, P. J. Embryonic POU5F1 is required for expanded bovine blastocyst formation. *Sci. Rep.* **8**, 7753. https://doi.org/10.1038/s41598-018-25964-x (2018).
49 Namula, Z. *et al.* Genome mutation after the introduction of the gene editing by electroporation of Cas9 protein (GEEP) system into bovine putative zygotes. *Vitro Cell. Dev. Biol. Anim.* **55**, 598-603. https://doi.org/10.1007/s11626-019-00385-w (2019).
50 Tanihara, F. *et al.* Effects of concentration of CRISPR/Cas9 components on genetic mosaicism in cytoplasmic microinjected porcine embryos. *J. Reprod. Dev.* **65**, 209-214 (2019).
51 Tanihara, F. *et al.* Generation of a TP53-modified porcine cancer model by CRISPR/Cas9-mediated gene modification in porcine zygotes via electroporation. *PLoS ONE* **13**, e0206360. https://doi.org/10.1371/journal.pone.0206360 (2018).

TABLES AND FIGURES

Table 1. Number of zygotes reaching the blastocyst developmental stage following microinjection of either Cas9 mRNA or protein and gRNAs targeting three loci (POLLED, H11, and ZFX) on different chromosomes. *In vitro* fertilized bovine embryos were injected 18 h post insemination, and the percentage of blastocysts with Cas9-induced mutations was determined by sequence analysis. Letters that differ in the same column are significantly different ($P < 0.01$).

Cas9	gRNA	Injected Groups	Total Embryos	Total Blasts (%)	Total Analyzed	Total Mutation (%)
mRNA	control	-	492	131 (27)[a]	-	-
	POLLED	4	114	22 (19)[b]	22	16 (73)[a]
	H11	7	191	28 (15)[b]	27	19 (70)[a]
	ZFX	14	372	63 (16)[b]	62	41 (67)[a]
protein	control	-	749	250 (33)[a]	-	-
	POLLED	12	316	53 (17)[b]	42	36 (86)[b]
	H11	8	234	39 (17)[b]	39	35 (90)[b]
	ZFX	22	562	91 (16)[b]	90	73 (81)[b]

Table 2. Editing efficiencies, mosaicism, average number of alleles and percent wild type reads as determined by PacBio sequencing of 63 blastocysts following microinjection of Cas9 mRNA or protein alongside gRNAs targeting three loci (POLLED, H11, and ZFX) on different chromosomes. *In vitro* fertilized bovine embryos were injected 18 h post insemination. Letters that differ in the same column are significantly different ($P < 0.05$). SEM = standard error of the mean.

Locus	n	Cas9	% non-edited	% edited non-mosaic	% mosaic embryos	Alleles	SEM	% Wild Type	SEM
POLLED	10	mRNA	0.0	0.0	100.0	5.4[a]	±0.365	42.5[a]	±7.52
	7	protein	0.0	14.3	85.7	3.0[b]	±0.398	9.1[b]	±8.11
H11	11	mRNA	36.4	0.0	100.0	5.1[a]	±0.396	70.9[a]	±7.01
	13	protein	15.4	7.7	92.3	4.8[a]	±0.353	33.7[b]	±6.69
ZFX	12	mRNA	25.0	0	100.0	5.1[a]	±0.375	79.7[a]	±6.94
	9	protein	11.1	11.1	88.9	4.5[a]	±0.386	43.5[b]	±7.47

Table 3. Published results of genome editing targeting the NHEJ pathway in livestock zygotes, and rates of mosaicism (where available). Modified from Mclean et al [3]. [a]Transcription activator-like effector (TALE), zinc finger (ZF). [b]Nuclease delivered as plasmid, mRNA, or ribonucleoprotein (RNP) complex. [c]Cytoplasmic injection (CI) or electroporation (E). [d]*In vitro* fertilization (IVF) or parthenogenetic activation (PA). [e]normalized on the total number of edited embryos or not determined (ND).

Nuclease[a]	Reagent[b]	Animal	Delivery Method[c]	Delivery time (post IVF)/h[d]	Target locus	Edited embryos %	Mosaic embryos %[e]	Edited offspring	Mosaic offspring	Reference
TALE	mRNA	Bovine	CI	19	*ACAN* or *GDF8*	2-50	20	-	-	[7]
TALE	mRNA	Bovine	CI	24	*GDF8*	31-57	ND	3/4	1/3	[8]
TALE	mRNA	Ovine	CI	24	*GDF8*	ND	ND	1/9	0/1	[8]
ZF	Plasmid	Bovine	CI	8	*LGB*	71	100	-	-	[9]
ZF	Plasmid	Bovine	CI	18	*LGB*	83	100	-	-	[9]
ZF	mRNA	Bovine	CI	8	*LGB*	70	75	-	-	[9]
ZF	mRNA	Bovine	CI	18	*LGB*	29	ND	-	-	[9]
Cas9	Plasmid	Porcine	CI	17	*GGTA1*	ND	ND	11/12	4/11	[43]
Cas9	mRNA	Ovine	CI	0	*PDX1*	67	38	2/4	2/2	[11]
Cas9	mRNA	Ovine	CI	6	*PDX1*	60	67	-	-	[11]
Cas9	mRNA	Ovine	CI	14-15	*BMPR-*	38	86	-	-	[44]
Cas9	mRNA	Ovine	CI	22	*MSTN*	50	80	10/22	4/10	[45]
Cas9	mRNA	Porcine	CI	3 (PA)	*Tet1*	94	30	-	-	[46]
Cas9	mRNA	Porcine	CI	8 (PA)	*Tet1*	100	33	-	-	[46]
Cas9	mRNA	Porcine	CI	18 (PA)	*Tet1*	83	100	-	-	[46]
Cas9	mRNA	Porcine	CI	?	*Npc1l1*	88	ND	11/11	9/11	[47]
Cas9	RNP	Bovine	CI	10 (IVF), 1 (PA)	*POU5F1*	86	34	-	-	[48]
Cas9	RNP	Bovine	E	10	*MSTN*	27-67	75-100	-	-	[49]
Cas9	RNP	Bovine	E	15	*MSTN*	19-67	92-100	-	-	[49]
Cas9	RNP	Porcine	CI	0	*GalT*	21	100	-	-	[50]
Cas9	RNP	Porcine	CI	0 + 6	*GalT*	23	100	-	-	[50]

Cas9	RNP	Porcine	CI	6	*GalT*	28-61	82-100	-	-	[50]
Cas9	RNP	Porcine	E	12	*TP53*	73-100	30-55	6/9	5/6	[51]
Cas9	mRNA	Bovine	CI	0	*PAEP* or *CSN2*	88	30	-	-	[14]
Cas9	RNP	Bovine	CI	0		87	30	-	-	[14]
Cas9	RNP	Bovine	CI	10		83	35	-	-	[14]
Cas9	mRNA	Bovine	CI	20		84	100	-	-	[14]
Cas9	RNP	Bovine	CI	20		83	100	-	-	[14]
Cas9	mRNA	Bovine	CI	18	POLLED	73	100	-	-	This study
Cas9	RNP	Bovine	CI	18	POLLED	86	86	-	-	This study
Cas9	mRNA	Bovine	CI	18	H11	70	100	-	-	This study
Cas9	RNP	Bovine	CI	18	H11	90	92	-	-	This study
Cas9	mRNA	Bovine	CI	18	ZFX	67	100	-	-	This study
Cas9	RNP	Bovine	CI	18	ZFX	81	89	-	-	This study

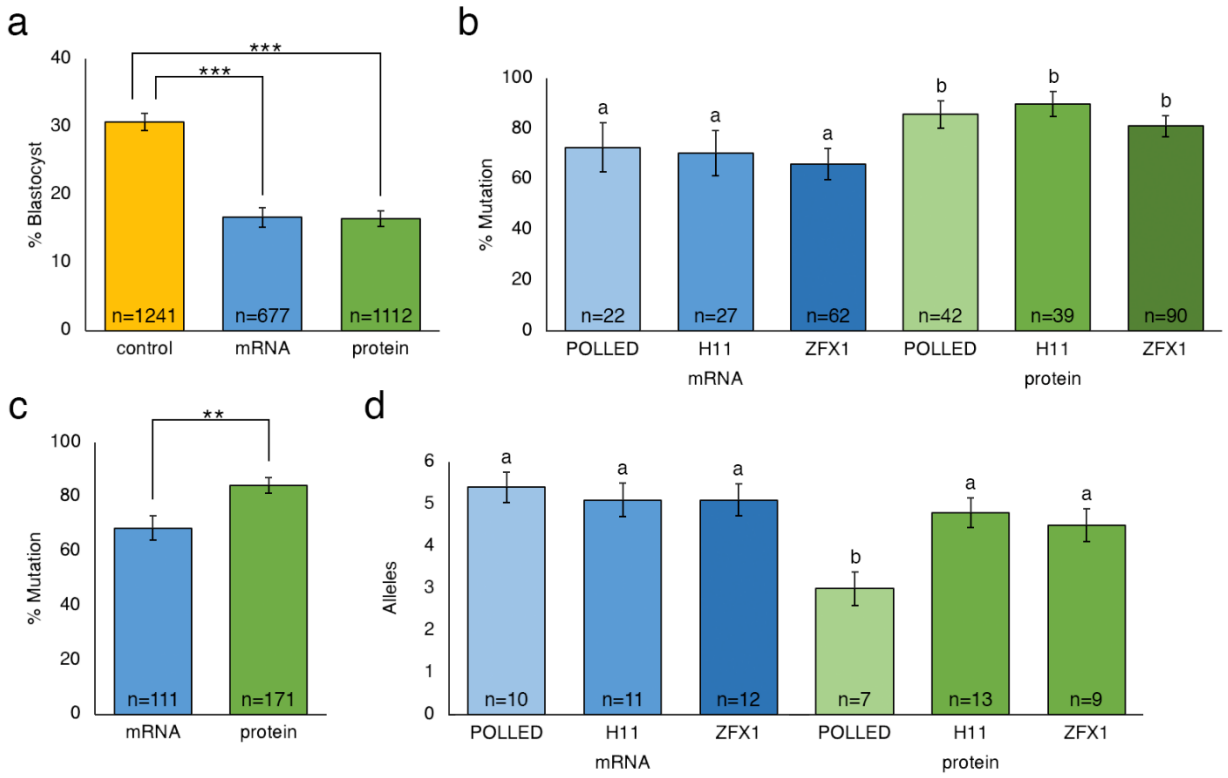

Figure 1. Percentage of uninjected control and microinjected zygotes reaching the blastocyst developmental stage following microinjection of either Cas9 mRNA or protein into in vitro fertilized bovine embryos 18 h post insemination, and percentage analyzed blastocysts with Cas9-induced mutations. (**a**) Blastocyst developmental percentage of CRISPR injected zygotes for all three loci compared to control non-injected zygotes. (**b**) Percentage of blastocysts with Cas9 mRNA or protein-induced mutation by all gRNAs targeting three loci (POLLED, H11, and ZFX) in the bovine genome. (**c**) Percentage of blastocysts with Cas9-induced mutations when injecting either Cas9 mRNA or protein alongside gRNAs targeting all three loci. (**d**) Average number of alleles per blastocyst when injecting Cas9 mRNA or protein targeting three loci (POLLED, H11, and ZFX) in the bovine genome. Error bars = standard error of the mean. $^{**}P < 0.005$; $^{***}P < 0.0005$. Columns with differing letters in the same graph are significantly different ($P < 0.05$).

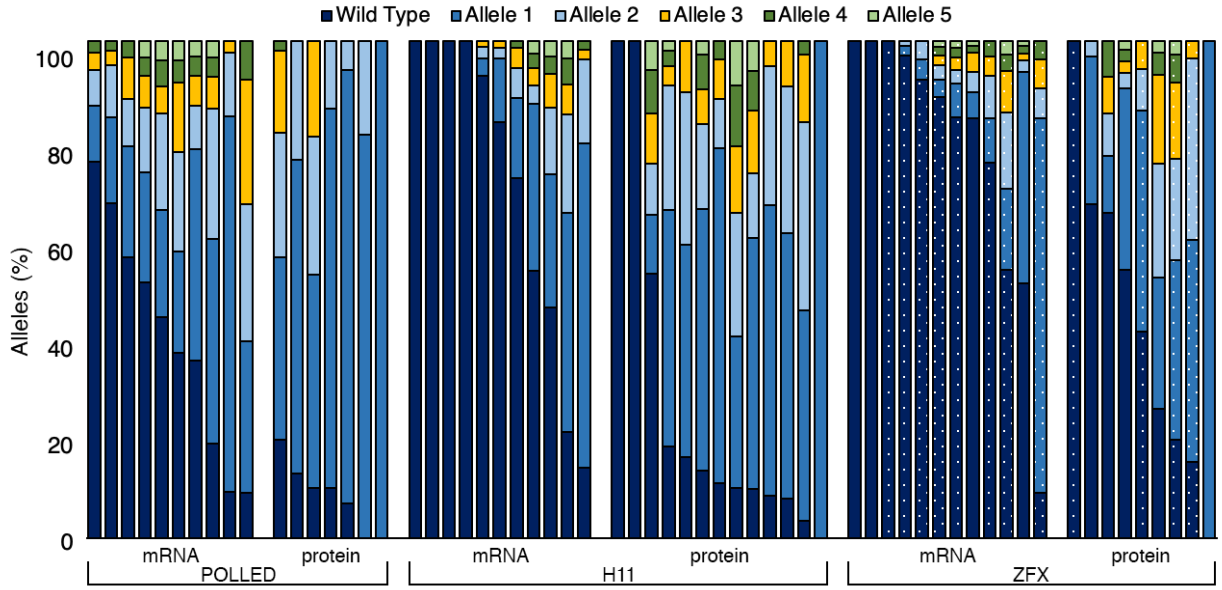

Figure 2. Bar graph depicting the percentage of alleles determined by PacBio sequencing in each of the 62 blastocysts microinjected 18 h post insemination with either Cas9 mRNA or protein and gRNAs targeting the POLLED, H11 and ZFX loci. Samples contained some combination of the wild type allele (dark blue) or an allele containing an insertion or deletion mediated by non-homologous end joining (blue, light blue, yellow, dark green and light green). For ZFX locus: dotted bars are female; solid bars are male.

SUPPLEMENTARY DATA

Supplementary Table S1. Sequence of primers used for PCR amplification of the POLLED, H11, or ZFX target regions, predicted off-target regions and gRNA sequences.

	Name	Sequence 5'- 3'	T_m (ºC)
On-Target primers	POLLEDgF	GAAGTGTGGCCGGTAGAAAA	62.8
	POLLEDgR	CGCTCCTTCCAAAACAAAAA	60.4
	H11gF	CCCCAGTGTTGTGCATGTAG	62.4
	H11gR	GTGAATGCCACTGCTGTGTT	60.4
	ZFXgF	AGCAGTGCTTCCAAACTTGAG	60.6
	ZFXgR	GATGAGAGCTTATGTAACTGTTGG	61.2
Off-Target primers	POLLEDoff1F	CAACTTCCCAGCTGTCTGC	59.0
	POLLEDoff1R	CCTTGTATGACGGCAACCTT	59.0
	POLLEDoff2F	TTCACTGCTCAAGGAAATGC	58.4
	POLLEDoff2R	AAGGCTATGAACTTGGGCTTT	58.7
	POLLEDoff3F	TTAAGCTTGGGCGTCTGAGT	59.0
	POLLEDoff3R	CATTTGGCTTTCGGCTACAC	59.0
	POLLEDoff4F	GAGGCAGATTTTGGCTTCAG	60.4
	POLLEDoff4R	GCCTCTGTCCACATGCTCTT	62.4
	POLLEDoff5F	CAGAGTCGGACACGACTGAA	62.4
	POLLEDoff5R	GCTGTGTCCTCCTAGGCTCA	64.5
	POLLEDoff6F	AAGGTTGTGTTGCATGTTGG	59.0
	POLLEDoff6R	AATTCCACTCCTCCAGAATCA	59.0
	POLLEDoff7F	TCTGGCATCACAGCATTTGT	58.4
	POLLEDoff7R	AAGATGCAAGAGACGCAGGT	60.4
	POLLEDoff8F	TTGGCCATGGACCTATGATT	59.0
	POLLEDoff8R	GGAGTGACATGGCACCTCATA	59.0
	H11off1F	GGAACAAAGATCCCACATGC	59.0
	H11off1R	GGCAGTCAAAACCCAAACAC	59.0
	H11off2F	GAATTCTGGGGGCATTGAC	60.2
	H11off2R	GAAGCCTAACCACCTCCACA	62.4
	H11off3F	CTCAGCTGGGTAACATGCAA	60.4
	H11off3R	GAGCAAATTGAGGTGGGTAA	58.4
	H11off4F	AATAAACCCCCAATTTGGCTA	56.7
	H11off4R	GGACTATCCCCTGGAGAAGG	64.5
	H11off5F	AGCCAGAGCTACTTGCTGGT	62.4
	H11off5R	AGGGTTCACTCTTGTTGGTG	60.4
	H11off6F	TGAATGGATAAGCTCCCTGTG	60.6
	H11off6R	GAATGGTCCAGTGGTTGTCC	62.4
	H11off7F	GGCAGAGAGGGAGAGAGACA	64.5
	H11off7R	TTGCCAGACATGAGAAGCAG	60.4
	H11off8F	CATGTAAATTTGGGGGTTGT	57.0
	H11off8R	CCTTCTAATTCTTGTCTGTTTGCTT	57.0
	H11off9F	CCTTGCAGATCAGCTCACAA	60.4

	H11off9R	AATGGCTTCTTCCCTCAGGA	60.4
	H11off10F	GGCTTTTTGCTCTGCTGTTT	58.4
	H11off10R	TCAGAGGACCAGATGATGGA	60.4
	H11off11F	GCACCGGGAGTTAATGTGTAA	60.6
	H11off11R	AAGGGACAAGGTGTGGACTG	62.4
	ZFXoff1F	GCAGCACCCAGAGTATCTCC	64.5
	ZFXoff1R	CCTGAGGTAGGGGGATTGTT	62.4
	ZFXoff2F	CCCCACTCCAGTACTCTTGC	64.5
	ZFXoff2R	TCCCGTGTTTTGTGTGATTT	56.3
	ZFXoff3F	TCATCTGGGCTGTTCTGAAG	60.4
	ZFXoff3R	AAGGTTCCTGCCTGCTTTTT	58.4
	ZFXoff4F	AAGGAAGGGGATTTTCTCCA	58.4
	ZFXoff4R	CACAGGGCTTTCTCCTTGAG	62.4
	ZFXoff5F	CAGCAAACTTTTCAGTGAGCA	58.7
	ZFXoff5R	TCCTCTCCTTTTTGGACATCA	58.7
Barcode Primers	BC1001F	CACATATCAGAGTGCGAGATCTCTCGAGGTT	62.0
	BC1001R	CACATATCAGAGTGCGGTAGTCGAATTCGTT	62.0
	BC1002F	ACACACAGACTGTGAGAGATCTCTCGAGGTT	62.0
	BC1002R	ACACACAGACTGTGAGGTAGTCGAATTCGTT	62.0
	BC1003F	ACACATCTCGTGAGAGAGATCTCTCGAGGTT	62.0
	BC1003R	ACACATCTCGTGAGAGGTAGTCGAATTCGTT	62.0
	BC1004F	CACGCACACACGCGCGAGATCTCTCGAGGTT	62.0
	BC1004R	CACGCACACACGCGCGGTAGTCGAATTCGTT	62.0
	BC1006F	CATATATATCAGCTGTAGATCTCTCGAGGTT	62.0
	BC1006R	CATATATATCAGCTGTGTAGTCGAATTCGTT	62.0
	BC1007F	TCTGTATCTCTATGTGAGATCTCTCGAGGTT	62.0
	BC1007R	TCTGTATCTCTATGTGGTAGTCGAATTCGTT	62.0
	BC1008F	ACAGTCGAGCGCTGCGAGATCTCTCGAGGTT	62.0
	BC1008R	ACAGTCGAGCGCTGCGGTAGTCGAATTCGTT	62.0
	BC1009F	ACACACGCGAGACAGAAGATCTCTCGAGGTT	62.0
	BC1009R	ACACACGCGAGACAGAGTAGTCGAATTCGTT	62.0
	BC1010F	ACGCGCTATCTCAGAGAGATCTCTCGAGGTT	62.0
	BC1010R	ACGCGCTATCTCAGAGGTAGTCGAATTCGTT	62.0
Guide RNA	POLLEDg1	GTCTATCCCAAAAGTGTGGG	-
	POLLEDg2	CCTGTGAAATGAAGAGTACG	-
	POLLEDg3	GATAGTTTTCTTGGTAGGC	-
	H11g1	TAGCCATAAGACTACCTAT	-
	H11g2	CTGGGGCAAAAGTCAACAGT	-
	H11g3	TGACTGGGAGGAGGAAGCCA	-
	ZFXg1	GCTAGTGGGCTAATGCCAGA	-
	ZFXg2	GCCGTCTCTCTATAGCTCAG	-
	ZFXg3	TCTTACAAGGGTGATAGTAC	-

Supplementary Table S2. Mutation rate in embryos for each guide injected 18 hours post insemination alongside Cas9 protein analyzed using PCR and Sanger sequencing. Multiple guides were tested targeting each locus to obtain highest efficiency guide. Letters that differ in the same column are significantly different ($P < 0.05$). Each chromosome independently tested using a two-by-two χ^2 test.

Allele	gRNA	Injected Embryos	Total Blastocysts (%)	Blastocysts Analyzed	Mutation Rate (%)
POLLED	1	47	15 (32[a])	13	0 (0)[a]
	2	75	14 (19[b])	13	10 (77)[b]
	3	90	25 (28[a])	25	2 (8)[a]
H11	1	65	12 (18[b])	12	10 (83)[b]
	2	45	13 (29[a])	13	5 (38)[a]
	3	47	10 (21[b])	10	6 (60)[ab]
ZFX	1	75	22 (29[a])	19	1 (5)[a]
	2	86	22 (26[a])	21	5 (24)[a]
	3	104	18 (17[b])	18	14 (78)[b]

Supplementary Table S3. List of sequencing barcodes used for PacBio sequencing for embryos injected 18 hours post insemination with gRNAs targeting the POLLED, H11, and ZFX loci alongside Cas9 mRNA or protein and corresponding reads per sample following sorting by barcode. Red highlighted samples were removed from analysis due to insufficient read count.

Locus	Cas9	Sample	Forward Barcode	Reverse Barcode	Reads per Sample
POLLED	mRNA	1	BC1001F	BC1001R	3359
		2	BC1001F	BC1002R	1049
		3	BC1001F	BC1003R	1446
		4	BC1001F	BC1004R	1075
		5	BC1001F	BC1006R	1118
		6	BC1001F	BC1007R	598
		7	BC1001F	BC1008R	472
		8	BC1001F	BC1009R	2632
		9	BC1001F	BC1010R	2662
		10	BC1002F	BC1001R	2236
	protein	1	BC1002F	BC1003R	24
		2	BC1002F	BC1004R	276
		3	BC1002F	BC1006R	812
		4	BC1002F	BC1007R	654
		5	BC1002F	BC1008R	12
		6	BC1002F	BC1009R	543
		7	BC1002F	BC1010R	1622
		8	BC1003F	BC1001R	1445
		9	BC1003F	BC1002R	417
H11	mRNA	1	BC1003F	BC1004R	3762
		2	BC1003F	BC1006R	3910
		3	BC1003F	BC1007R	1203
		4	BC1003F	BC1008R	3111
		5	BC1003F	BC1009R	3267
		6	BC1003F	BC1010R	2745
		7	BC1004F	BC1001R	7681
		8	BC1004F	BC1002R	1624
		9	BC1004F	BC1003R	1579
		10	BC1004F	BC1004R	1552
		11	BC1004F	BC1006R	1937
	protein	1	BC1004F	BC1008R	37
		2	BC1004F	BC1009R	1693
		3	BC1004F	BC1010R	8
		4	BC1006F	BC1001R	6795
		5	BC1006F	BC1002R	1197
		6	BC1006F	BC1003R	1567
		7	BC1006F	BC1004R	1926

		8	BC1006F	BC1006R	2045
Locus	**Cas9**	**Sample**	**Forward Barcode**	**Reverse Barcode**	**Reads per Sample**
H11	protein	9	BC1006F	BC1007R	1108
		10	BC1006F	BC1008R	1472
		11	BC1006F	BC1009R	1213
		12	BC1006F	BC1010R	1937
		13	BC1007F	BC1001R	2163
		14	BC1007F	BC1002R	1838
		15	BC1007F	BC1003R	1500
ZFX	mRNA	1	BC1007F	BC1007R	1630
		2	BC1007F	BC1008R	1603
		3	BC1007F	BC1009R	3973
		4	BC1007F	BC1010R	3531
		5	BC1008F	BC1001R	4960
		6	BC1008F	BC1002R	1720
		7	BC1008F	BC1003R	1521
		8	BC1008F	BC1004R	1530
		9	BC1008F	BC1006R	1039
		10	BC1008F	BC1007R	17
		11	BC1008F	BC1008R	2037
		12	BC1008F	BC1009R	1484
		13	BC1008F	BC1010R	1614
	protein	1	BC1009F	BC1001R	4954
		2	BC1009F	BC1002R	1240
		3	BC1009F	BC1003R	27
		4	BC1009F	BC1004R	1564
		5	BC1009F	BC1006R	1280
		6	BC1009F	BC1007R	1324
		7	BC1009F	BC1008R	2102
		8	BC1009F	BC1009R	2304
		9	BC1009F	BC1010R	74
		10	BC1010F	BC1001R	4014
		11	BC1010F	BC1002R	1812

Supplementary Table S4. Number of PacBio sequencing reads of PCR products from 69 blastocysts microinjected with Cas9 editing reagents targeting three loci (POLLED, H11, and ZFX) in the bovine genome, and the percentage of reads that were <700 bp read length, and additionally had a unique blastocyst sample identifying barcode.

Filtered By	Locus	Passed	Total	Percent
Read length	Total	171,545	236,518	72.5
Barcode	POLLED	22,416	26,460	84.7
Barcode	H11	58,815	78,305	75.1
Barcode	ZFX	47,236	66,780	70.7

Supplementary Table S5. Prevalence of different allele types from PacBio sequencing of targeted PCR products < 700 bp from 69 blastocysts microinjected with Cas9 editing reagents targeting three loci (POLLED, H11, and ZFX) in the bovine genome. Types of mutations = location relative to the cut site (3bp upstream of the PAM sequence): type of deletion; D = deletion, I = insertion. "Other" mutations indicate those with reads too few to report.

Locus	Total Number of Reads	Wild Type Alleles (%)	Type of Mutation				
			# of Reads (%)				
POLLED	26460	12719 (48)	**-16:7D**	**-14:11D**	**-13:4D**	**-10:1I**	**Other**
			1672 (6)	1751 (7)	6356 (24)	2250 (19)	1712 (6)
H11	78305	59302 (76)	**-14:11D**	**-13:6D**	**-12:3D**	**-10:1D**	**-8:1D**
			3246 (4)	3813 (5)	4091 (5)	5061 (6)	2792 (4)
ZFX	66780	47939 (71)	**-10:14D**	**-4:9D**	**-1:3D**	**1:1I**	**2:1I**
			4222 (6)	2998 (4)	3198 (5)	2194 (3)	6532 (10)

Supplementary Table S6. Number of alleles and percentage of each corresponding allele per sample detected at the cut-site of Cas9 mRNA or protein injected embryos. WT = percentage of reads that were wild type sequence. Alleles 1-5 are percent reads with each of the alleles found in the samples. Bold samples contained no wild type sequence. n/a = not applicable; genotypic sex was only determined for samples targeting the X chromosome.

Locus	Cas9	Sample	Sex	# of alleles	% of Reads for Each Allele					
					WT	Allele 1	Allele 2	Allele 3	Allele 4	Allele 5
POLLED	mRNA	1	n/a	5	57	22	10	8	3	-
		2	n/a	5	76	11	7	4	2	-
		3	n/a	6	37	44	9	6	4	3
		4	n/a	5	9	31	28	25	8	-
		5	n/a	6	46	22	20	6	6	4
		6	n/a	5	67	17	11	3	2	-
		7	n/a	4	9	75	13	2	-	-
		8	n/a	6	20	43	27	7	4	3
		9	n/a	6	53	23	13	7	4	3
		10	n/a	6	39	21	21	15	5	4
	protein	1	n/a	4	10	43	28	19	-	-
		2	n/a	3	13	63	24	-	-	-
		3	n/a	3	7	87	6	-	-	-
		4	n/a	3	10	76	14	-	-	-
		5	n/a	**2**	**-**	**81**	**19**	**-**	**-**	**-**
		6	n/a	5	20	37	25	16	2	-
		7	n/a	**1**	**-**	**100**	-	-	-	-
H11	mRNA	1	n/a	6	54	34	4	3	3	3
		2	n/a	6	21	44	20	6	5	4
		3	n/a	5	14	65	17	2	2	-
		4	n/a	6	46	27	14	7	3	3
		5	n/a	5	72	16	6	4	2	-
		6	n/a	4	84	13	2	1	-	-

		7	n/a	4	93	4	2	1	-	-
		8	n/a	1	100	-	-	-	-	-
Locus	**Cas9**	**Sample**	**Sex**	**# of alleles**	**% of Reads for Each Allele**					
					WT	**Allele 1**	**Allele 2**	**Allele 3**	**Allele 4**	**Allele 5**
H11	mRNA	9	n/a	1	100	-	-	-	-	-
		10	n/a	1	100	-	-	-	-	-
		11	n/a	1	100	-	-	-	-	-
	protein	1	n/a	1	100	-	-	-	-	-
		2	n/a	6	53	12	10	10	9	6
		3	n/a	6	10	50	13	13	8	6
		4	n/a	6	14	53	17	7	7	3
		5	n/a	1	100	-	-	-	-	-
		6	n/a	6	18	48	25	4	3	2
		7	n/a	4	8	54	29	9	-	-
		8	n/a	4	8	59	28	5	-	-
		9	n/a	**1**	**-**	**100**	-	-	-	-
		10	n/a	5	11	67	10	8	4	-
		11	n/a	6	10	30	25	13	12	9
		12	n/a	5	4	42	38	14	3	-
		13	n/a	4	16	43	31	10	-	-
ZFX	mRNA	1	female	5	9	75	6	6	4	-
		2	male	6	51	43	2	1	1	1
		3	female	5	76	9	9	4	3	-
		4	female	3	97	2	1	-	-	-
		5	male	6	85	5	4	4	1	1
		6	female	6	54	16	15	8	3	3
		7	male	1	100	-	-	-	-	-
		8	female	3	92	4	4	-	-	-
		9	female	6	85	7	3	3	2	2
		10	female	6	89	4	3	2	2	1

		11	female	1	100	-	-	-	-	-
		12	male	1	100	-	-	-	-	-
	protein	1	male	5	65	12	8	7	7	-
					% of Reads for Each Allele					
Locus	**Cas9**	**Sample**	**Sex**	**# of alleles**	**WT**	**Allele 1**	**Allele 2**	**Allele 3**	**Allele 4**	**Allele 5**
ZFX	protein	2	male	6	54	37	3	2	2	2
		3	female	1	100	-	-	-	-	-
		4	female	4	42	44	8	6	-	-
		5	male	6	26	26	23	18	5	2
		6	male	**1**	**-**	**100**	-	-	-	-
		7	male	3	67	30	3	-	-	-
		8	female	6	20	36	20	16	6	3
		9	female	4	15	45	36	4	-	-

Supplementary Table S7. Predicted off-target sites for each of the three guides targeting the POLLED, H11, or ZFX locus. DNA = sequence of off-target site (lower case bases are mismatches). Position is relative to the start of the bosTau8 reference genome. Total reads aligned = number of reads mapped to the off-target sequence from overlapped MiSeq data. Coverage = reads per sample per target.

Target Locus	Off-Target Chromosome	DNA	Position	Direction	Total Reads Aligned	Coverage
POLLED	2	CaTGTGAAtTGAAGAGTACc	17859417	+	301211	35X
	10	CCTcTGgAATGAAGAGTACc	23332597	-	94118	11X
	12	CCTGTGAAATGActAGTACa	57833284	+	256177	30X
	14	CCTcTGAAATGAAGAGaACc	83079285	+	85603	10X
	18	CCTGaGAAATGAAGAGgAtG	34058298	-	54877	6X
	18	CtTGTGcAAaGAAGAGTACG	46423386	-	301211	35X
	X	CCTGTGAgATGAtGAtTACG	31206746	+	430923	51X
	X	gCTGTGAAATGAAGAGgAtG	129076601	+	713874	84X
H11	1	TAGCCATAAGcaTACCaAT	3616887	+	21658	2X
	1	TAGCCATAAGtCaACaTAT	7454978	+	1022399	97X
	1	TAGCCAcAAGtCTACaTAT	12203491	-	878840	84X
	1	gAGaCATAAGACTACCcAT	111862587	+	226674	22X
	4	TAGCCATAAGAaTtCCTAa	102992457	-	249056	24X
	7	TAGCaATAAGAgTACCTAa	8578648	-	162124	15X
	7	TAGtCATAAttCTACCTAT	75383424	-	12118	1X
	7	aAGCCATAcaACTACCTAT	75200649	-	265923	25X
	8	TAGCCATcAGACTACCaAg	62416292	-	717812	68X
	10	TAGCCAaAAGACaACaTAT	59699661	+	1104588	105X
	X	TAGCaATAAGAgTAaCTAT	125300735	+	1179081	112X
ZFX	7	TCTTAaAAGGGTGATAaTAt	112332349	+	125193	13X
	12	TCTTACAgaGaTGATAGTAC	22046100	-	474201	47X
	21	aaTTACAgGGGTGATAGTAC	28506796	-	470743	47X
	21	TCTTACAAGaGTcATAGTgC	48414495	-	329628	33X
	27	TCcTAgAAGGGTGATcGTAC	8648733	-	924826	92X

Supplementary Table S8. Results for development and mutation rate from each replicate of control embryos, and groups injected 18 hours post insemination with gRNAs targeting the POLLED, H11, and ZFX loci alongside Cas9 mRNA or protein

Locus	Cas9	# Embryos	# Blastocyst	% Blastocyst	# Blastocysts evaluated	# Blastocysts With mutation	% Mutation
POLLED	mRNA	30	7	23.3	7	5	71.4
POLLED	mRNA	29	5	17.2	5	4	80
POLLED	mRNA	26	4	15.4	5	3	60
POLLED	mRNA	29	6	20.7	5	4	80
POLLED	protein	26	4	15.4	3	3	100
POLLED	protein	27	5	18.5	4	3	75
POLLED	protein	27	3	11.1	2	2	100
POLLED	protein	28	5	17.9	4	3	75
POLLED	protein	26	6	23.1	5	4	80
POLLED	protein	27	4	14.8	3	2	66.7
POLLED	protein	26	4	15.4	3	3	100
POLLED	protein	26	5	19.2	4	3	75
POLLED	protein	27	5	18.5	4	3	75
POLLED	protein	26	4	15.4	3	3	100
POLLED	protein	26	5	19.2	4	4	100
POLLED	protein	24	3	12.5	3	3	100
H11	mRNA	26	3	11.5	3	2	66.7
H11	mRNA	27	5	18.5	4	3	75
H11	mRNA	26	3	11.5	3	2	66.7
H11	mRNA	27	4	14.8	4	3	75
H11	mRNA	25	3	12	3	2	66.7
H11	mRNA	30	6	20	6	4	66.7
H11	mRNA	30	4	13.3	4	3	75
H11	protein	28	5	17.9	5	5	100
H11	protein	30	6	20	6	5	83.3
H11	protein	28	4	14.3	4	4	100
H11	protein	28	4	14.3	4	4	100

H11	protein	30	6	20	6	5	83.3
H11	protein	30	5	16.7	5	4	80
H11	protein	30	4	13.3	4	3	75
H11	protein	30	5	16.7	5	5	100
ZFX	mRNA	26	4	15.4	4	3	75
ZFX	mRNA	26	4	15.4	4	2	50
ZFX	mRNA	27	5	18.5	5	3	60
ZFX	mRNA	26	5	19.2	5	3	60
ZFX	mRNA	26	4	15.4	4	3	75
ZFX	mRNA	27	4	14.8	4	2	50
ZFX	mRNA	26	3	11.5	3	2	66.7
ZFX	mRNA	25	5	20	5	4	80
ZFX	mRNA	26	3	11.5	3	1	33.3
ZFX	mRNA	25	4	16	4	3	75
ZFX	mRNA	26	5	19.2	5	4	80
ZFX	mRNA	26	4	15.4	4	2	50
ZFX	mRNA	30	6	20	6	5	83.3
ZFX	mRNA	30	7	23.3	6	4	66.7
ZFX	protein	26	4	15.4	4	3	75
ZFX	protein	26	4	15.4	4	3	75
ZFX	protein	27	5	18.5	5	4	80
ZFX	protein	26	5	19.2	5	5	100
ZFX	protein	26	4	15.4	4	3	75
ZFX	protein	24	4	16.7	4	3	75
ZFX	protein	26	3	11.5	3	3	100
ZFX	protein	25	5	20	5	4	80
ZFX	protein	26	3	11.5	3	2	66.7
ZFX	protein	25	4	16	4	3	75
ZFX	protein	26	5	19.2	5	4	80
ZFX	protein	26	4	15.4	4	4	100
ZFX	protein	26	4	15.4	4	3	75
ZFX	protein	25	5	20	5	4	80

ZFX	protein	25	4	16	4	3	75
ZFX	protein	26	4	15.4	4	4	100
ZFX	protein	24	3	12.5	3	2	66.7
ZFX	protein	25	4	16	4	3	75
ZFX	protein	26	4	15.4	4	3	75
ZFX	protein	26	3	11.5	3	2	66.7
ZFX	protein	25	4	16	4	4	100
ZFX	protein	25	6	24	5	4	80
control	-	30	9	30	-	-	-
control	-	30	8	26.7	-	-	-
control	-	30	7	23.3	-	-	-
control	-	30	6	20	-	-	-
control	-	30	13	43.3	-	-	-
control	-	30	8	26.7	-	-	-
control	-	30	10	33.3	-	-	-
control	-	29	9	31	-	-	-
control	-	30	8	26.7	-	-	-
control	-	30	13	43.3	-	-	-
control	-	30	8	26.7	-	-	-
control	-	30	9	30	-	-	-
control	-	30	7	23.3	-	-	-
control	-	30	8	26.7	-	-	-
control	-	27	9	33.3	-	-	-
control	-	30	10	33.3	-	-	-
control	-	30	8	26.7	-	-	-
control	-	30	5	16.7	-	-	-
control	-	29	7	24.1	-	-	-
control	-	30	6	20	-	-	-
control	-	30	8	26.7	-	-	-
control	-	29	9	31	-	-	-
control	-	30	8	26.7	-	-	-
control	-	30	14	46.7	-	-	-

control	-	30	8	26.7	-	-	-
control	-	28	13	46.4	-	-	-
control	-	30	8	26.7	-	-	-
control	-	30	7	23.3	-	-	-

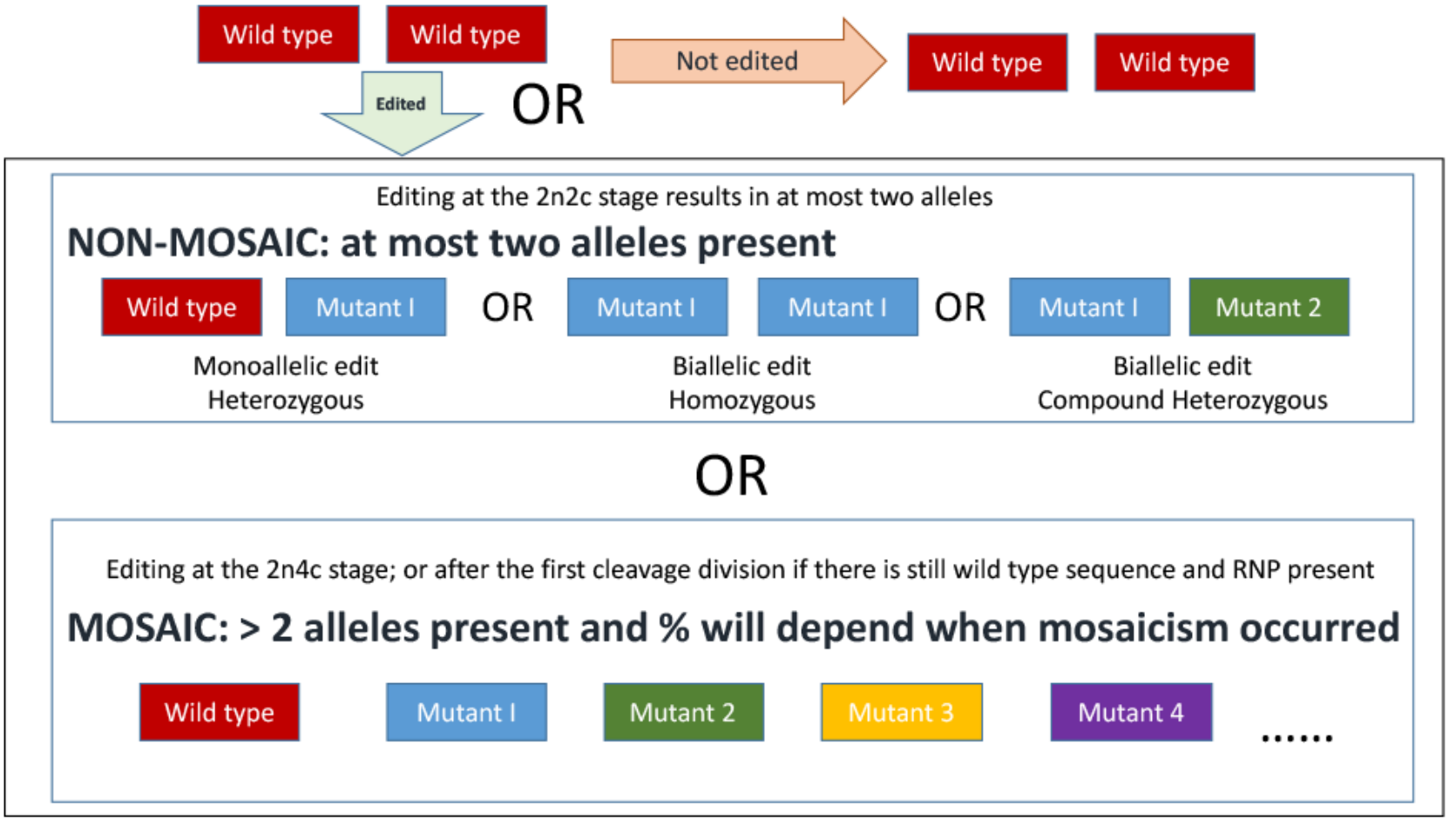

Supplementary Figure S1. Schematic representation of possible outcomes from CRISPR-mediated mutation by cytoplasmic injection of an *in vitro* fertilized embryo 18 hours post insemination. 2n = number of homologous chromosomes, i.e. diploid. 2c/4c = number of copies of chromosomes either before DNA replication or after.

Chapter 3: A deletion at the polled P_C locus alone is not sufficient to cause a polled phenotype in cattle

Sadie L. Hennig[1], Joseph R. Owen[1], Jason C. Lin[1], Bret R. McNabb[2], Alison L. Van Eenennaam[1] and James D. Murray[1,2]

[1]Department of Animal Science, University of California – Davis, Davis, CA
[2]Department of Population Health and Reproduction, School of Veterinary Medicine, University of California – Davis, Davis, CA

Corresponding Author email: jdmurray@ucdavis.edu

ABSTRACT

Dehorning is a common practice in the dairy industry, but raises animal welfare concerns. A naturally occurring genetic mutation (Pc allele) comprised of a 212 bp duplicated DNA sequence replacing a 10-bp sequence at the polled locus is associated with the hornless phenotype (polled) in cattle. To test the hypothesis that the 10 bp deletion alone is sufficient to result in polled, a CRISPR-Cas9 dual guide RNA approach was optimized to delete a 133 bp region including the 10 bp sequence. Timing of ribonucleoprotein complex injections at various hours post insemination (hpi) (6, 8, and 18 hpi) as well as *in vitro* transcribed (IVT) vs synthetic gRNAs were compared. Embryos injected 6 hpi had a significantly higher deletion rate (53%) compared to those injected 8 (12%) and 18 hpi (7%), and synthetic gRNAs had a significantly higher deletion rate (84%) compared to IVT gRNAs (53%). Embryo transfers were performed, and bovine fetuses were harvested between three and five months of gestation. All fetuses had mutations at the target site, with two of the seven having biallelic deletions, and yet they

displayed horn bud development indicating that the 10 bp deletion alone is not sufficient to result in the polled phenotype.

INTRODUCTION

Dehorning and disbudding are common practices used in the beef and dairy industry to physically remove an animal's horns. These procedures are done as preventative measures to protect both animals and handlers, however they are costly to the producer and painful to the animal. Recent studies have shown roughly half of producers that perform these procedures use some sort of pain management[1]. Taking the welfare of the animal into consideration, it has been proposed to eliminate the need for dehorning by introducing a naturally occurring hornless allele into elite horned cattle lines via genome editing to prevent horn bud development[2-5].

A dominant allele (P) at the polled locus on *Bos taurus* chromosome 1 resulting in the hornless (polled) phenotype in cattle is common among some cattle breeds, such as Angus, but is rare in breeds such as Charolais and Holstein, especially in the elite breeding lines[1]. Four variants of the polled allele have been discovered[6]. These variants are referred to as Mongolian polled (P_M)[7], Guarani polled (P_G)[8], Friesian polled (P_F)[9-11], and Celtic polled (P_C)[9,10]. This study focused on the P_C variant which is found in northern European beef breeds, such as Angus, and consists of the deletion of a 10 base pair (bp) segment replaced by a 212 bp duplication (Supplementary Fig. S1)[6,7,9]. There is no known transcript or protein associated with any polled variant, and the underlying mechanism resulting in the polled phenotype is not well understood.

Carlson et al. demonstrated that recapitulating the deletion and duplication of the P_C allele is sufficient to result in the polled phenotype. This was done by substituting the P_C allele for the p allele at the polled locus in a cell lined derived from a horned dairy bull, followed by somatic cell nuclear transfer (SCNT) cloning to produce two polled dairy bull calves[3]. A more

recent study by Young et al. demonstrated that the P_C allele from the genome edited bull created by Carlson et al. is heritable[12]. Although successful introgression of the P_C allele was achieved and calves were produced, the overall efficiency of this process was low. Due to complications associated with cloning, three of the five calves were not viable and needed to be euthanized within 24 hours of birth[3]. Only two calves survived to 60 days after birth; an overall efficiency of 7%[3]. Using a CRISPR-Cas12a gene editing approach, Schuster et al. also demonstrated the P_C allele is sufficient to result in the polled phenotype, however they too struggled with the inefficiencies of SCNT[13]. Low efficiency for producing calves via SCNT is not uncommon[14]. Due to low success, cloning would be an inefficient way to successfully integrate the Pc allele into elite genetic lines of horned cattle. An alternative option would be to edit the genome through direct injection of zygotes. Methods for producing *in vitro* fertilized (IVF) embryos have resulted in higher pregnancy rates[15-17]. Live, healthy genome edited animals produced through direct injection of bovine zygotes with either TALENs or CRISPRs have been reported at more efficient rates as well[18-20].

The previously described studies showed that the P_C allele was sufficient to induce the polled phenotype, however it is not clear whether the 212 bp duplication, the 10 bp deletion, or both are necessary to result in the polled phenotype. In this study, we directly tested whether the deletion of the 10 bp segment alone can result in the polled phenotype by creating a targeted deletion in genotypically horned embryos to see if a polled phenotype would occur. Here, we also addressed the inefficiency of SCNT by directly editing zygotes using the CRISPR-Cas9 gene editing system. A dual guide RNA (gRNA) deletion approach was taken to delete a 133 bp region including the 10 bp missing at the polled locus (Supplementary Fig. S2). Timing of zygote microinjection and type of gRNA (synthetic or *in vitro* transcribed) were analyzed to

optimize deletion efficiency. Once optimized, embryo transfers of presumptive 133 bp deletion embryos were performed, and the resulting fetuses were analyzed to determine if the deletion alone was sufficient to result in the polled phenotype.

RESULTS

Guide-RNA Testing

To optimize production of a 133 bp deletion in the bovine genome, gRNAs were designed targeting the 5' and 3' ends flanking the 10 bp sequence that is present in the horned allele but deleted in the P_C allele at the polled locus on bovine chromosome 1 (Supplementary Table S1; Supplementary Fig. S2). The top two gRNAs targeting the 5' region (btHP 5'g1 and btHP 5'g2) and 3' region (btHP 3'g1 and btHP 3'g2) were *in vitro* transcribed, incubated with Cas9 protein to form a ribonucleoprotein (RNP) complex and independently microinjected into zygotes 18 hours post insemination (hpi). Groups of non-injected embryos were also cultured and used as developmental controls. The blastocyst rates for btHP 5'g1 and btHP 5'g2 were 27% and 13%, respectively (Fig. 1a; Supplementary Table S2). Non-injected controls developed at a rate of 35%, which was significantly higher than embryos microinjected with btHP 5'g2 (P = 0.005), but not btHP 5'g1 (P = 0.49). The development between the two microinjected groups was not significantly different (P = 0.17). btHP 5'g2 was chosen to be the 5' guide due to its higher mutation rate (75%) compared to btHP 5'g1 (36%), though the difference was not statistically significant (Fig. 1c; Supplementary Table S2; P = 0.1). Of the 3' target gRNAs, there was no significant difference in development between embryos microinjected with btHP 3'g1 (35%), btHP 3'g2 (28%) and non-injected controls (35%) (Fig. 1b; Supplementary Table S2). Embryos microinjected with btHP 3'g2 had a mutation rate of 62% which was significantly higher than the mutation rate of embryos microinjected with btHP 3'g1 (6%; P = 0.006) (Fig. 1d;

Supplementary Table S2). Based on these results, btHP 3'g2 was used for the 3' gRNA, which would result in a 133 bp deletion when microinjected in tandem with btHP 5'g2 (Supplementary Fig. S3).

Timing of Guide-RNA Co-Injection and Deletion Efficiency

To test if the timing of the co-injection of the btHP 5'g2 and btHP 3'g2 RNP complexes affected deletion efficiency, zygotes were divided into three groups, and three trials of co-injections were done at 6, 8 or 18 hpi. The blastocyst rate of embryos microinjected 8 hpi (51%) was significantly higher than embryos microinjected 6 (28%; $P = 0.025$) and 18 hpi (and 23%; $P = 0.022$). Non-injected control embryos had a blastocyst rate of 35% (Fig. 2a; Supplementary Table S3). An embryo was considered positive for a mutation if a mutation was detected at either or both gRNA target sites. The individual mutation rates for each microinjected group were not significantly different (Fig. 2b; Supplementary Table S3), however the targeted 133 bp deletion rate, when both gRNAs cut in tandem, for the 6 hpi microinjected group (53%) was significantly higher when compared to either the 8 hpi (12%, $P = 0.026$) and 18 hpi (7%, $P = 0.036$) groups (Fig. 2c; Supplementary Table S3). An embryo was classified as mosaic if more than two alleles were detected. Of the embryos that had deletions, embryos microinjected 6 hpi had the lowest rate of mosaicism (24%) and only monoallelic deletions were detected (76%) (Fig. 2d; Supplementary Table S3). One embryo had a monoallelic deletion and one had a mosaic deletion in the 8 hpi microinjected group, and only one embryo with a deletion was detected in the 18 hpi group, and it was mosaic. Due to small sample sizes, it was not possible to detect a significant difference in the types of deletions when comparing times of injections.

***In Vitro* Transcribed vs Synthetic Guide-RNA Efficiency**

To determine if deletion efficiency could be further improved, a comparison of *in vitro* transcribed (IVT) and synthetic gRNAs was performed. Embryos were divided into two groups

and microinjected in three trials at 6 hpi with RNP complexes using either IVT or synthetic btHP 5'g2 and btHP 3'g2 guides. The IVT gRNA group had a development rate of 28% while the synthetic gRNA group developed at a rate of 20%. Control non-injected embryos had a development rate of 36% (Fig. 3a; Supplementary Table S4). There was a significant difference in development rates between the non-injected controls and the synthetic gRNA group (P = 0.001), but there was no difference in development between the IVT gRNA group and non-injected controls (P = 0.151) or the IVT and synthetic gRNA microinjected group (P = 0.143). The mutation rate of embryos injected with either IVT or synthetic gRNAs was not significantly different (88% and 97%, respectively; P = 0.146) (Fig. 3b; Supplementary Table S4), but there was a significant difference in 133 bp deletion rates (P = 0.006) – embryos injected with IVT gRNAs had a 53% deletion rate while synthetic gRNA injected embryos had an 84% deletion rate (Fig. 3c; Supplementary Table S4). Of the embryos that had deletions, there were significant differences in monoallelic and biallelic deletions between IVT and synthetic gRNA injected embryos, with 100% of the IVT gRNA injected embryos having monoallelic deletions compared to 34% of synthetic gRNA injected embryos ($P = 3.9 \times 10^{-7}$). Furthermore, 63% of synthetic gRNA injected embryos had biallelic deletions while none were seen in IVT gRNA injected embryos ($P = 1 \times 10^{-6}$) (Fig. 3d; Supplementary Table S4). There was no significant difference in mosaicism between either gRNA types.

Embryo Transfers

In total, 78 day-7 presumptive 133 bp deletion embryos were transferred into 28 synchronized recipients – 42 IVT gRNA edited embryos into 14 recipients and 36 synthetic gRNA edited embryos into 14 recipients (Table 1). Seven of the 14 recipients that received IVT gRNA edited embryos were pregnant at day 35 of gestation (50% pregnancy rate), with 12, possibly 13, fetuses detected (29-31% fetal development rate), but at 80 days of gestation, a total

of three recipients were pregnant (21% pregnancy rate) with five fetuses detected (12% fetal development rate). Due to the high deletion rates we discovered using synthetic gRNAs, two embryo transfers were done using synthetic gRNA edited embryos. Only one of the 14 recipients that received synthetic gRNA edited embryos was pregnant at 35 and 80 days of gestation (7% pregnancy rate) with three fetuses (8% fetal development rate) detected.

Phenotypic and Genotypic Analysis of Fetuses

Overall, a total of four IVT gRNA edited fetuses were harvested – three at 151 days of gestation and one at 123 days of gestation – (overall 10% fetal development rate), and three synthetic gRNA edited fetuses were harvested at 95 days of gestation (overall 8% fetal development rate) (Table 1). All fetuses presented small dimples in the horn bud region, indicating horn bud development had occurred (Fig. 4a-c). PCR and Sanger sequencing revealed that all had mutations at one or both target sites (Fig. 5a; Supplementary Table S5). Only two of the four IVT gRNA edited fetuses contained the 133 bp deletion, while all three synthetic gRNA edited fetuses had the deletion (Fig. 5b; Fig. 6a-c; Supplementary Table S5). Both IVT gRNA edited fetuses that had the deletion were mosaic, while only one synthetic gRNA edited fetus was mosaic, with the other two having biallelic deletions and no mosaicism detected (Fig. 5c; Supplementary Table S5). Due to small sample sizes, it was not possible to detect significant differences in the frequency of deletions or mosaicism rates between IVT or synthetic gRNA edited fetuses.

The polled (P_C) allele was detected in all three fetal PCRs for ET1 (Fig. 6a), despite the fetuses clearly presenting a horned phenotype. It was deduced that there was maternal DNA contamination, as the recipients were polled Angus (positive for the P_C allele). Extra precaution and more thorough sample washes were done for the subsequent fetal harvests to avoid future maternal DNA contamination. Recipient DNA was taken for ETs 2 and 4 as a control due to the

maternal DNA contamination issues from ET1. The P_C allele was only detected in the polled Angus recipient and no longer detected in the fetuses, demonstrating the modified sample processing protocol was effective (Fig. 6b-c). All fetuses were also tested for the P_F allele and all were negative.

Histological Analysis of Fetuses

Histological analysis of fetuses from ET1, ET2 and ET4 revealed that all fetuses had horn bud development consistent with wild type horned control fetuses in that the horn bud region had several structural differences compared to their respective frontal skin (Supplementary Fig. S4-S10). Extensive layering of vacuolated keratinocytes was seen in the horn bud region of edited fetuses (Fig. 7c, f, i) as well as horned controls (Fig. 7b, e, h). The layering of the vacuolated keratinocytes in the frontal skin of all fetuses and the horn bud region of polled controls was not as prominent. Also like the horned controls (Fig. 7e, h), nerve bundles were seen in the horn bud region of edited fetuses (Fig. 7f, i), with little to no hair follicles present (Supplementary Fig. S7 – S10). The frontal skin of all fetuses (Supplementary Fig. S7 – S10) and the horn bud region of polled controls (Fig. 7d, g; Supplementary Fig. S7 – S10) lacked nerve bundles and many hair follicles were present. In fetuses harvested at 151 days of gestation, sebaceous gland development was seen in the horn bud region of horned control fetuses (Fig. 7b) and edited fetuses (Fig. 7c), but was lacking in the frontal skin of all fetuses as well as the horn bud region of polled control fetuses (Fig. 7a; Supplementary Fig. S4 – S6).

DISCUSSION

The findings from this study demonstrated that CRISPR-Cas9 dual (synthetic) guide RNAs microinjected as RNPs 6 hpi in bovine embryos is an efficient method to obtain biallelic

deletion animals, however the 133 bp deletion, including the10 bp deletion found in the P_C allele, is not sufficient to result in the polled phenotype.

We designed gRNAs targeting the 5' and 3' regions surrounding the targeted 10 bp in genotypically horned embryos that resulted in high rates of mutation and, when co-injected, resulted in the predicted 133 bp deletion, the smallest possible deletion containing the 10 bp we could achieve based on gRNA design and mutation efficiency in embryos. We found that embryos microinjected 6 hpi with IVT gRNAs had much higher rates of deletion (53%) compared to those injected 8 or 18 hpi (12% and 7%, respectively) (Fig. 2c; Supplementary Table S3). Due to the high mutation efficiency when microinjecting embryos 6 hpi, this protocol was used for subsequent studies conducted in our lab[21-23]. It was interesting to note that the development rate for embryos microinjected 8 hpi was significantly higher compared to embryos injected 6 or 18 hpi (Fig. 2a; Supplementary Table S3). This could potentially be attributed to two factors: concentration of sperm used in IVF and higher editing efficiency. A concentration of 2×10^6 sperm per mL was used for embryos microinjected 6 or 8 hpi, while a concentration of only 1×10^6 sperm per mL was used for embryos microinjected 18 hpi. The sperm concentration was increased for embryos that were microinjected 6 or 8 hpi to help compensate for the shorter IVF incubation period. This increase in sperm concentration may have played a role in the higher blastocyst rate between embryos injected 8 hpi and 18 hpi. Embryos injected 6 hpi may have had a lower development rate because of the higher mutation and deletion rates compared to embryos microinjected 8 hpi. Our previous study[24] demonstrated an inverse correlation between development and mutation rates generally occurs, with more efficient gRNAs resulting in lower blastocyst development rates. A trend was also seen among embryos that had deletions where the earlier the embryo was microinjected post-insemination, the lower the mosaicism rate became

(Fig. 2d; Supplementary Table S3), but due to the small sample sizes in the 8 and 18 hpi groups, we were not able to detect a significant difference between the groups. This is consistent with the study by Lamas-Toranzo et al. where they microinjected gRNAs and Cas9 mRNA or RNP complexes into bovine embryos 0, 10 or 20 hpi and evaluated mosaicism levels. They found that the earlier the embryos were microinjected, the lower the mosaicism rate[25]. It is feasible that by introducing the editing reagents early, the genome can be edited before DNA replication occurs, resulting in a lower rate of mosaicism.

After synthetic gRNAs became available, we compared them with our IVT gRNAs to see if we could improve our deletion efficiency at 6 hpi. Interestingly, the synthetic gRNAs outperformed the IVT gRNAs in many respects. Although similar mutation efficiencies were seen between the two groups, a significantly higher number of embryos injected with synthetic gRNAs had the targeted 133 bp deletion (84%) compared to those injected with IVT gRNAs (53%) (Fig. 3c; Supplementary Table S4). Furthermore, of the embryos that had deletions, the majority of those injected with synthetic gRNAs had biallelic deletions, whereas only monoallelic deletions were detected in IVT injected embryos (Fig. 3d; Supplementary Table S4). This could be due to several factors. One could be quality control of gRNAs. We did not have easy access to a mass spectrometer to accurately measure product purity of the IVT gRNAs we produced ourselves. Conversely, commercial production companies can provide this with their synthetic gRNA products, allowing for a purer and more reliable product. The proprietary scaffold of synthetic gRNAs may also influence editing efficiency by potentially having a stronger or more readily forming bond with the Cas9 protein. It should also be noted that IVT gRNAs have been shown to trigger an innate immune response, whereas synthetic gRNAs do not[26]. Although this immune response was demonstrated in primary cell lines, one may question

if this could translate over into embryos. Little is known about the innate immune response in early embryos, but a recent study unveiled the existence of what can be described as the earliest observable innate immune response in the developing embryo[27]. They discovered that epithelial cells were able to detect, consume, and destroy defective cells, thus aiding in the embryo's ability to survive. We did not observe a significant difference in lethality between the IVT and synthetic gRNA injected embryos, but is an area for future research.

Although our pregnancy and fetal development rates following transfer of edited embryos to surrogate dams are not as high as those routinely obtained in industry, they are still superior to those of SCNT embryos. A total of four embryo transfers were done, two using IVT gRNA edited embryos and two with synthetic gRNA embryos. Overall, a total of four out of 28 recipients became pregnant (14% pregnancy rate) and a total of seven fetuses out of the 78 transferred embryos were recovered (development rate of 9%) (Table 1).

The results from ET1 were consistent with expectations. The conception rate of *in vivo* produced embryos is around 50%, whereas IVF produced embryos is typically between 30-40%[28]. With this decrease in conception rate of uninjected IVF produced embryos, we predicted a similar or slightly lower conception rate with IVF produced gene edited embryos, which we saw for ET1 (pregnancy rate of 33%). The pregnancy rates of embryo transfers 2-4 were much lower, ranging from 0-13%. There are several possible explanations for the low rates we experienced. At the first pregnancy check for ET2, there was a 63% pregnancy rate and a 33-38% fetal development rate, however at the second ultrasound, all but one pregnancy was lost. During the period between the first and second ultrasound check, our area was heavily affected by the Camp Fire that started in Paradise, California, with the air quality index (AQI) being in the hazardous classification for several days. It is possible this could have caused extreme stress

on the recipients, resulting in early pregnancy fetal losses. A similar phenomenon was seen in rhesus macaques at the California National Primate Research Center (CNPRC), only a mile away from where our recipients were housed. The rate of pregnancy loss in rhesus macaques exposed to the Camp Fire was almost double that of controls[29]. Although the miscarriage rate seen at the CNPRC (18%) was not as high as was seen in our recipients (50%), it is still possible the Camp Fire played a role in the fetal losses experienced in ET2.

No pregnancies were achieved from ET3. It is possible heat could have played a factor since the transfer was done in July with temperature highs between 32 – 38°C. At this time of the year, we typically see a drop in the quality of embryos produced, but we proceeded due to the availability of recipient heifers. The fourth embryo transfer was scheduled later in the year when embryo quality improved.

Although we experienced lower pregnancy and fetal development rates with our IVF edited fetuses compared to normal IVF rates, the rates were still higher than those achieved with SCNT, and no phenotypic anomalies were seen. The percent of SCNT embryos that develop to term is typically 0.5 – 5%[16] and developmental abnormalities are not uncommon[14]. It is possible that transferring 2-3 blastocysts per recipient played a role in lower pregnancy rates due to potential competition of space and resources, but taking into consideration cost, resources, reduction in experimental animal numbers and the early pregnancy termination timeline for fetal harvests, it was deemed an appropriate approach to obtain a greater number of fetuses.

All genotypically horned edited fetuses that contained the 133 bp deletion presented with a horned phenotype. Although unlikely, it is still feasible the absent 10 bp in the P_C allele is solely responsible for the polled phenotype. It is possible the 10 bp deletion could be important based on spatial architecture of the chromosomal DNA. It remains a possibility that since the 133

bp deletion we created was larger than the 10 bp deletion alone, it may have not altered the DNA in a similar manner, thus the polled phenotype did not occur.

The histological findings of our edited fetuses resembled those of horned control fetuses (Fig. 7). There were noticeable structural differences between the horn bud region of our edited fetuses and horned controls compared to the horn bud region of polled and the frontal skin of all fetuses. Among these differences were increases in layering of vacuolated keratinocytes in the horn bud region of edited and horned control fetuses as well as the presence of nerve bundles and sebaceous glands. These results are consistent with the histological findings seen in the work by others[9,30]. Thickening in the layering of vacuolated keratinocytes and the development of nerve bundles are the first notable differences in the differentiation of the horn bud region, occurring as early as 2-3 months of gestation[30]. The development of sebaceous glands in the horn bud region of horned fetuses occurs a few months later, approximately 4-5 months of gestation. Interestingly, the horn bud region of horned fetuses tends to differentiate before the forehead region as shown by a matured epidermis and the presence of sebaceous glands, with the maturation of the frontal skin being delayed about 1-2 months in comparison[30].

Overall, this study reports the creation of an optimized CRISPR-Cas9 dual guide approach. We demonstrated that the time in which gene editing reagents are introduced into the zygote has a significant effect on deletion efficiency, and the use of synthetic gRNAs results in significantly higher deletion rates as well as lower levels of mosaicism compared to IVT gRNAs. Genotypically 133 bp biallelic deletion fetuses were obtained, but all displayed horn bud development, indicating that removal of the 133 bp encompassing the 10 bp DNA sequence typically present in the horned allele of the polled locus in genotypically horned (pp) embryos is not sufficient to result in the polled phenotype. Further research is needed to fully elucidate how

the 212 bp duplication/10 bp deletion in the Celtic polled (P_C) allele results in the dominant polled phenotype.

MATERIALS AND METHODS

Animal Care

All experiments carried out utilizing animals were approved and completed in compliance with the Institutional Animal Care and Use Committee (IACUC) protocol #20746 at the University of California, Davis. Housing and maintenance of recipient cattle was conducted at the University of California, Davis Beef Barn and Feedlot.

Guide-RNA Design and Construction

Guide sequences were designed using the online tools sgRNA Scorer 2.0[31,32] and Cas-OFFinder[33] targeting the 5' and 3' regions flanking the 10 bp target at the polled locus. Guides were selected with no less than three mismatches in the guide sequence for off-target sites using the UMD3.1.1 bovine reference genome[34], and at least one mismatch in the seed region (8–11 bp upstream of the PAM sequence). Oligonucleotides were ordered from Eurofins USA (Louisville, KY) for the top four guides for construction of the gRNAs (two targeting upstream and two targeting downstream of the 10 bp target). *In vitro* transcription of the oligonucleotides was done using the AmpliScribe T7-Flash Transcription kit (Lucigen, Palo Alto, CA) and purified using the MEGAclear Transcription Clean-Up kit (Thermo Fisher, Chicago, IL) as described by Vilarino et al[35]. Synthetic guides targeting the same sequences were also ordered from Synthego (Menlo Park, CA) with the option of no modifications being done to the gRNAs. Cleavage efficiency was tested using an *in vitro* cleavage assay by combining 60 ng of PCR amplified product, 100 ng of gRNA, 150 ng of Cas9 protein (PNA Bio, Inc., Newbury Park, CA), 1 μL of 10X BSA, 1 μL of NEB Buffer 3.1 and water bringing the total volume to 10 μL in a 0.2 μL tube

and incubated at 37°C for 1 hr. The incubated product was then run on a 2% agarose gel with 5 μL of SYBR Gold (Invitrogen, Waltham, MA) at 100 V for 1 hr and visualized using a ChemiDoc-ItTS2 Imager (UVP, LLC, Upland, CA).

Embryo Production

Bovine ovaries were collected from a local processing plant and transported to the laboratory at 35–37°C in sterile saline. Cumulus-oocyte complexes (COCs) were aspirated from follicles and groups of 50 COCs were transferred to 4-well dishes containing 500 μL of maturation media (BO-IVM, IVF Bioscience, Falmouth, United Kingdom). COCs were incubated for 20–22 hr at 38.5°C in a humidified 5% CO_2 incubator. Approximately 25 oocytes per drop were fertilized in 60 μL drops of SOF-IVF with either 2×10^6 sperm per mL for an incubation period of 6 or 8 hr or 1×10^6 sperm per mL for an incubation period of 18 hr at 38.5°C in a humidified 5% CO_2 incubator using the protocol described in Bakhtari et al[36]. Sperm used was from a known genotypically horned sire. Previous preliminary experiments we conducted revealed the majority of ovaries obtained from the processing plant were from horned cattle, allowing for the creation of genotypically horned embryos. Presumptive zygotes were denuded by light vortex in SOF-HEPES medium[36] for 5 min. 25 zygotes per drop were incubated in 50 μL drops of culture media (Bo-IVC, IVF Bioscience, Falmouth, United Kingdom) at 38.5°C in a humidified atmosphere of 5% CO_2, 5% O_2 and 90% N_2 for 7–8 days from insemination.

Guide-RNA Testing

Mutation rates for each guide were determined by laser-assisted cytoplasmic injection[37] of *in vitro* fertilized embryos with 6pL of a solution containing 67 ng/μL of gRNA and 167 ng/μL of Cas9 protein (PNA Bio, Inc., Newbury Park, CA) incubated at room temperature for 30 min prior to injection to allow for the formation of RNP complexes. Injected embryos were

incubated for 7–8 days from insemination. Embryos that reached blastocyst stage were lysed in 10 μL of Epicenter DNA extraction buffer (Lucigen, Palo Alto, CA) using a Simpli-Amp Thermal Cycler (Applied Biosystems, Foster City, CA) at 65°C for 6 min, 98°C for 2 min and held at 4°C. The target region was amplified by two rounds of the polymerase chain reaction (PCR) using primers developed with Primer3 (Supplementary Table S6)[38,39]. The first round of PCR was performed on a SimpliAmp Thermal Cycler (Applied Biosystems, Foster City, CA) with 10 μL GoTAQ Green Master Mix (Promega Biosciences LLC, San Luis Obispo, CA), 0.4 μL of each primer at 10 mM and 9.2 μL of DNA in lysis buffer for 5 min at 95°C, 35 cycles of 30 s at 95°C, 30 s at 62°C, and 2 min at 72°C, followed by 5 min at 72 °C. The second round of PCR was run with 10 μL GoTAQ Green Master Mix (Promega Biosciences LLC, San Luis Obispo, CA), 4.2 μL of water, 0.4 μL of each primer at 10 mM and 5 μL of first round PCR for 3 min at 95°C, 35 cycles of 30 s at 95°C, 30 s at 60°C, and 1 min at 72°C, followed by 5 min at 72°C. Products were visualized on a 1.3% agarose gel using a ChemiDoc-ItTS2 Imager (UVP, LLC, Upland, CA), purified using the QIAquick Gel Extraction Kit (Qiagen, Valencia, CA), Sanger sequenced (GENEWIZ, LLC, South Plainfield, NJ) and analyzed with CRISP-ID[40] and Synthego's ICE analysis. Mutation rates for co-injected *in vitro* fertilized embryos were determined using the same methods described above – injecting RNP complexes of the most efficient 5' and 3' IVT or synthetic gRNAs (67 ng/μL each) and 167 ng/μL of Cas9 protein (PNA Bio, Inc., Newbury Park, CA).

Embryo Transfers

Estrus synchronization of recipient cattle began 16 days prior to the embryo transfer with the use of an intravaginal progesterone releasing device (1.38 g; Eazi-Breed CIDR; Zoetis) and the administration of gonadorelin (100 mcg; Factrel; Zoetis) done on day 0. On day 7, the CIDR was removed and prostaglandin (25 mg; Lutalyse; Zoetis) was administered. A second dose of

gonadorelin (100 mcg; Factrel; Zoetis) was given on day 9 and recipients were monitored for signs of estrus. Confirmation of recipient synchronization was done on day 15 via corpus luteum detection using a transrectal ultrasound. On day 16, embryo transfers were performed. Recipients received a caudal epidural of 100 mg 2% lidocaine (Xylocaine; Fresenius) prior to embryo transfer. Two to three blastocysts were loaded into 0.25cc straws and transferred using the non-surgical transcervical technique into the uterine horn ipsilateral to the corpus luteum. On day 35 of gestation, transrectal ultrasonography (5.0 MHz linear probe; EVO Ibex, E.I. Medical Imaging) was done to confirm pregnancies, and reconfirmed on day 80. A total of four embryo transfers were performed, and recipients were resynchronized for subsequent embryo transfers if they did not become pregnant from prior embryo transfers.

Phenotypic and Genotypic Analysis of Fetuses

Recipient cattle were slaughtered between 95 – 151 days of gestation via penetrating captive bolt and subsequent exsanguination. The fetuses were retrieved from the uterine horns, and horn bud phenotyping was performed by the large animal veterinarian onsite. Fetal liver and tail samples were taken for later genotypic analysis, and the frontal skin and horn bud regions were taken for histological analysis. Recipient muscle tissue was also taken for experimental controls. All samples were washed three times in PBS before collection.

To determine fetal genotypes, DNA was extracted from tissue samples using the DNeasy Blood & Tissue Kit (Qiagen, Valencia, CA) and PCR amplified with the 2nd round primers used for gRNA testing. PCR was done using a SimpliAmp Thermal Cycler (Applied Biosystems, Foster City, CA) with 12.5 μL GoTAQ Green Master Mix (Promega Biosciences LLC, San Luis Obispo, CA), 1 μL of each primer at 10 mM, 9.5 μL of water and 100 ng of DNA for 5 min at 95°C, 35 cycles of 30 s at 95°C, 30 s at 60°C, and 1 min at 72°C, followed by 5 min at 72°C. Products were visualized on a 1.3% agarose gel using a ChemiDoc-ItTS2 Imager (UVP, LLC,

Upland, CA), purified using the QIAquick Gel Extraction Kit (Qiagen, Valencia, CA), Sanger sequenced (GENEWIZ, LLC, South Plainfield, NJ) and analyzed with CRISP-ID[40] and Synthego's ICE analysis. Fetuses were also tested for the P_F allele using the same PCR protocol with a modified anneal and extension temp for the P_F primers given in Supplementary Table S6. The P_M and P_G alleles were not tested for as they were not applicable based on the breeds of cattle used to produce the fetuses.

Histological Analysis of Fetuses

Fetal horn bud and frontal skin tissue samples were fixed in 4% paraformaldehyde at 4°C for 18 hr, washed 3x in phosphate-buffered saline (PBS) on a rocker for 30 min and placed in 70% ethanol. They were subsequently processed in a vacuum infiltration processor (Sakura Tissue-Tek VIP 5, Torrance, CA) where they were dehydrated in a graded ethanol series and cleared with xylene. Samples were then embedded in paraffin blocks and 5 µm microtome sections were cut (Leica RM2255, Leica Biosystems, Buffalo Grove, IL) and stained with hematoxylin and eosin. Digital images were obtained with an Echo Revolve (Discover Echo Inc., San Diego, CA) microscope.

Statistical Analysis

Comparison between blastocyst and fetal development, mutation and deletion rates were evaluated using logistic regression models created with the glm "general linear model" function in R with gRNA, gRNA type, and time of injection modeled as fixed effects. Differences were considered significant when $P < 0.05$.

ACKNOWLEDGEMENTS

The authors wish to thank Ashley Young and Rebecca Ozeran for their help in the collection and transport of ovaries from the processing plant to UC Davis. This project was

supported in part by the USDA Regional Research Project W4171: Germ Cell and Embryo Development and Manipulation for the Improvement of Livestock, the Agricultural Experiment Station of the University of California, the Russell L. Rustici Rangeland and Cattle Research Endowment and the Henry A. Jastro Research Fellowship in the College of Agricultural and Environmental Science at UC Davis, and the National Institute for Food and Agriculture National Needs Graduate and Postgraduate Fellowship no. 2017-38420-26790 from the U.S. Department of Agriculture.

AUTHOR'S CONTRIBUTION

SLH performed the experiments with feedback and input from JDM and ALV. SLH, JRO and JCL participated in sample processing and data analysis. BRM performed embryo transfers. SLH and JDM wrote the manuscript with suggestions from all the co-authors. All authors read and approved the final version.

COMPETING INTERESTS

The authors declare no competing interests.

DATA AVAILABILITY

Data generated and analyzed during this study are included in this published article and its Supplementary Information file.

REFERENCES

1 Winder, C. B. *et al.* Practices for the disbudding and dehorning of dairy calves by veterinarians and dairy producers in Ontario, Canada. *J. Dairy Sci.* **99**, 10161-10173. https://doi.org/10.3168/jds.2016-11270 (2016).

2 Tan, W. *et al.* Efficient nonmeiotic allele introgression in livestock using custom endonucleases. *Proc. Natl. Acad. Sci. USA* **110**, 16526-16531. https://doi.org/10.1073/pnas.1310478110 (2013).

3 Carlson, D. F. *et al.* Production of hornless dairy cattle from genome-edited cell lines. *Nat. Biotechnol.* **34**, 479-481. https://doi.org/10.1038/nbt.3560 (2016).

4 Mueller, M. L., Cole, J. B., Sonstegard, T. S. & Van Eenennaam, A. L. Simulation of introgression of the *POLLED* allele into the Jersey breed via conventional breeding vs. gene editing. *Transl. Anim. Sci.* **2**, S57-S60. https://doi.org/10.1093/tas/txy054 (2018).
5 Mueller, M. L., Cole, J. B., Sonstegard, T. S. & Van Eenennaam, A. L. Comparison of gene editing versus conventional breeding to introgress the POLLED allele into the US dairy cattle population. *J. Dairy Sci.* **102**, 4215-4226. https://doi.org/10.3168/jds.2018-15892 (2019).
6 Schafberg, R. & Swalve, H. H. The history of breeding for polled cattle. *Livest. Sci.* **179**, 54-70. https://doi.org/10.1016/j.livsci.2015.05.017 (2015).
7 Medugorac, I. *et al.* Whole-genome analysis of introgressive hybridization and characterization of the bovine legacy of Mongolian yaks. *Nat. Genet.* **49**, 470-475. https://doi.org/10.1038/ng.3775 (2017).
8 Utsunomiya, Y. T. *et al.* Hornless Nellore cattle (Bos indicus) carrying a novel 110 kbp duplication variant of the polled locus. *Anim. Genet.* **50**, 187-188. https://doi.org/10.1111/age.12764 (2019).
9 Allais-Bonnet, A. *et al.* Novel insights into the bovine polled phenotype and horn ontogenesis in Bovidae. *PLoS One* **8**, e63512. https://doi.org/10.1371/journal.pone.0063512 (2013).
10 Medugorac, I. *et al.* Bovine polledness--an autosomal dominant trait with allelic heterogeneity. *PLoS One* **7**, e39477. https://doi.org/10.1371/journal.pone.0039477 (2012).
11 Rothammer, S. *et al.* The 80-kb DNA duplication on BTA1 is the only remaining candidate mutation for the polled phenotype of Friesian origin. *Genet. Sel. Evol.* **46**, 1-5. https://doi.org/10.1186/1297-9686-46-44 (2014).
12 Young, A. E. *et al.* Genomic and phenotypic analyses of six offspring of a genome-edited hornless bull. *Nat. Biotechnol.* **38**, 225-232. https://doi.org/10.1038/s41587-019-0266-0 (2020).
13 Schuster, F. *et al.* CRISPR/Cas12a mediated knock-in of the Polled Celtic variant to produce a polled genotype in dairy cattle. *Sci. Rep.* **10**, 13570. https://doi.org/10.1038/s41598-020-70531-y (2020).
14 Akagi, S., Geshi, M. & Nagai, T. Recent progress in bovine somatic cell nuclear transfer. *Anim. Sci. J.* **84**, 191-199. https://doi.org/10.1111/asj.12035 (2013).
15 Morotti, F. *et al.* Pregnancy rate and birth rate of calves from a large-scale IVF program using reverse-sorted semen in Bos indicus, Bos indicus-taurus, and Bos taurus cattle. *Theriogenology* **81**, 696-701. https://doi.org/10.1016/j.theriogenology.2013.12.002 (2014).
16 Heyman, Y. *et al.* Frequency and occurrence of late-gestation losses from cattle cloned embryos. *Biol. Reprod.* **66**, 6-13. https://doi.org/10.1095/biolreprod66.1.6 (2002).
17 Wilmut, I. *et al.* Somatic cell nuclear transfer. *Nature* **419**, 583-586. https://doi.org/10.1038/nature01079 (2002).
18 Proudfoot, C. *et al.* Genome edited sheep and cattle. *Transgenic Res.* **24**, 147-153. https://doi.org/10.1007/s11248-014-9832-x (2015).
19 Park, K. E. *et al.* One-step homology mediated CRISPR-Cas editing in zygotes for generating genome edited cattle. *CRISPR J.* **3**, 523-534. https://doi.org/10.1089/crispr.2020.0047 (2020).

20 Wei, J. *et al.* Cattle with a precise, zygote-mediated deletion safely eliminate the major milk allergen beta-lactoglobulin. *Sci. Rep.* **8**, 7661. https://doi.org/10.1038/s41598-018-25654-8 (2018).
21 Owen, J. R. *et al.* Harnessing endogenous repair mechanisms for targeted gene knock-in of bovine embryos. *Sci. Rep.* **10**, 16031. https://doi.org/10.1038/s41598-020-72902-x (2020).
22 Owen, J. R. *et al.* One-step generation of a targeted knock-in calf using the CRISPR-Cas9 system in bovine zygotes. *BMC Genomics* **22**, 118. https://doi.org/10.1186/s12864-021-07418-3 (2021).
23 Owen, J. R. *et al.* Improved rate of targeted gene knock-in of in-vitro fertilized bovine embryos. *Proc. Assoc. Advmt. Anim. Breed. Genet.* **23**, 7-10 (2019).
24 Hennig, S. L. *et al.* Evaluation of mutation rates, mosaicism and off target mutations when injecting Cas9 mRNA or protein for genome editing of bovine embryos. *Sci. Rep.* **10**, 22309. https://doi.org/10.1038/s41598-020-78264-8 (2020).
25 Lamas-Toranzo, I. *et al.* Strategies to reduce genetic mosaicism following CRISPR-mediated genome edition in bovine embryos. *Sci. Rep.* **9**, 14900. https://doi.org/10.1038/s41598-019-51366-8 (2019).
26 Wienert, B., Shin, J., Zelin, E., Pestal, K. & Corn, J. E. In vitro-transcribed guide RNAs trigger an innate immune response via the RIG-I pathway. *PLoS Biol.* **16**, e2005840. https://doi.org/10.1371/journal.pbio.2005840 (2018).
27 Hoijman, E. *et al.* Cooperative epithelial phagocytosis enables error correction in the early embryo. *Nature* **590**, 618-623. https://doi.org/10.1038/s41586-021-03200-3 (2021).
28 Rizos, D. *et al.* Consequences of in vitro culture conditions on embryo development and quality. *Reprod. Domest. Anim.* **43 Suppl 4**, 44-50. https://doi.org/10.1111/j.1439-0531.2008.01230.x (2008).
29 Willson, B. E. *et al.* Effects of the 2018 Camp Fire on birth outcomes in non-human primates: Case-control study. *Reprod. Toxicol.* **105**, 128-135. https://doi.org/10.1016/j.reprotox.2021.08.005 (2021).
30 Wiener, D. J., Wiedemar, N., Welle, M. M. & Drogemuller, C. Novel features of the prenatal horn bud development in cattle (Bos taurus). *PLoS One* **10**, e0127691. https://doi.org/10.1371/journal.pone.0127691 (2015).
31 Aach, J., Mali, P. & Church, G. M. CasFinder: Flexible algorithm for identifying specific Cas9 targets in genomes. *bioRxiv*. https://doi.org/10.1101/005074 (2014).
32 Chari, R., Yeo, N. C., Chavez, A. & Church, G. M. sgRNA Scorer 2.0: A species-independent model to predict CRISPR/Cas9 activity. *ACS Synth. Biol.* **6**, 902-904. https://doi.org/10.1021/acssynbio.6b00343 (2017).
33 Bae, S., Park, J. & Kim, J. S. Cas-OFFinder: a fast and versatile algorithm that searches for potential off-target sites of Cas9 RNA-guided endonucleases. *Bioinformatics* **30**, 1473-1475. https://doi.org/10.1093/bioinformatics/btu048 (2014).
34 Elsik, C. G. *et al.* The genome sequence of taurine cattle: a window to ruminant biology and evolution. *Science* **324**, 522-528. https://doi.org/10.1126/science.1169588 (2009).
35 Vilarino, M. *et al.* CRISPR/Cas9 microinjection in oocytes disables pancreas development in sheep. *Sci. Rep.* **7**, 17472. https://doi.org/10.1038/s41598-017-17805-0 (2017).

36 Bakhtari, A. & Ross, P. J. DPPA3 prevents cytosine hydroxymethylation of the maternal pronucleus and is required for normal development in bovine embryos. *Epigenetics* **9**, 1271-1279. https://doi.org/10.4161/epi.32087 (2014).
37 Bogliotti, Y. S., Vilarino, M. & Ross, P. J. Laser-assisted cytoplasmic microinjection in livestock zygotes. *J. Vis. Exp.* https://doi.org/10.3791/54465 (2016).
38 Koressaar, T. & Remm, M. Enhancements and modifications of primer design program Primer3. *Bioinformatics* **23**, 1289-1291. https://doi.org/10.1093/bioinformatics/btm091 (2007).
39 Untergasser, A. *et al.* Primer3--new capabilities and interfaces. *Nucleic Acids Res.* **40**, e115. https://doi.org/10.1093/nar/gks596 (2012).
40 Dehairs, J., Talebi, A., Cherifi, Y. & Swinnen, J. V. CRISP-ID: decoding CRISPR mediated indels by Sanger sequencing. *Sci. Rep.* **6**, 28973. https://doi.org/10.1038/srep28973 (2016).

TABLES AND FIGURES

Table 1. Results from embryo transfers (ETs) of zygotes injected 6 hr post insemination with *in vitro* transcribed (IVT) or synthetic gRNAs and Cas9 protein. Two to three blastocysts were transferred per recipient. Pregnancies were confirmed on 35 and 80 days of gestation.

ET	gRNA Type	Blastocysts Transferred	Recipients	35 Days of Gestation		80 Days of Gestation		Fetuses Harvested (%)
				Pregnant (%)	**Fetuses Detected (%)**	**Pregnant (%)**	**Fetuses Detected (%)**	
1	IVT	18	6	2 (33)	4 (22)	2 (33)	4 (22)	3 (17)
2	IVT	24	8	5 (63)	8 - 9 (33 - 38)	1 (13)	1 (4)	1 (4)
Total	**IVT**	**42**	**14**	**7 (50)**	**12 - 13 (29 - 31)**	**3 (21)**	**5 (12)**	**4 (10)**
3	Synthetic	12	4	0 (0)	0 (0)	-	-	-
4	Synthetic	24	10	1 (10)	3 (8)	1 (7)	3 (13)	3 (13)
Total	**Synthetic**	**36**	**14**	**1 (7)**	**3 (8)**	**1 (7)**	**3 (8)**	**3 (8)**
Overall Total	**IVT & Synthetic**	**78**	**28**	**8 (29)**	**15 – 16 (19 - 21)**	**4 (14)**	**8 (10)**	**7 (9)**

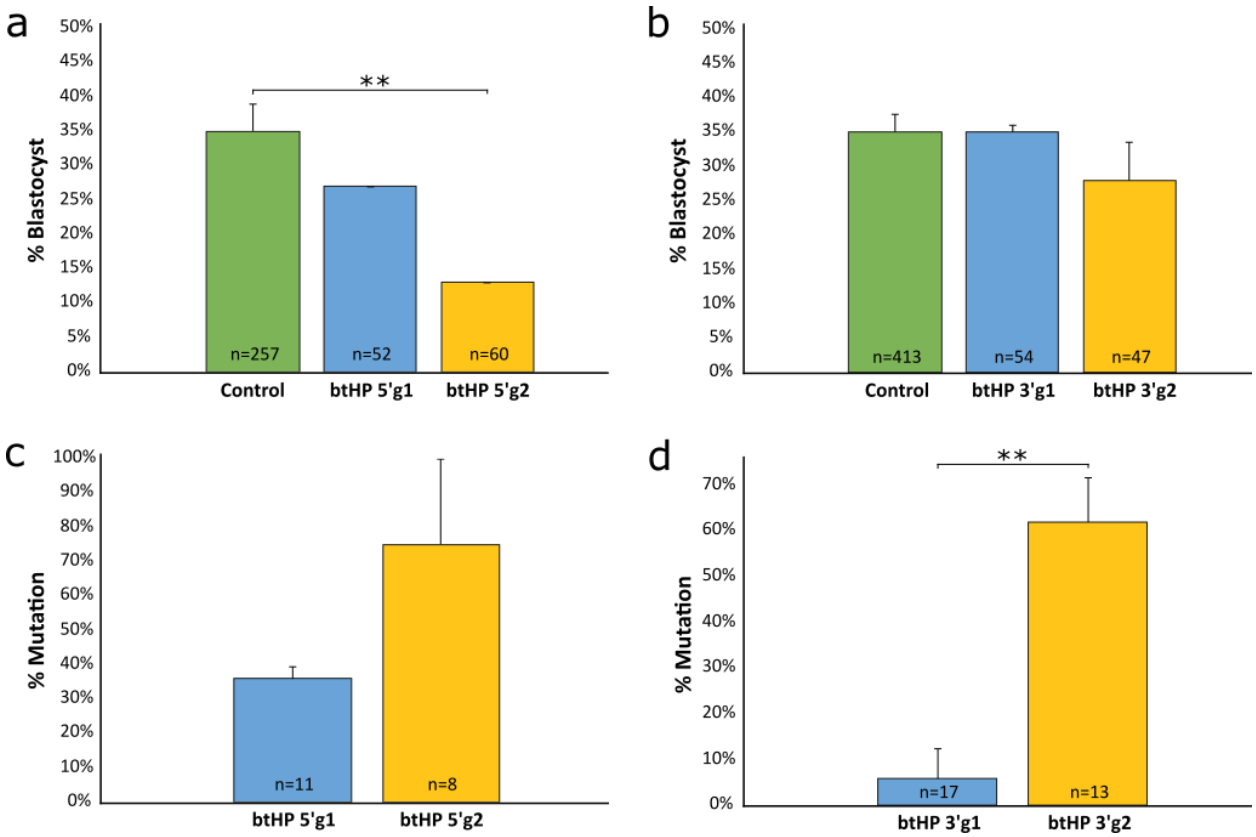

Figure 1. Non-injected and microinjected zygote development rates to the blastocyst stage and mutation efficiencies following microinjection of Cas9 protein and *in vitro* transcribed (IVT) test gRNAs targeting the 5' and 3' regions flanking the 10 bp on the polled locus at 18 hours post insemination. (**a**) Blastocyst development rate of microinjected and non-injected control embryos (green) when targeting the 5' and (**b**) 3' regions flanking the 10 bp target region. (**c**) Mutation rates in embryos injected with Cas9 and gRNAs targeting the 5' and (**d**) 3' regions flanking the 10 bp target region. Error bars = SEM. $^{**}P < 0.01$.

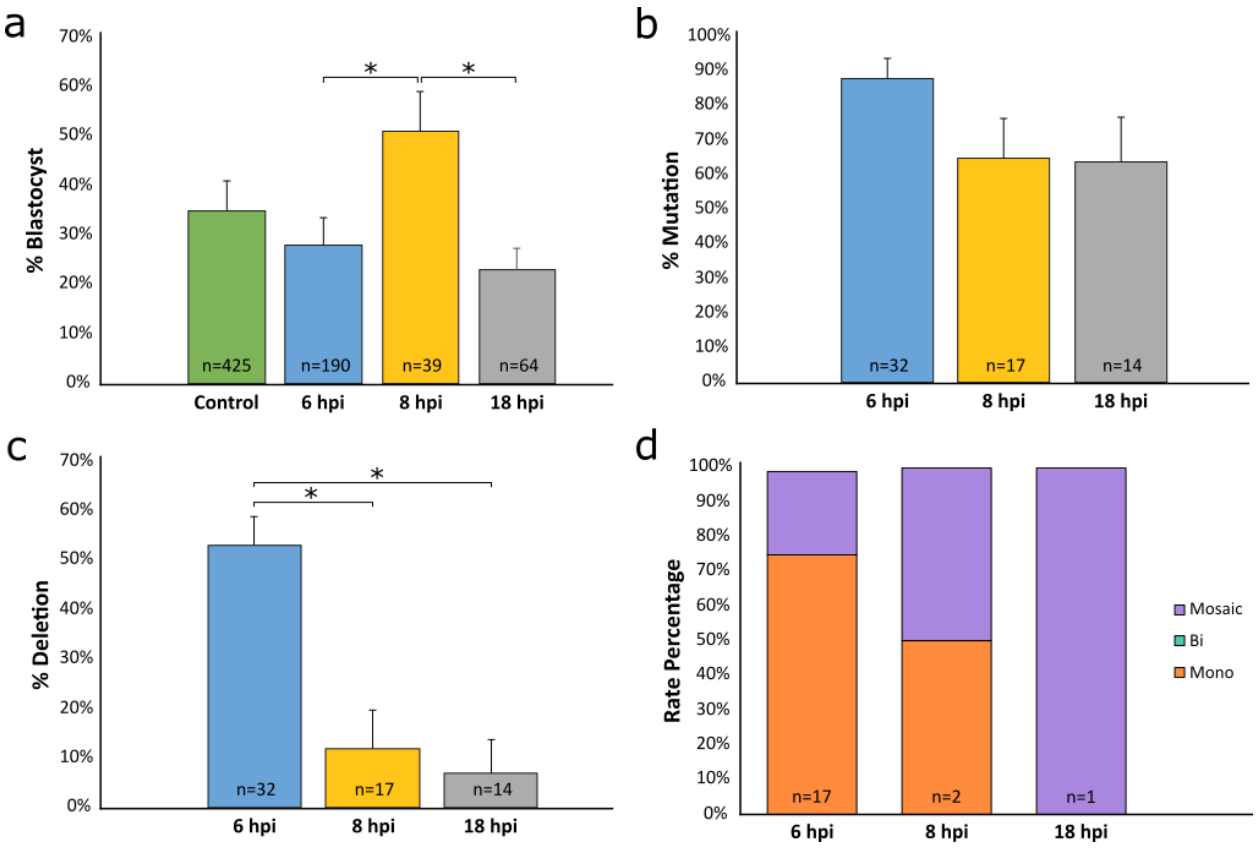

Figure 2. Non-injected and microinjected zygote blastocyst development rates and mutation and deletion efficiencies following microinjection of Cas9 protein and *in vitro* transcribed (IVT) gRNAs btHP 5'g2 and btHP 3'g2 at 6, 8 or 18 hours post insemination (hpi). (**a**) Blastocyst development rate of microinjected and non-injected control embryos (green). (**b**) Mutation rates and (**c**) deletion rates in embryos injected with Cas9 protein, btHP 5'g2 and btHP 3'g2. A blastocyst was considered mutated if a mutation was detected at one or both target sites. (**d**) Frequency of types of deletions detected in microinjected embryos. Mono = monoallelic (orange); Bi = biallelic (aqua), Mosaic (purple). Error bars = SEM. **P* < 0.05.

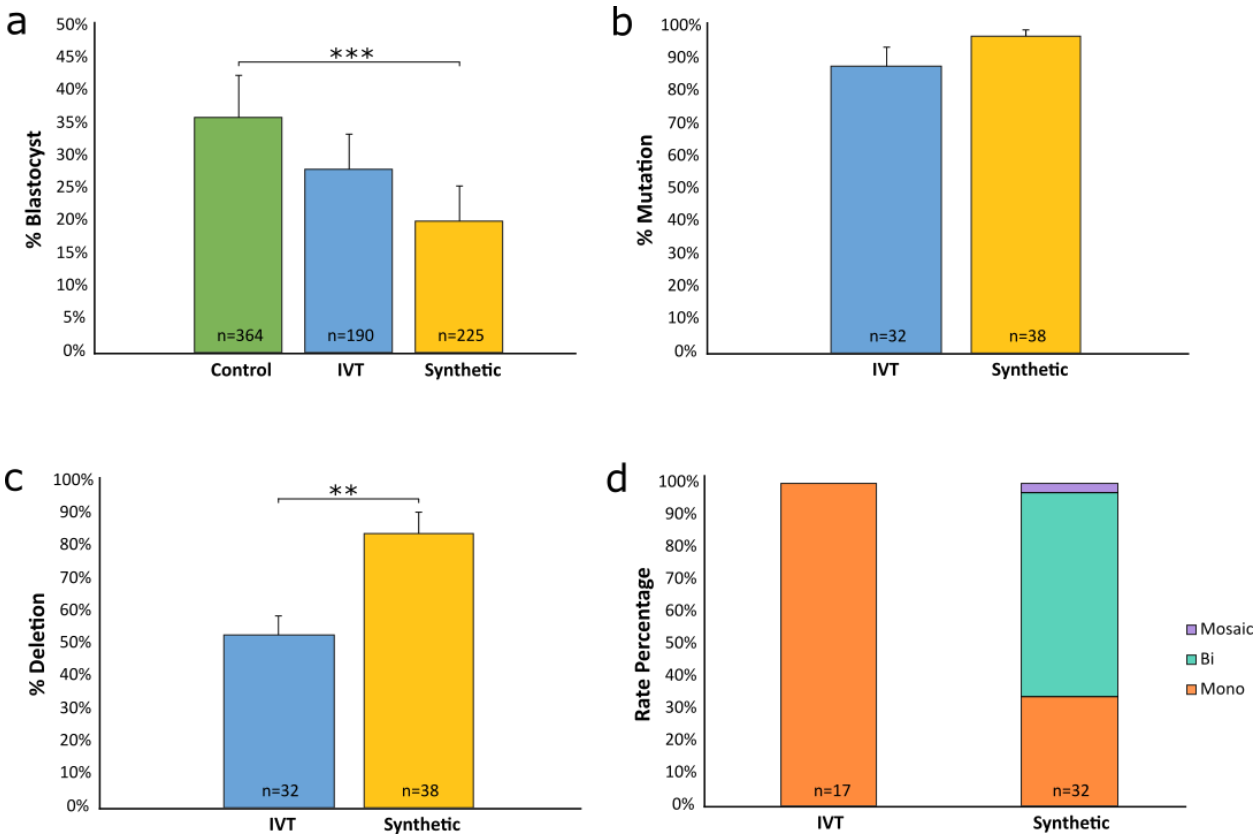

Figure 3. Non-injected and microinjected zygote blastocyst development rates and mutation and deletion efficiencies following microinjection of Cas9 protein and either *in vitro* transcribed (IVT) or synthetic gRNAs btHP 5'g2 and btHP 3'g2 at 6 hours post insemination. (**a**) Blastocyst development rate of microinjected and non-injected control embryos (green). (**b**) Mutation rates and (**c**) deletion rates in embryos injected with Cas9 protein, btHP 5'g2 and btHP 3'g2. A blastocyst was considered mutated if a mutation was detected at one or both target sites. (**d**) Frequency of types of deletions detected in microinjected embryos. Mono = monoallelic (orange); Bi = biallelic (aqua), Mosaic (purple). Error bars = SEM. $^{**}P < 0.01$; $^{***}P < 0.001$.

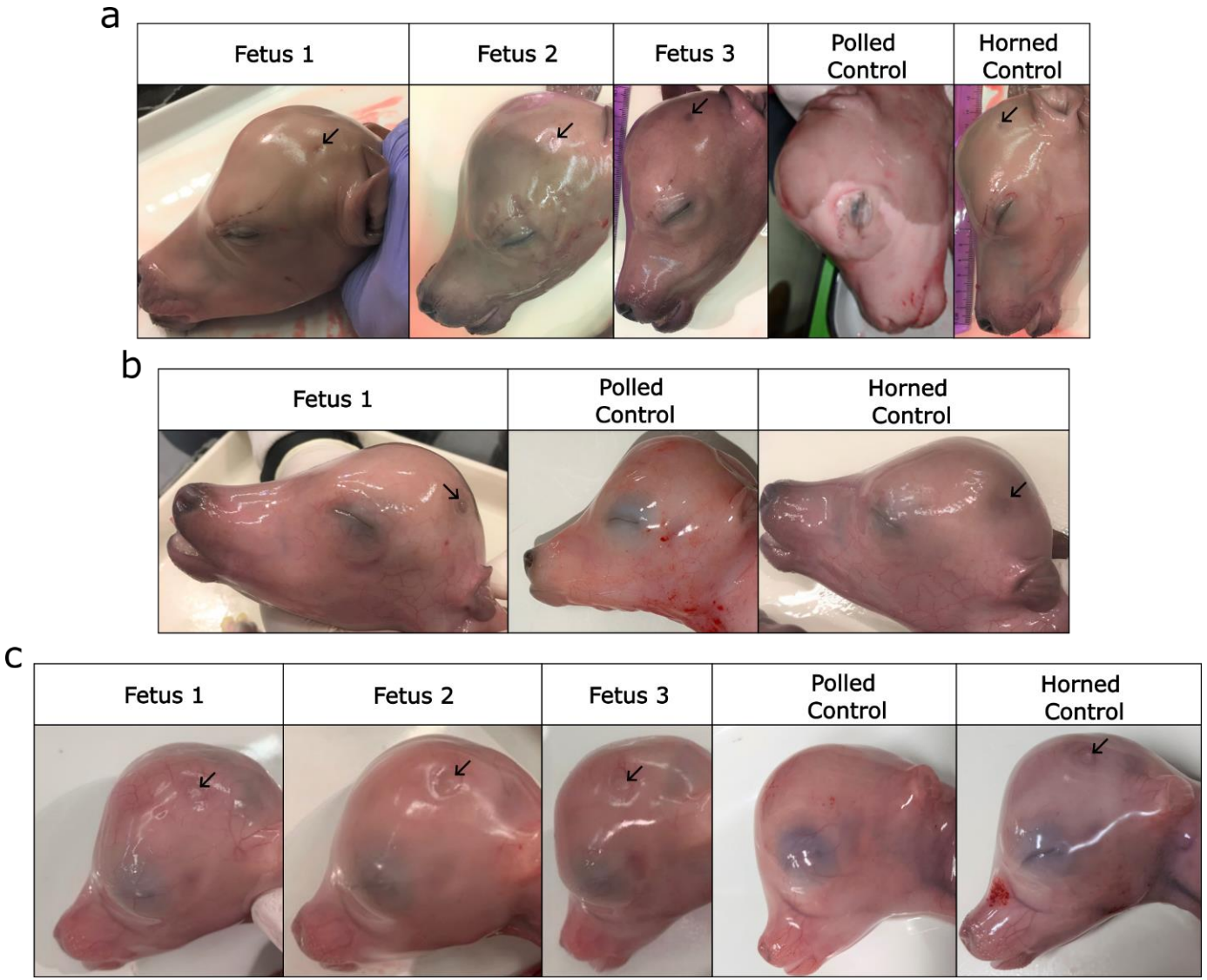

Figure 4. Phenotypic analysis of fetuses harvested from embryo transfers (ETs). (**a**) Fetuses from ET 1, (**b**) 2 and (**c**) 4 along with aged matched horned and polled controls. Fetuses were harvested at 151, 123 and 95 days of gestation, respectively. Horn bud development can be seen by the presence of small dimples (black arrows).

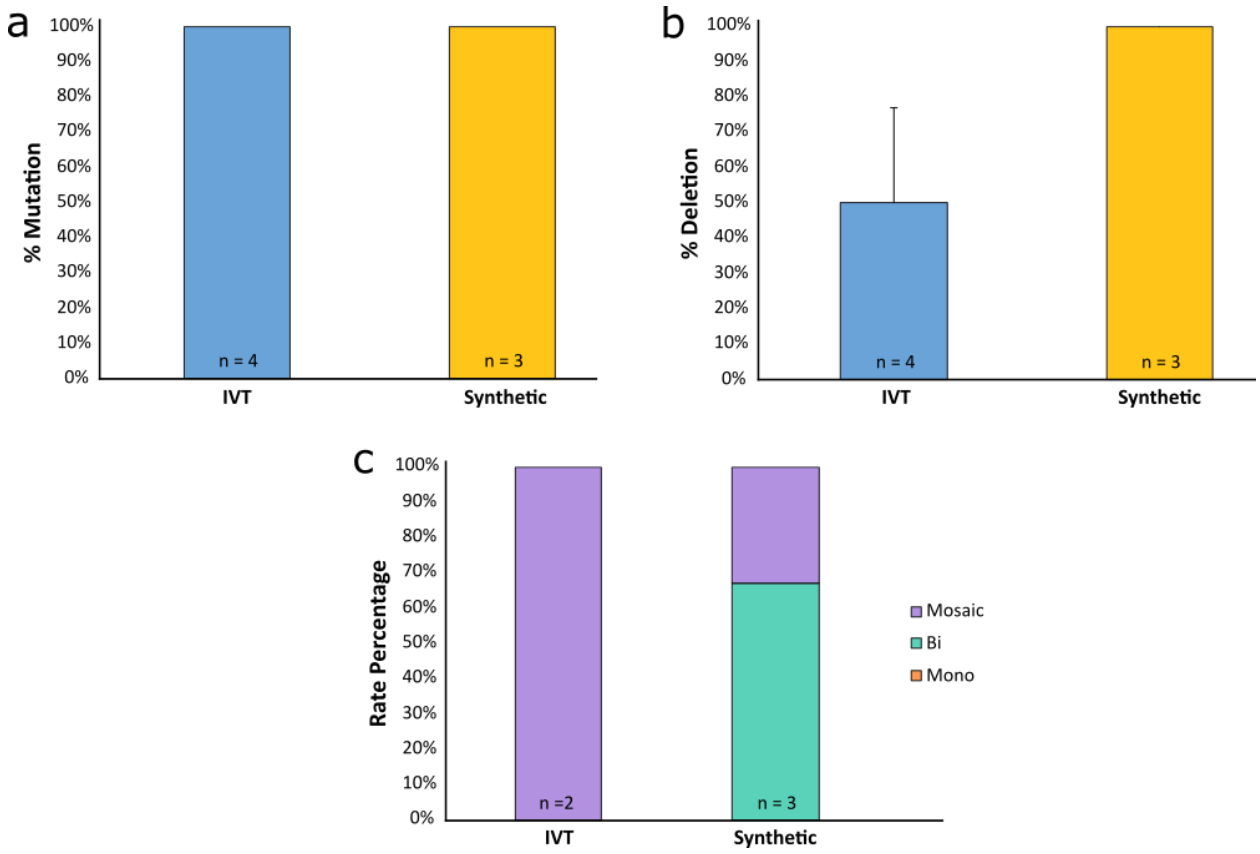

Figure 5. Mutation and deletion efficiencies of fetuses harvested from *in vitro* transcribed (IVT) and synthetic gRNA edited embryo transfers. (**a**) Mutation rates and (**b**) deletion rates in fetuses edited with Cas9 protein and either IVT or synthetic gRNAs btHP 5'g2 and btHP 3'g2. A fetus was considered mutated if a mutation was detected at one or both target sites. (**c**) Frequency of types of deletions detected in edited fetuses. Mono = monoallelic (orange); Bi = biallelic (aqua), Mosaic (purple). Error bars = SEM.

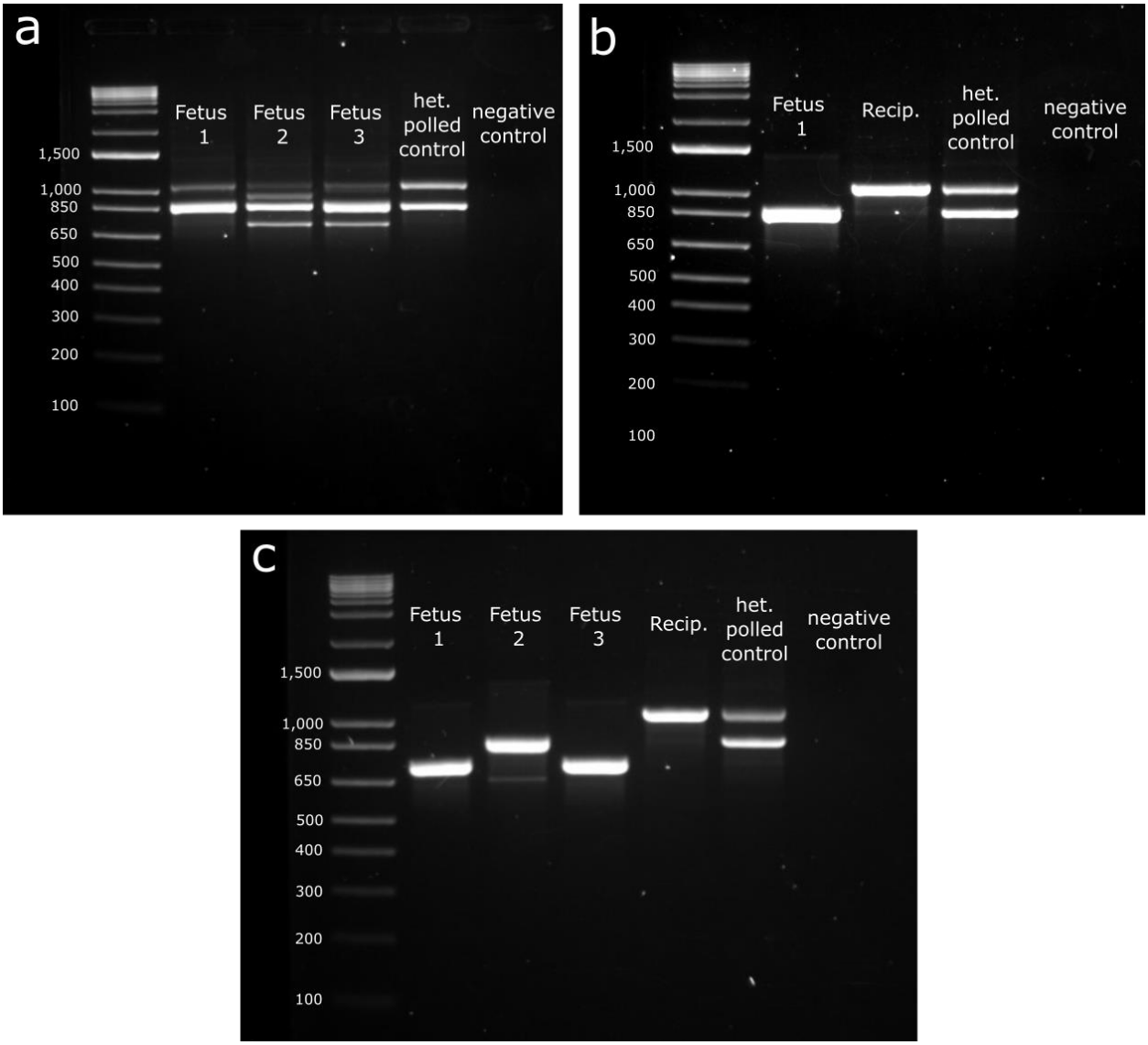

Figure 6. Genotypic analysis of fetuses harvested from embryo transfers (ETs). (**a**) Gel showing fetal genotypes from ET 1, (**b**) 2 and (**c**) 4. DNA was extracted from tail tissue and PCR amplified. Gel electrophoresis was done to visualize the 133 bp targeted deletion. Polled amplicon is 1,078 bp, horned amplicon is 866 bp and expected size with deletion is 733 bp. Polled maternal DNA contamination can be seen in fetuses from ET1 (1,078 bp bands).

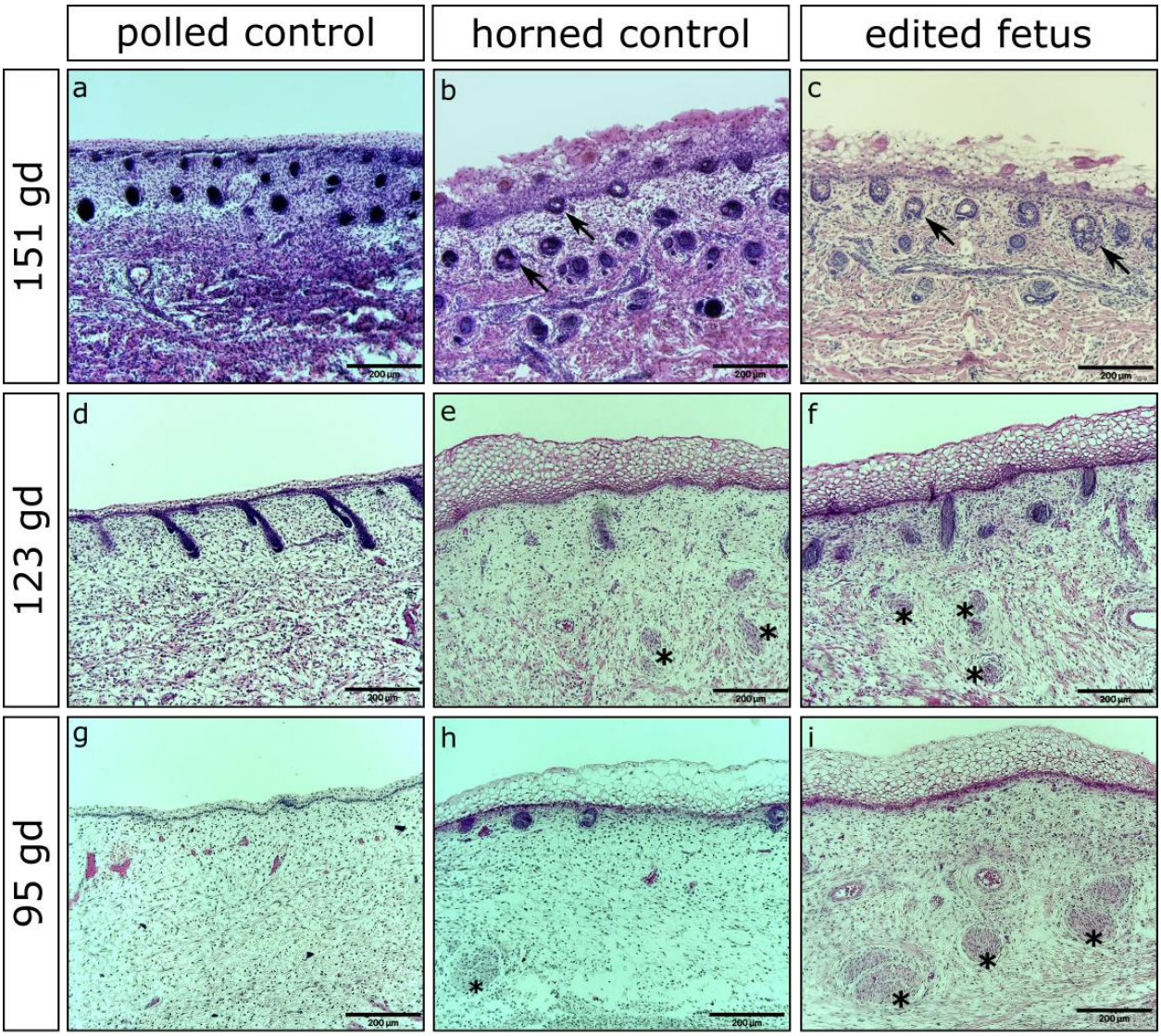

Figure 7. Histological analysis of gene edited fetuses along with polled and horned controls. (**a, d, g**) Horn bud region of aged matched polled and (**b**, **e**, **h**) horned control fetuses alongside representative fetuses from (**c**) ETs 1, (**f**) 2 and (**i**) 4. Multiple layers of vacuolated keratinocytes can be seen in the horn bud region of horned fetuses along with sebaceous glands (black arrows) and nerve bundles (black stars). Stained with Hematoxylin and eosin. gd = gestation days.

SUPPLEMENTARY DATA

Supplementary Table S1. Guide RNA targets surrounding the 10 bp on the P_C allele. The location is given in respect to the 10 bp targeted deletion.

Location	Name	Sequence
5’	btHP 5’g1	GATAGTTTTCTTGGTAGGC
	btHP 5’g2	TCTTTGTAGTGAGAGCAGGC
3’	btHP 3’g1	GTCTATCCCAAAAGTGTGGG
	btHP 3’g2	GATGTTGAATTATAGGCAGA

Supplementary Table S2. Blastocyst and mutation rates of zygotes following microinjection of Cas9 protein and *in vitro* transcribed (IVT) test gRNAs targeting the 5' and 3' regions flanking the 10 bp on the polled locus. Bovine embryos were *in vitro* fertilized and microinjected 18 hours post insemination. Blastocysts were counted on day 8 and mutations were determine using Sanger sequencing. Letters that differ in the same column are significantly different ($P < 0.01$).

Target Region	gRNA	Total Embryos	Total Blastocysts (%)	Total Analyzed	Total Mutation (%)
5'	Non-Injected Control	257	90 (35)^{A}	-	-
	btHP 5'g1	52	14 (27)^{AB}	11	4 (36)^{A}
	btHP 5'g2	60	8 (13)^{B}	8	6 (75)^{A}
3'	Non-Injected Control	413	144 (35)^{A}	-	-
	btHP 3'g1	54	19 (35)^{A}	17	1 (6)^{A}
	btHP 3'g2	47	13 (28)^{A}	13	8 (62)^{B}

Supplementary Table S3. Blastocyst, mutation and targeted deletion rates of zygotes following microinjection of Cas9 protein and *in vitro* transcribed (IVT) gRNAs btHP 5'g2 and btHP 3'g2 targeting the polled locus. Bovine embryos were *in vitro* fertilized and microinjected 6, 8 or 18 hours post insemination (hpi). Blastocysts were counted on day 8 and mutations were determine using Sanger sequencing. A blastocyst was classified as mutated if a mutation was detected at either or both gRNA target sites. Total deletion rates are broken down into subsets of monoallelic (mono), biallelic (bi) and mosaic deletions. Letters that differ in the same column are significantly different ($P < 0.05$).

Time of Injection	Total Embryos	Total Blastocysts (%)	Total Analyzed	Total Mutation (%)	Total Deletion (%)	Subset of Deletion Embryos		
						Non-Mosaic		Mosaic
						Mono (%)	Bi (%)	
Non-Injected Control	425	148 (35)[ab]	-	-	-	-	-	-
6 hpi	190	53 (28)[b]	32	28 (88)[a]	17 (53)[a]	13 (76)	0 (0)	4 (24)
8 hpi	39	20 (51)[a]	17	11 (65)[a]	2 (12)[b]	1 (50)	0 (0)	1 (50)
18 hpi	64	15 (23)[b]	14	9 (64)[a]	1 (7)[b]	0 (0)	0 (0)	1 (100)

Supplementary Table S4. Blastocyst, mutation and targeted deletion rate of zygotes following microinjection of Cas9 protein and *in vitro* transcribed (IVT) or synthetic gRNAs btHP 5'g2 and btHP 3'g2 targeting the polled locus. Bovine embryos were *in vitro* fertilized and microinjected 6 hours post insemination (hpi). Blastocysts were counted on day 8 and mutations were determine using Sanger sequencing. A blastocyst was classified as mutated if a mutation was detected at either or both gRNA target sites. Total deletion rates are broken down into subsets of monoallelic (mono), biallelic (bi) and mosaic deletions. Letters that differ in the same column are significantly different, with capital letters at the 0.001 level ($P < 0.001$) and lowercase letters at the 0.01 level ($P < 0.01$).

gRNA Type	Total Embryos	Total Blastocysts (%)	Total Analyzed	Total Mutation (%)	Total Deletion (%)	Subset of Deletion Embryos		
						Non-Mosaic		Mosaic
						Mono (%)	Bi (%)	
Non-Injected Control	364	130 (36)^{A}	-	-	-	-	-	-
IVT	190	53 (28)^{AB}	32	28 (88)^{a}	17 (53)^{a}	17 (100)^{A}	0 (0)^{A}	0 (0)^{a}
Synthetic	225	45 (20)^{B}	38	37 (97)^{a}	32 (84)^{b}	11 (34)^{B}	20 (63)^{B}	1 (3)^{a}

Supplementary Table S5. Fetal genotyping results from embryo transfers (ETs) of zygotes injected 6 hr post insemination with *in vitro* transcribed (IVT) or synthetic gRNAs and Cas9 protein. A fetus was classified as mutated if a mutation was detected at either or both gRNA target sites. Total deletion rates are broken down into subsets of monoallelic (mono), biallelic (bi) and mosaic.

ET	gRNA Type	Days of Gestation	Total Fetuses	Total Mutation (%)	Total Deletion (%)	Subset of Deletion Fetuses		
						Non-Mosaic		Mosaic
						Mono (%)	Bi (%)	
1	IVT	151	3	3 (100)	2 (67)	0 (0)	0 (0)	2 (100)
2	IVT	123	1	1 (100)	0 (0)	-	-	-
Total	**IVT**	**-**	**4**	**4 (100)**	**2 (50)**	**0 (0)**	**0 (0)**	**2 (100)**
4	Synthetic	95	3	3 (100)	3 (100)	0 (0)	2 (67)	1 (33)
Overall Total	**IVT & Synthetic**	**-**	**7**	**7 (100)**	**5 (71)**	**0 (0)**	**2 (40)**	**3 (60)**

Supplementary Table S6. Primers used for PCR amplification of the P_C allele containing the targeted deletion and the P_F allele.

Target	PCR Round (1st or 2nd)	Forward	Reverse	Tm (°C)	Extension Time
P_C allele	1st	GGGCAAGTTGCTCAGCTGTTTTTG	TCCGCATGGTTTAGCAGGATTCA	62	2 min
	2nd	GAAGTGTGGCCGGTAGAAAA	TCCGCATGGTTTAGCAGGATTCA	60	1 min
P_F allele	1st	CCATCTTGGGTACAGCGTTT	TGTTCTGTGTGGGTTTGAGG	60	30 s

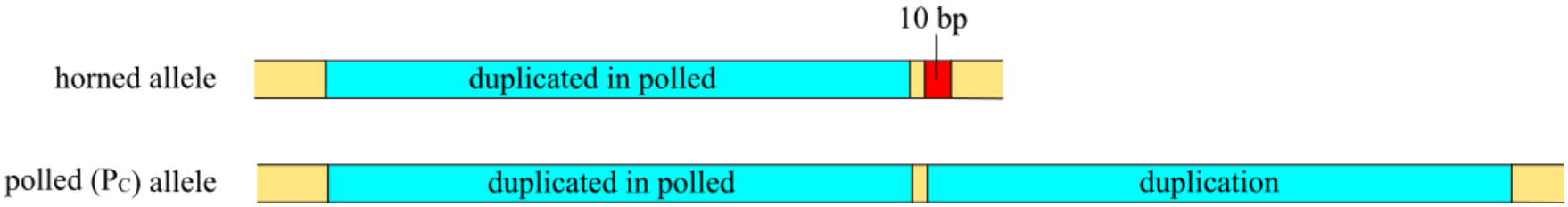

Supplementary Figure S1. Schematic representation of the horned versus the polled (P_C) allele.

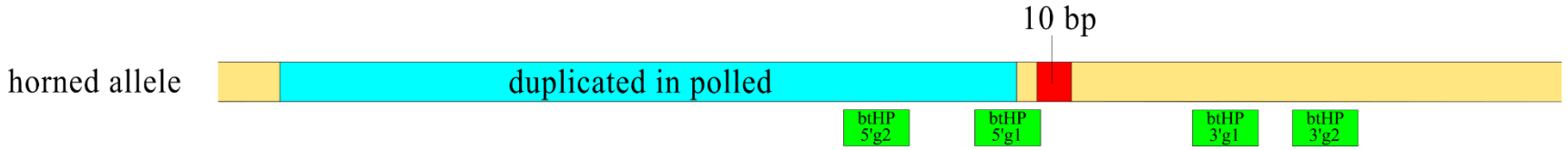

Supplementary Figure S2. Schematic representation of the designed gRNA locations targeting the 10 bp on the horned allele.

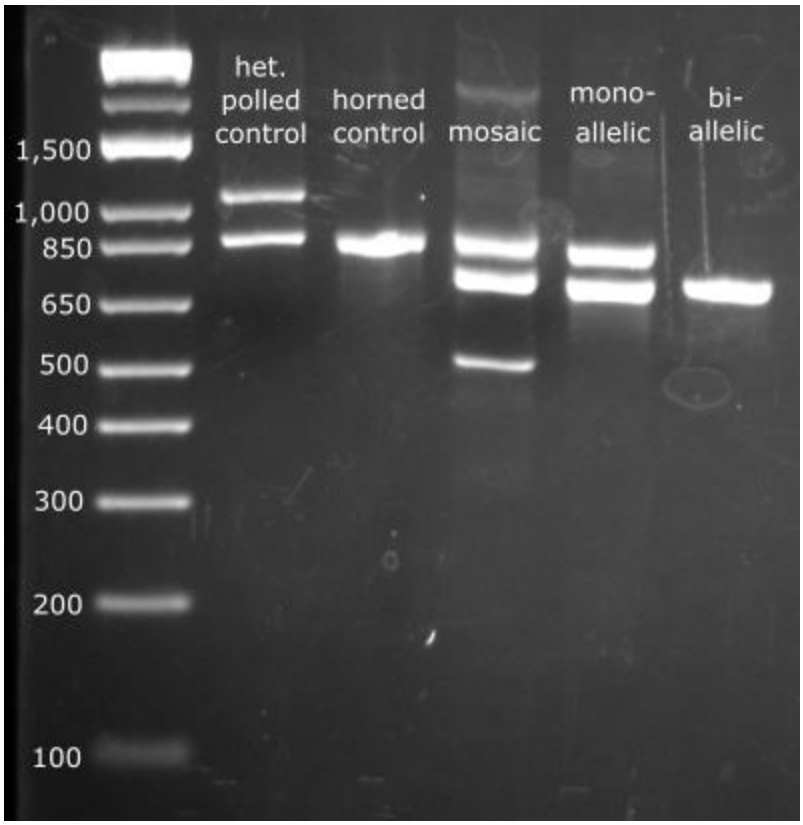

Supplementary Figure S3. Deletion detection at the polled locus of embryos injected with RNP complexes containing gRNAs btHP 5'g2 and btHP 3'g2. Following culture to day-8 blastocysts, DNA was extracted and gel electrophoresis was done. Polled amplicon is 1,078 bp, horned amplicon is 866 bp and expected size with deletion is 733 bp.

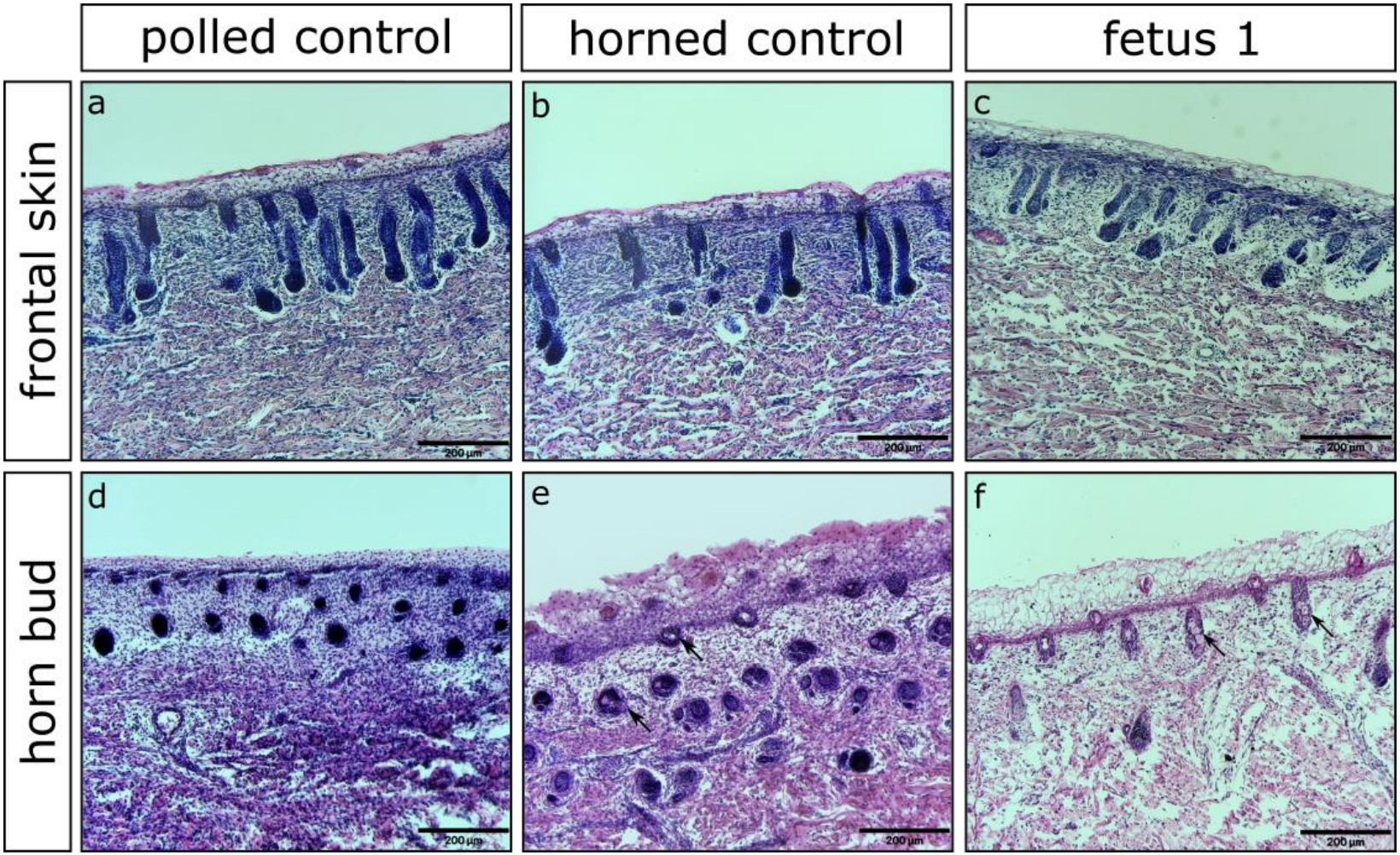

Supplementary Figure S4. Histological analysis of fetus 1 from embryo transfer 1 along with horned and polled control fetuses. (**a-c**) Frontal skin and (**d-f**) horn bud region of fetus 1 and age matched polled and horned controls at 151 days of gestation. Multiple layers of vacuolated keratinocytes can be seen in the horn bud region of horned fetuses along with sebaceous glands (black arrows). Stained with Hematoxylin and eosin.

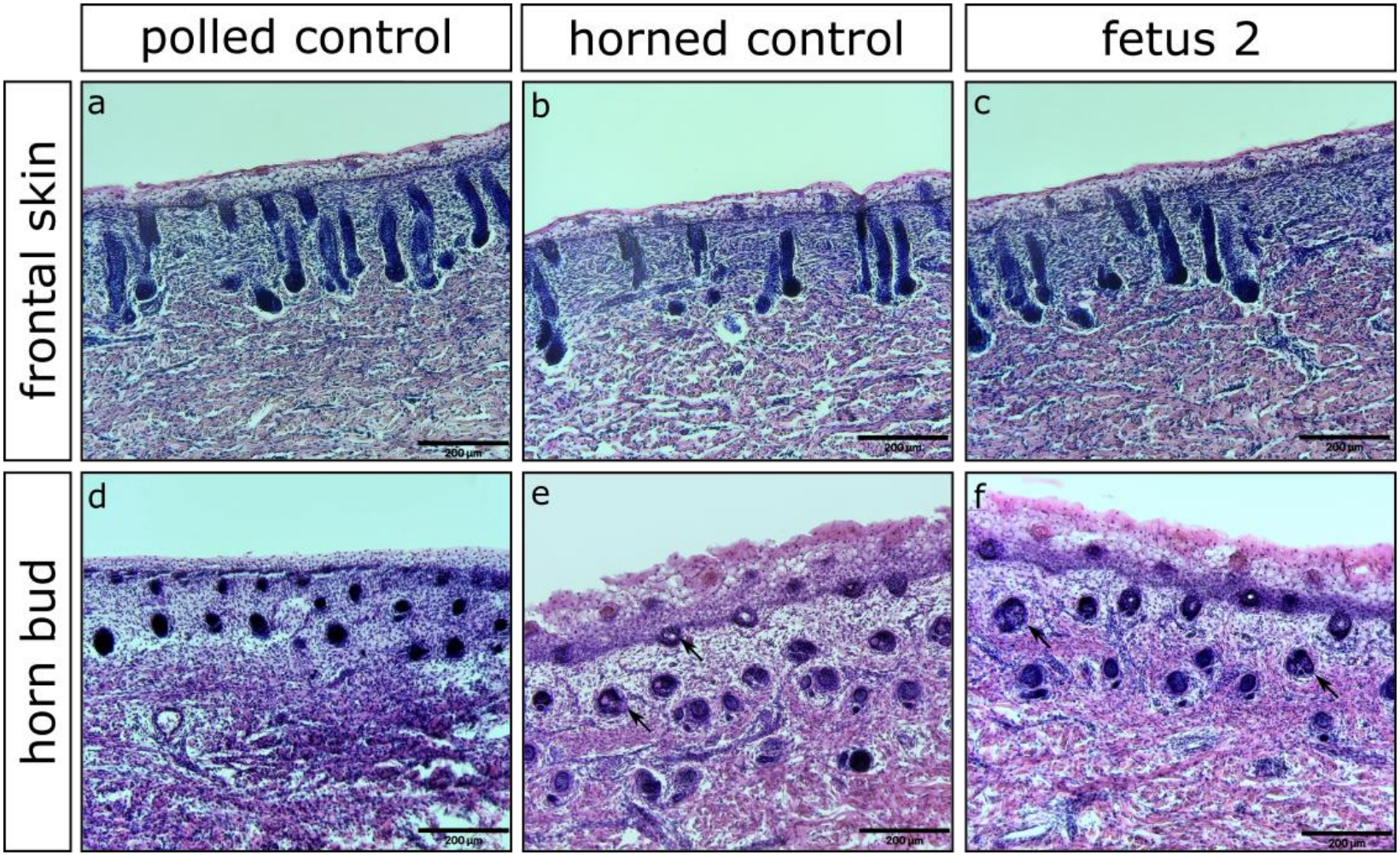

Supplementary Figure S5. Histological analysis of fetus 2 from embryo transfer 1 along with horned and polled control fetuses. (**a-c**) Frontal skin and (**d-f**) horn bud region of fetus 2 and age matched polled and horned controls at 151 days of gestation. Multiple layers of vacuolated keratinocytes can be seen in the horn bud region of horned fetuses along with sebaceous glands (black arrows). Stained with Hematoxylin and eosin.

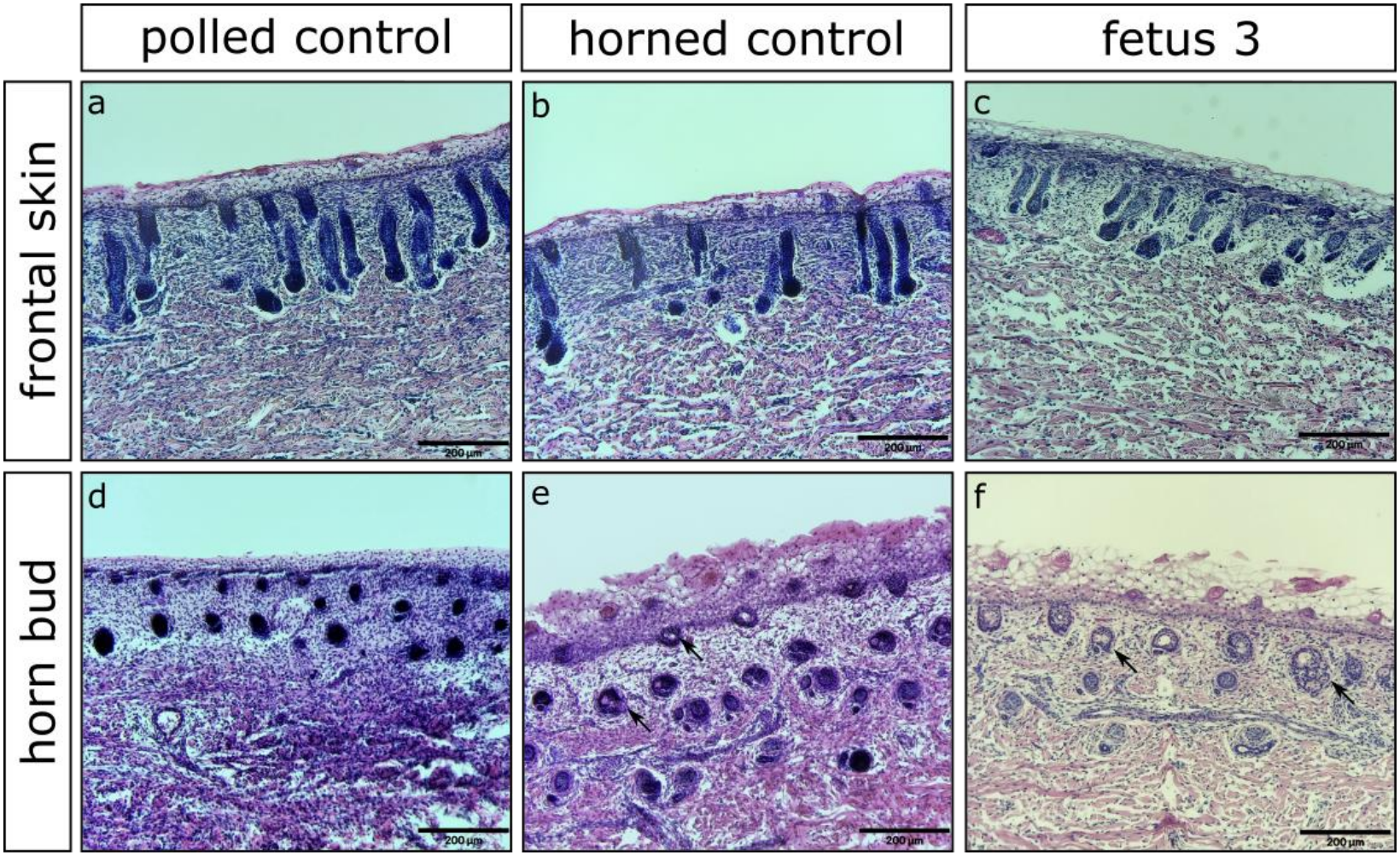

Supplementary Figure S6. Histological analysis of fetus 3 from embryo transfer 1 along with horned and polled control fetuses. (**a-c**) Frontal skin and (**d-f**) horn bud region of fetus 3 and age matched polled and horned controls at 151 days of gestation. Multiple layers of vacuolated keratinocytes can be seen in the horn bud region of horned fetuses along with sebaceous glands (black arrows). Stained with Hematoxylin and eosin.

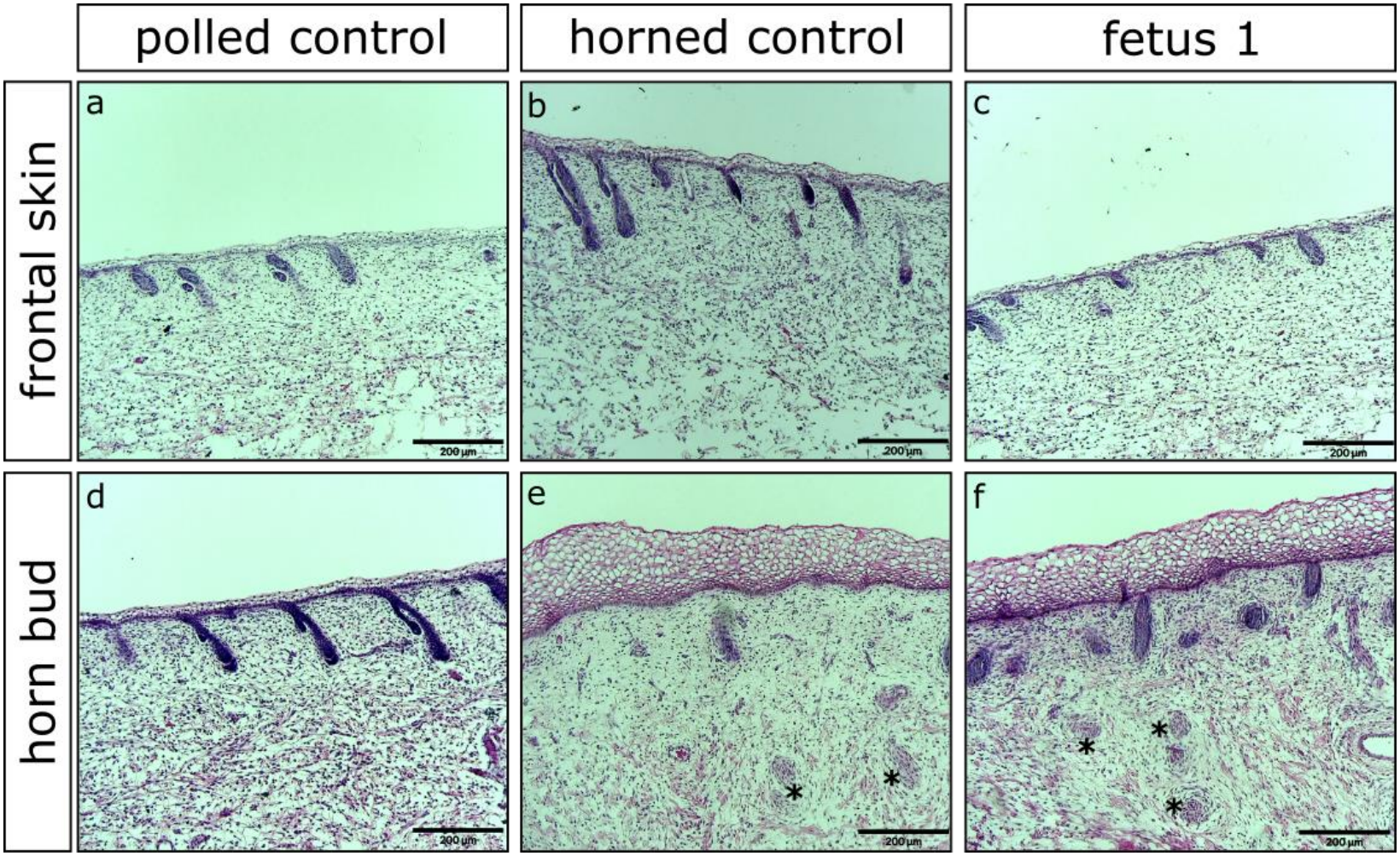

Supplementary Figure S7. Histological analysis of fetus 1 from embryo transfer 2 along with horned and polled control fetuses. (**a-c**) Frontal skin and (**d-f**) horn bud region of fetus 1 and age matched polled and horned controls at 123 days of gestation. Multiple layers of vacuolated keratinocytes can be seen in the horn bud region of horned fetuses along with thick nerve bundles (black stars). Stained with Hematoxylin and eosin.

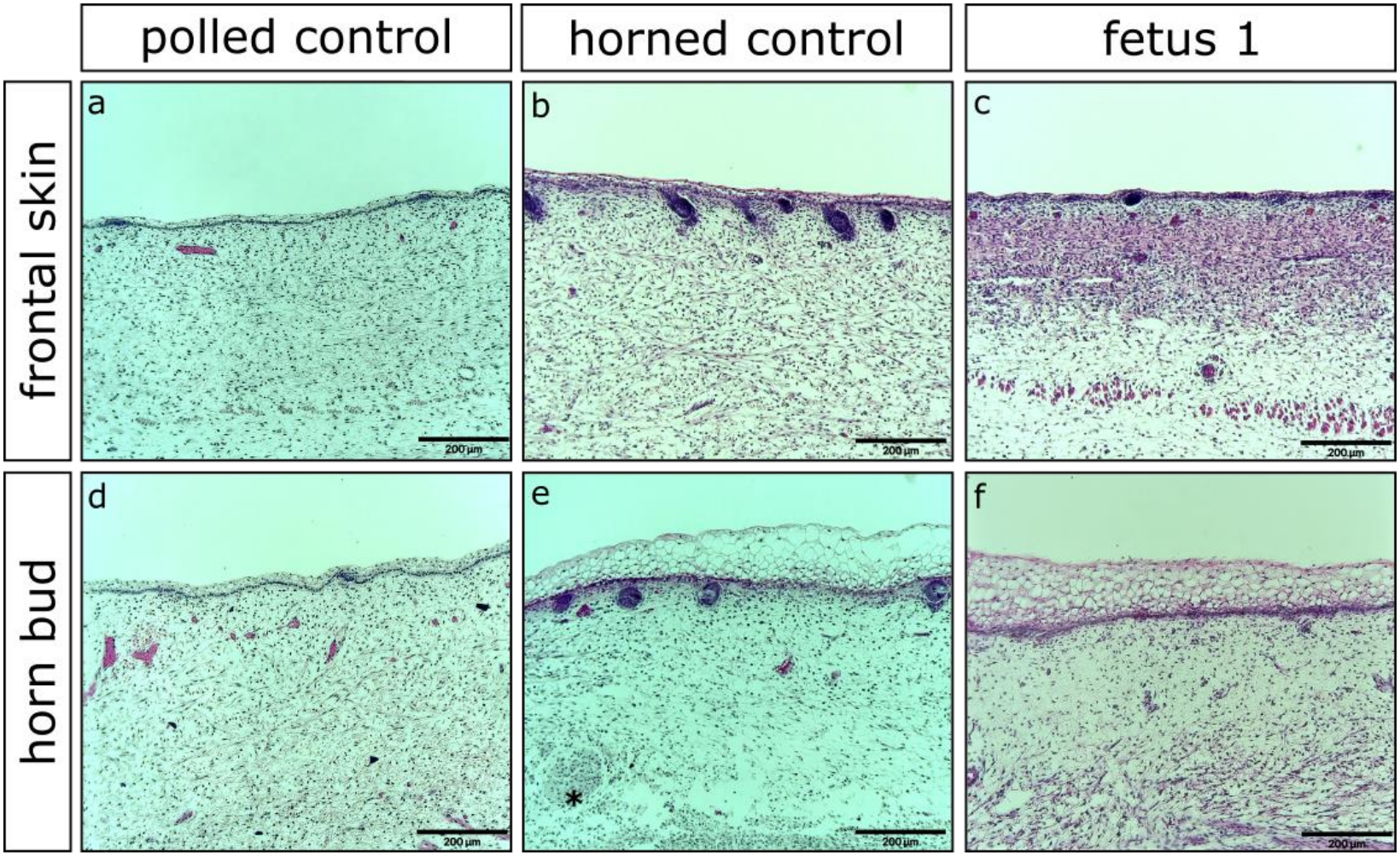

Supplementary Figure S8. Histological analysis of fetus 1 from embryo transfer 4 along with horned and polled control fetuses. (**a-c**) Frontal skin and (**d-f**) horn bud region of fetus 1 and age matched polled and horned controls at 95 days of gestation. Multiple layers of vacuolated keratinocytes can be seen in the horn bud region of horned fetuses along with thick nerve bundles (black stars). Stained with Hematoxylin and eosin.

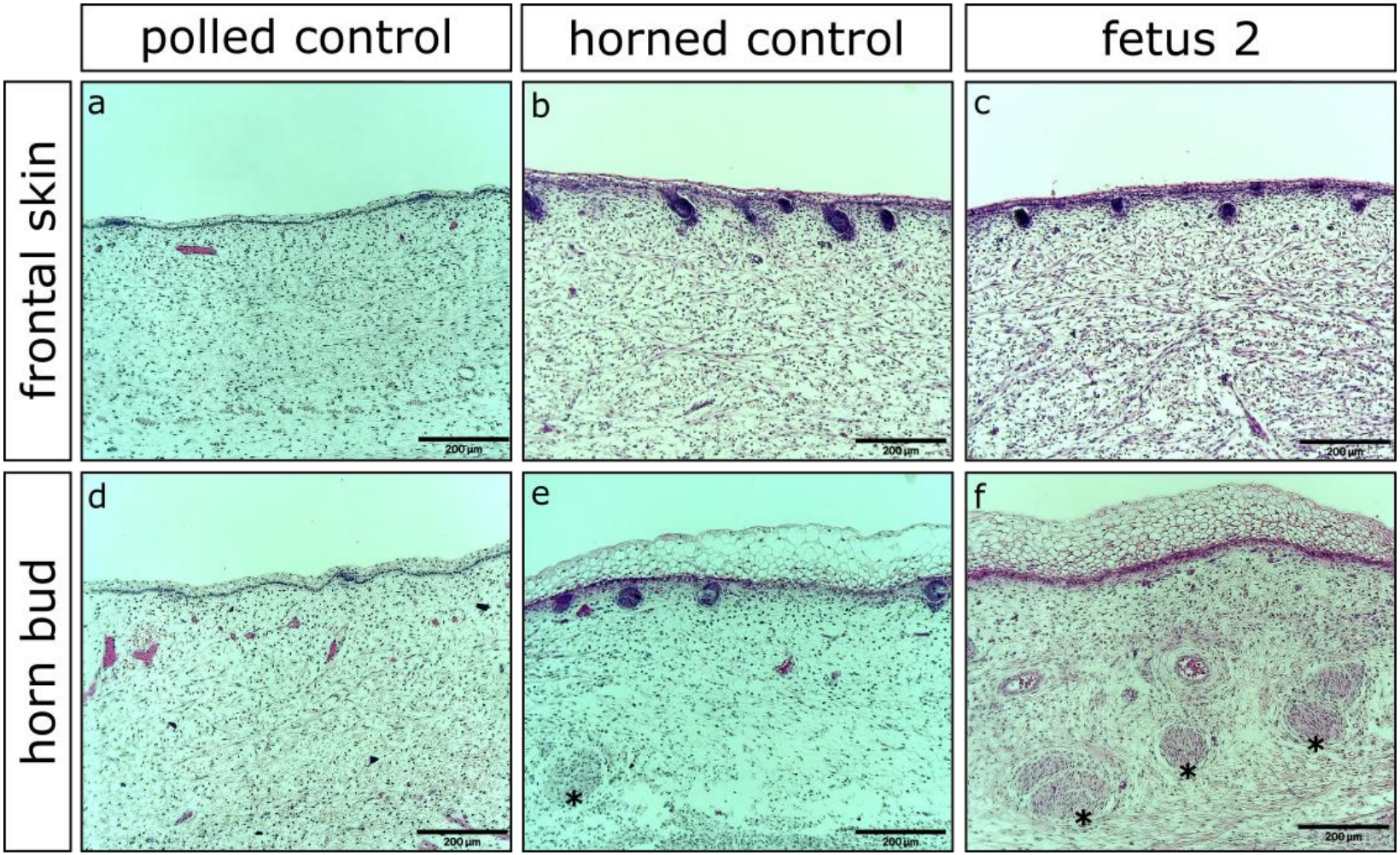

Supplementary Figure S9. Histological analysis of fetus 2 from embryo transfer 4 along with horned and polled control fetuses. (**a-c**) Frontal skin and (**d-f**) horn bud region of fetus 2 and age matched polled and horned controls at 95 days of gestation. Multiple layers of vacuolated keratinocytes can be seen in the horn bud region of horned fetuses along with thick nerve bundles (black stars). Stained with Hematoxylin and eosin.

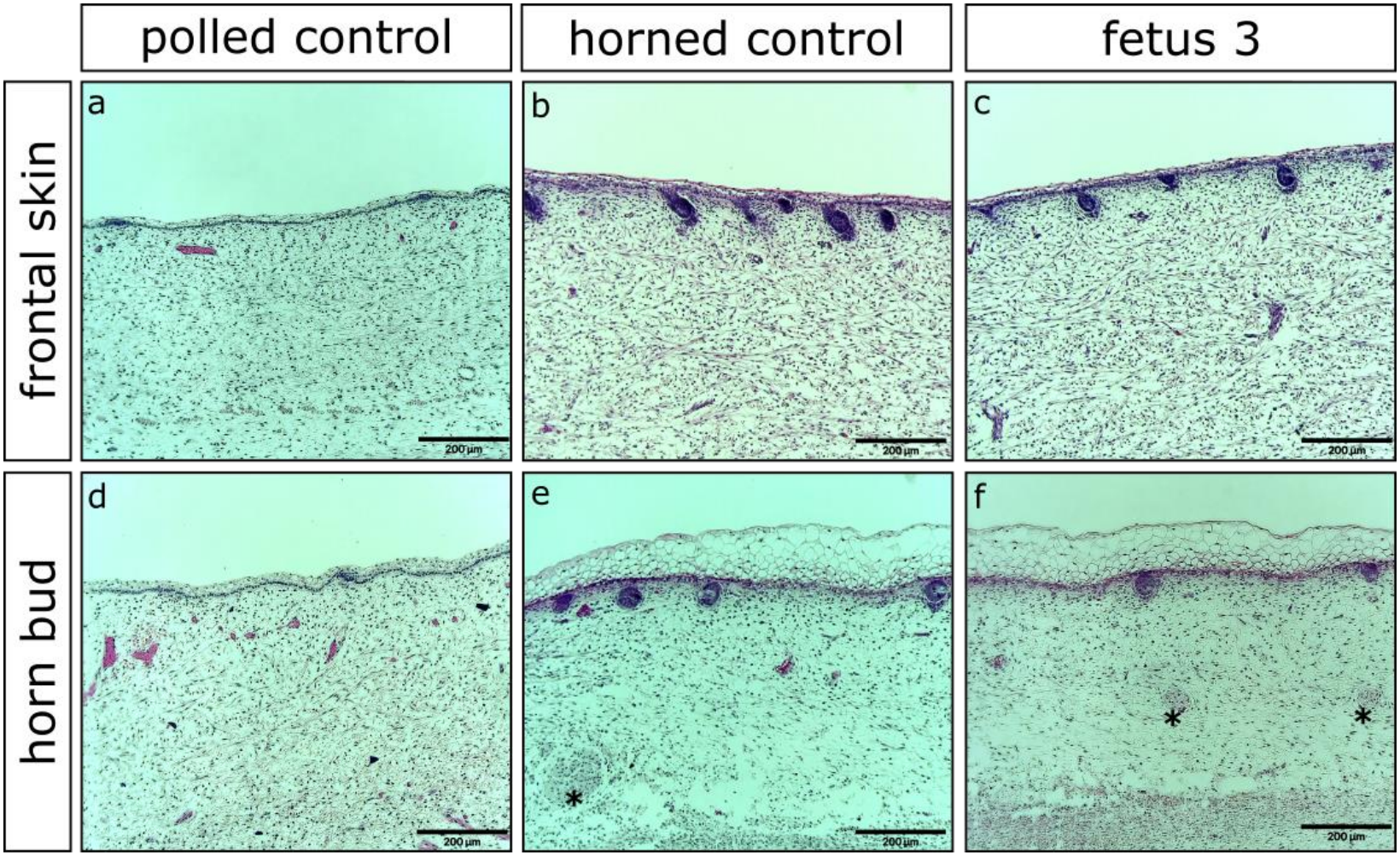

Supplementary Figure S10. Histological analysis of fetus 3 from embryo transfer 4 along with horned and polled control fetuses. (**a-c**) Frontal skin and (**d-f**) horn bud region of fetus 3 and age matched polled and horned controls at 95 days of gestation. Multiple layers of vacuolated keratinocytes can be seen in the horn bud region of horned fetuses along with thick nerve bundles (black stars). Stained with Hematoxylin and eosin.

***LincRNA#1* Knockout does not Affect Polled Phenotype in Cattle**

Sadie L. Hennig[1], Bret R. McNabb[2], Josephine F. Trott[1], Alison L. Van Eenennaam[1] and James D. Murray[1,2]

[1]Department of Animal Science, University of California – Davis, Davis, CA
[2]Department of Population Health and Reproduction, School of Veterinary Medicine, University of California – Davis, Davis, CA

Corresponding Author: jdmurray@ucdavis.edu

ABSTRACT

A long intergenic non-coding RNA (*lincRNA#1*) has been shown to be overexpressed in the horn bud region of polled (hornless) bovine fetuses, suggesting a potential role in horn bud suppression. Genome editing was used to test whether the absence of this sequence was associated with the horned phenotype. Two gRNAs with high mutation efficiencies targeting the 5' and the 3' regions flanking the *lincRNA#1* sequence were co-injected with Cas9 as ribonucleoprotein complexes into bovine zygotes (n=121) 6 hours post insemination. Of the resulting blastocysts (n=31), 84% had the expected 3.7 kb deletion, with 88% of the embryos being biallelic knockouts. Thirty-nine presumptive edited seven-day blastocysts were transferred to 13 synchronized recipient cows resulting in ten pregnancies, five with embryos heterozygous for the dominant P_C polled allele at the POLLED locus, and five with the recessive pp genotype. Eight (80%) of the resulting fetuses were biallelic *lincRNA#1* knockouts, with the remaining two being mosaic. RT-qPCR analysis was used to confirm the absence of *lincRNA#1* expression in knockout fetuses. Phenotypic and histological analysis of the genotypically (P_Cp) polled,

lincRNA#1 knockout fetuses revealed similar morphology to non-edited, control polled fetuses, indicating the absence of *lincRNA#1* alone does not result in a horned phenotype.

INTRODUCTION

Several studies have identified causal mutations for the polled (hornless) phenotype in cattle, but the underlying biological mechanism causing polled remains unclear[1-5]. The two known *Bos taurus* allelic variants at the POLLED gene associated with the polled phenotype, Friesian P_F[1,2,4] and Celtic P_C[1,4], are not associated with any known transcript or protein. Carlson et al.[6] demonstrated that the POLLED variant found in beef breeds (P_C), when introgressed using genome editing to replace the recessive horned allele (p) in a cell line derived from a horned dairy bull, resulted in polled homozygous P_CP_C bull calves when the edited cell line was subsequently used in somatic cell nuclear transfer (SCNT) cloning to produce live calves. A follow up study investigating the progeny of these genome edited bulls bred to horned Hereford cows demonstrated that the introgressed P_C allele was inherited as a dominant trait and resulted in six heterozygous P_Cp calves with a polled phenotype, further demonstrating the casual role of the P_C allele for the polled phenotype[7].

Allais-Bonnet et al.[1] identified an additional genetic component potentially associated with the polled phenotype – a long intergenic non-coding RNA (lincRNA) that is annotated as *LOC100848368* and which was termed *lincRNA#1*. LincRNAs are a form of RNA that have very similar characteristics to mRNA, however they do not code for any known proteins. There is still uncertainty as to why lincRNAs exist, but some play important roles in the regulatory functions of vital biological processes[8-10]. The *lincRNA#1* locus is located approximately 80 kb downstream of the P_C allele and was identified by reverse transcription quantitative PCR (RT-

qPCR) to be overexpressed in the horn bud region of 90-day polled (P_Cp) fetuses as compared to the horn bud region of wild type (pp) horned fetuses[1].

Several studies have demonstrated lincRNAs can be cis-acting elements regulating neighboring genes, often located within a few kb of the lincRNA sequence[11-13]. OLIG1, a transcription factor involved in neural crest differentiation pathways[14], is located approximately 8 kb away from the *lincRNA#1* locus and is the closest gene with a known function. Wiedemar et al.[15] found that *OLIG1* is overexpressed in the horn bud region of 150 day old horned fetuses when compared to the horn bud region of polled fetuses, and another study investigated how the evolution and development of pecoran (ruminants, excluding Tragulidae) headgear was likely influenced by OLIG1[16]. The inverse correlation between expression of *lincRNA#1* and *OLIG1* suggests an inhibitory or repressive relationship. Downregulation of *OLIG1* expression by upregulation of *lincRNA#1* might be associated with the absence of horn bud development in polled cattle.

In this study, we directly tested whether *lincRNA#1* plays a role in the polled phenotype and investigated a possible regulatory role with respect to *OLIG1*. Little is known about *lincRNA#1*, particularly the functional region, so we decided to take a complete knockout (KO) approach. Using two guide RNAs (gRNAs) with the CRISPR-Cas9 system to create large deletions of greater than 1 kb in length has been successfully achieved in zebrafish[17] and mice embryos[18], but has yet to be attempted in livestock. Here, we deployed a dual-guide approach in microinjected zygotes to delete an approximately 3.7 kb region in the bovine genome, thereby completely knocking out *lincRNA#1*. Presumptive *lincRNA#1* KO bovine embryos were transferred to synchronized recipient cows, and the resulting fetuses were harvested at 90 days of gestion. Fetuses were analyzed to determine if knocking out *lincRNA#1* in a heterozygous (P_Cp)

background would result in a horned phenotype, and the expression of both *lincRNA#1* and *OLIG1* expression were assayed using RT-qPCR to investigate their relative expression levels.

RESULTS

Guide-RNA Testing and *lincRNA#1* Knockout Testing in Embryos

Generating a *lincRNA#1* KO bovine fetus began by designing gRNAs targeting the 5' and 3' regions flanking *lincRNA#1* on bovine chromosome 1 (Supplementary Table S1). Using our previously described protocol[19], we identified two possible gRNAs targeting the 5' region (linc 5'g1 and linc 5'g2) and two gRNAs targeting the 3' region (linc 3'g1 and linc 3'g2). The gRNAs were incubated with Cas9 protein to form a ribonucleoprotein (RNP) complex and independently microinjected into zygotes 6 hours post insemination (hpi), following a previously established protocol[19]. Uninjected embryos were cultured as a developmental control. For gRNAs targeting the 5' region, there were no differences in development to the blastocyst stage between uninjected controls (27%), linc 5'g1 (26%), linc 5'g2 (17%), or between the two gRNAs (Fig. 1a; Supplementary Table S2). There were also no differences in mutation rates between linc 5'g1 (95%) and linc 5'g2 (80%) (Fig. 1b, Supplementary Table S2). When testing gRNAs targeting the 3' region, there was again no difference in blastocyst development between the non-injected control group (31%), linc 3'g1 (33%), linc 3'g2 (42%) groups or between the two test gRNAs (Fig. 1c; Supplementary Table S2). However, there was a difference in mutation rate between linc 3'g1 (100%) and linc 3'g2 (75%; $P = 0.005$) (Fig.1d, Supplementary Table S2). Due to the higher mutation rate, linc 3'g1 was selected for further analysis.

To determine the best gRNA combination to use to achieve the *lincRNA#1* KO, two co-injection groups were tested, with co-injection group 1 (Co1) consisting of linc 3'g1 and linc 5'g1 RNP complexes and co-injection group 2 (Co2) consisting of linc 3'g1 and linc 5'g2 RNP

complexes. There were no differences in blastocyst development rates between the non-injected controls (36%) and either Co1 (30%) or Co2 (34%) or between the two co-injection groups (Fig. 2a; Supplementary Table S3). There was also no difference in the mutation rate between Co1 or Co2 (both 100%), when a blastocyst was considered positive if a mutation was found in at least one target site (Fig. 2b; Supplementary Table S3). However, the KO rate for Co1 (84%) was 38% higher than the KO rate for Co2 (61%; P = 0.045) (Fig. 2c, Supplementary Table S3). There was an 88% biallelic KO rate and a 12% mosaicism rate in Co1 injected embryos, whereas the biallelic and mosaic KO rates in Co2 injected embryos were 77% and 23%, respectively (Fig. 2d; Supplementary Table S3). No differences were detected between Co1 and Co2 biallelic and mosaic KO rates, however based on the difference in overall KO rates, Co1 was selected as the best combination for producing KO embryos to transfer into synchronized recipient cows.

Embryo Transfers

Once the deletion of *lincRNA#1* was optimized *in vitro*, recipient heifers were synchronized for embryo transfers. For the first trial (ET1), 15 presumptive edited blastocysts heterozygous (P_Cp) at the POLLED locus, and nine presumptive edited blastocysts homozygous (pp) at the POLLED locus, which would be expected to be horned (negative controls), were non-surgically transferred into eight synchronized recipients (three blastocysts per recipient) (Table 1). At day 30 of gestation, three out of the eight recipient cows were pregnant based on pregnancy-associated glycoprotein (PAG) testing, one from the heterozygous (P_Cp) embryo transfers, and two from the homozygous (pp) embryo transfers. At day 35 of gestation, transrectal ultrasounds confirmed pregnancies and fetal counts. Two fetuses were detected in the recipient that was carrying the heterozygous (P_Cp) fetuses and five were detected in the recipients carrying the homozygous (pp) fetuses, one carrying twins and the other triplets. Recheck examinations at 75 days of gestation via transrectal ultrasound found only the recipients

carrying the five homozygous (pp) fetuses remained pregnant, though none of the fetuses were viable. It was estimated that fetal demise had occurred at roughly 45 – 50 days of gestation based on fetal measurements. The fetal remnants from these homozygous (pp) fetal demises were recovered the following week for analysis.

Due to these fetal losses, a second embryo transfer (ET2) was performed, however because of the limited availability of recipients, only blastocysts with the P_Cp genotype at the POLLED locus were transferred. These were expected to be polled in the presence of *lincRNA#1* and horned in its absence. A total of 15 heterozygous P_Cp day-seven presumptive *lincRNA#1* KO blastocysts, obtained from two microinjection groups of 50 to 60 embryos each, were transferred into five synchronized recipients (three blastocysts per recipient) (Table 1). Blastocysts that were not transferred in ET2 were analyzed to establish an editing profile for the transferred embryos. Twelve blastocysts were analyzed, and ten blastocysts had *lincRNA#1* KOs (83%), while the remaining two embryos had mutations only at the linc 3'g1 target site (Supplementary Fig. S1). Of the ten KO embryos, seven were biallelic KOs (70%) and three were mosaic (30%).

At day 29 of gestation, all five recipients were pregnant based on PAG testing. At 35 days of gestation, transrectal ultrasounds confirmed four of the five recipients remained pregnant, with three recipients carrying singletons and one carrying twins. Given the high rate of pregnancy losses from ET1, we performed weekly ultrasounds to monitor fetal development and viability until the five fetuses were harvested at 90 days of gestation.

Overall, nine genetically horned (pp) edited embryos were transferred into three recipients and 30 genetically polled (P_Cp) presumptive edited embryos were transferred into 10 recipients (Table 1). At 75 days of gestation for ET1, ultrasounds revealed that fetal demise had occurred, resulting in an overall pregnancy and fetal viability rate of 0%. The fetal remains of the

five genetically horned (pp) fetuses were recovered for analysis. For ET2, four of the ten recipients were pregnant at 75 days of gestation with five viable fetuses (40% pregnancy rate; 17% fetal viability rate), and a total of five genetically polled (P_CP) fetuses were harvested at 90 days of gestation.

Phenotypic and Genotypic Analysis of Fetuses

The fetal remnants from the five ET1 genetically horned (pp) fetuses were harvested at 83 days of gestation. Two of the fetuses detected in one recipient were almost fully resorbed, and it was estimated they were lost between 35 – 45 days of gestation (Table 2). Three fetuses from the second recipient were not as far along in the resorption process. The basic anatomy was still present, but they were severely degraded. Based on crown-rump length (approximately 2.5 – 3 cm), it was estimated that fetal demise occurred between 45 – 50 days of gestation. Although the horned phenotype could not be determined due to the age and state of the fetuses, PCR and Sanger sequencing analysis revealed that all five fetuses had biallelic *lincRNA#1* KOs, with fetuses 1 and 2 being compound heterozygous KOs (fetus 1: 3,733 bp and 3,736 bp deletions; fetus 2: 3,736 bp deletion and a 3,740 bp deletion - 7 bp insertion) and fetuses 3, 4 and 5 being homozygous biallelic KOs (3,755 bp deletions; Fig. 3a; Table 2).

Five genetically polled (P_CP) fetuses from ET2 were harvested at 90 days of gestation (Table 2). All five fetuses displayed a polled phenotype (Fig. 4). PCR and Sanger sequencing analysis revealed that fetuses 2, 4 and 5 were homozygous biallelic KO fetuses (fetus 2: 3,751 bp deletions; fetuses 4 and 5: 3,733 bp deletions; Fig. 3b; Table 2). Fetus 1 was a mosaic KO, and fetus 3 was also a mosaic, with mutations identified at the linc 3’g1 target site and only low KO levels detected. In total, ten (100%) of the edited fetuses contained a *lincRNA#1* KO, however only eight of these (80%) were biallelic KOs. Two (20%) were mosaic with some sequences

having an incomplete deletion of the *lincRNA#1* locus (Fig. 3b). Of the sequences that were not the full 3.7 kb *lincRNA#1* KO, none contained an unmutated (wild type) sequence.

Histological Analysis of Fetuses

Although histological analysis could not be performed on fetuses from ET1, histological analysis of fetuses from ET2 showed the lack of fetal horn bud development consistent with 90-day polled control fetuses (Fig. 5; Supplementary Fig. S2 – S3). There was no substantial layering of vacuolated keratinocytes or nerve bundles present in the horn bud region of edited fetuses (Fig. 5f; Supplementary Fig. S2), unlike the horn bud region of horned control fetuses (Fig. 5d). The horn bud regions of edited fetuses were histologically identical to the frontal skin of all fetuses (Fig. 5a-c), with few layers of vacuolated keratinocytes, no nerve bundles, and hair follicles throughout, and were histologically comparable to the horn bud region of the polled control (Fig. 5e; Supplementary Fig. S2 – S3).

Reverse Transcription Quantitative PCR (RT-qPCR) Analysis of Fetuses

RT-qPCR analysis was performed on tissue collected from the horn bud region of edited fetuses from ET2 as well as one unedited horned (pp), and two unedited polled (P_Cp) age-matched controls. We found *lincRNA#1* to have an elevated expression in the horn bud region of the polled control fetuses as compared to the horn bud region of the horned control fetus, although expression varied more than 2-fold between the two polled controls (Fig. 6). When analyzing the genome edited fetuses, *lincRNA#1* expression was only detected in one mosaic fetus (fetus 3), at nearly identical expression levels as in the polled control, confirming that our biallelic KOs did eliminate this transcript. Due to low sample numbers, no significance can be ascribed to differences in *lincRNA#1* expression levels.

To determine if there was a relationship between *lincRNA#1* and *OLIG1* expression levels, RT-qPCR analysis was also performed on transcripts from both loci. *OLIG1* expression

levels were highly variable (Fig. 6). No differences in OLIG1 expression were observed among the different experimental groups, although sample sizes were small. Expression of *OLIG1* tended to be higher in the 90-day polled control fetuses as compared to the horned control, in contrast to the previous study[15] with 150-day fetuses, however, the highest level of *OLIG1* expression was observed in one of the biallelic *lincRNA#1* KO fetuses (fetus 2). *OLIG1* expression was not detectable in fetus 1 (mosaic) or fetus 5 (biallelic KO), but fetus 4 (biallelic KO) showed similar expression levels to horned controls. The fact that *OLIG1* expression was variably present and absent in *lincRNA#1* biallelic KO fetuses, led us to conclude that knocking out *lincRNA#1* did not have an obvious direct effect on *OLIG1* expression in the horn bud of 90-day old bovine fetuses. It should be noted that expression levels for both *lincRNA#1* and *OLIG1* were extremely low, and detection of both proved challenging in the horn bud region of 90-day old fetuses.

DISCUSSION

Allais-Bonnet et al. first identified that *lincRNA#1*[1] was more highly expressed in the horn bud region of polled compared to horned bovine fetuses. LincRNAs may function as cis-acting elements to regulate neighboring genes[11-13] and *OLIG1*, a gene that codes for a transcription factor involved in neural crest differentiation pathways[14] that potentially influences horn development[16], is the closest neighboring gene at approximately 8 kb from the *lincRNA#1* locus. Given previous findings that *OLIG1* is overexpressed in the horn bud region of horned fetuses when compared to the horn bud region of polled fetuses[15], we hypothesized that the P_C allele results in the overexpression of *lincRNA#1* which downregulates the expression of *OLIG1*, thereby inhibiting horn development and resulting in a polled phenotype.

A CRISPR-Cas9 dual-guide approach was deployed in bovine zygotes to achieve large fragment (approximately 3.7 kb) deletion, homozygous KO fetuses, and in this study specifically, KO of *lincRNA#1*. Although we were able to achieve high KO rates, the absence of the *lincRNA#1* transcript, and elimination of any downstream effects of *lincRNA#1* expression, did not result in phenotypically horned fetuses. All genetically polled (P_Cp) *lincRNA#1* KO fetuses still presented a polled phenotype, suggesting that *lincRNA#1* does not play a role in horn bud suppression and is not responsible for the polled phenotype.

Histological analysis of the genetically polled (P_Cp) *lincRNA#1* KO fetuses revealed similar morphology to control P_Cp polled fetuses. At 90 days of gestation, the horn bud and frontal skin regions of polled control fetuses were histologically identical, with abundant hair follicles, few layers of vacuolated keratinocytes, and no nerve bundles present, corresponding to other fetal histological studies[1,20]. This same morphology was seen in our *lincRNA#1* edited fetuses. These histology results support the gross phenotypic observations, indicating that even though our genetically polled (P_Cp) fetuses had the *lincRNA#1* deletion, they nonetheless had a polled phenotype.

Analyzing expression levels of *lincRNA#1* and *OLIG1* in the horn bud region of edited and control 90-day bovine fetuses proved challenging. Although we were ultimately able to detect both *lincRNA#1* and *OLIG1* transcripts, the assay required five times the amount of cDNA per qPCR reaction to detect expression in 90-day old bovine fetuses as compared to the study conducted by Allais-Bonnet et al.[1] (100 ng vs 20 ng, respectively). Wiedemar et al. attempted to analyze *lincRNA#1* and *OLIG1* expression levels across a range of fetal ages, but they were unable to detect these transcripts by qPCR using ~16 ng[15] of cDNA in early stage fetuses, although they were able to detect *OLIG1* expression in 150-158-day old fetuses. It is common for

lincRNAs to be minimally expressed, with as little as a few molecules per cell, thus making them extremely difficult to detect[21]. It is possible that cattle breed may also affect *lincRNA#1* expression. Allais-Bonnet et al. used known breeds of cattle (Charolais and Holstein X Normande crossbred cull cows)[1], whereas we obtained fetuses of unknown breed from a local slaughterhouse, similar to Wiedemar et al.[15]. There was evident (>2-fold difference) expression variation with our two polled control fetuses. Even though *lincRNA#1* was difficult to detect, overall our results were consistent with those seen in the study by Allais-Bonnet et al.[1]. It was interesting to observe *lincRNA#1* expression in the mosaic KO fetus (fetus 3), despite the fact that there was no completely wild type sequence of *lincRNA#1* remaining in this fetus. This suggest that whatever mutation was introduced in the sequence did not prevent the expression of *lincRNA#1* and highlights the importance of generating complete KOs of functionally unknown regions/genes to unambiguously study their function.

OLIG1 also proved difficult to detect and was extremely variable in expression between control and edited fetuses, possibly as a result of its very low concentration in our cDNA preparations. Across the biallelic *lincRNA#1* edited fetuses, *OLIG1* expression varied from non-detectable (fetus 2), to low (fetus 4), to high (fetus 5). Wiedemar et al. also had difficulty detecting *OLIG1* in early developing fetuses, but detection was possible by 150-158 days of gestation[15]. Further studies need to be performed to analyze *OLIG1* expression in *lincRNA#1* KO fetuses at later gestational stages to determine if *lincRNA#1* has any regulatory role over *OLIG1* during gestation. Additionally, a different lincRNA locus *LOC100848215* which is expressed only in horned ruminants and has decreased or even absent expression in the presence of one or two copies of the P_C polled allele[15], would be another interesting candidate to KO to determine if its expression is required for horn bud formation in cattle.

High rates of embryonic loss and death were observed in the first embryo transfer performed in this study, with all the fetuses recovered being nonviable. Abortion diagnostic panels were performed on the recipients to rule out infectious causes for the fetal losses, but no diagnosis was reached. Because the function of *lincRNA#1* is unknown, we speculated that it could be a lethal KO, however several studies have shown that long non-coding RNAs are dispensable, and their absence does not result in the organism's death[12,14,22]. A second embryo transfer was performed with the same recipient pool and veterinarian, and a much higher rate of success was achieved. Since all the fetuses harvested from the second embryo transfer were viable at 90-days and three were complete biallelic *lincRNA#1* KOs, it was determined to be a non-lethal KO, leaving the exact cause of the fetal demises observed in ET1 undiagnosed.

Mosaicism is a common problem observed when using genome editing reagents in developing embryos. Our previous work reported an inverse correlation between mosaicism rate and timing of injections hours post insemination (hpi), with the lowest mosaicism rates being seen in embryos edited 6 hpi[23]. Interestingly, we saw this same trend in the work presented here. Based on the blastocyst developmental rates in our preliminary studies, it was determined that around 100-120 embryos would be needed to obtain sufficient blastocysts for embryo transfers. To ensure editing reagents were at their highest editing efficiency and to limit the time embryos were exposed to suboptimal conditions outside of the incubator, two groups of 50-60 zygotes were injected separately using newly prepared editing reagents per injection group. This means that one group (group 1) was injected 6 hpi and the second group (group 2) was injected around 6.5 - 7 hpi. Any remaining blastocysts not transferred to recipients were analyzed to obtain an editing profile of those embryos that were transferred. Although all the embryos from ET1 were transferred, there were 12 non-transferred embryos from ET2 that were analyzed, eight from

group 1 and four from group 2. It was interesting to observe that the deletion rate was higher and the mosaicism rate was lower in embryos injected in group 1 as compared to embryos injected group 2 (Supplementary Fig. S1). Furthermore, of the edited fetuses harvested, the two mosaic fetuses were both from group 2 embryos. These results lend further support to the importance of early introduction of genome editing agents into zygotes to promote high editing efficiency and low mosaicism rates. These data also highlight one of the downfalls of microinjection. Microinjection is time consuming, even if done by a skilled individual. A better approach would be to edit all embryos simultaneously in a shorter amount of time using recently developed electroporation techniques[24]. The optimization of electroporation methods to simultaneously introduce editing reagents into hundreds of livestock zygotes may increase the obtainment of genome edited biallelic KO embryos with low mosaicism rates.

Overall, this paper describes how a CRISPR-Cas9 dual-guide approach was used to create a large (>3 kb) targeted deletion in bovine embryos. Embryo transfers of presumptive *lincRNA#1* KO embryos were performed, and although all of the pregnancies from the first embryo transfer resulted in fetal demise, five phenotypically normal 90-day fetuses were harvested from the second embryo transfer for analysis. Of those five genotypically polled (P_Cp) fetuses, all carried a deletion containing *lincRNA#1*, and all but one mosaic fetus showed no *lincRNA#1* expression. However, all fetuses presented with a polled phenotype. Based on these results, we established that absence of *lincRNA#1* alone does not result in a horned phenotype, suggesting that *lincRNA#1* expression is not required for horn bud suppression.

MATERIALS AND METHODS

Animal Care

All experiments including animals were approved and conducted in accordance with the Institutional Animal Care and Use Committee (IACUC) protocol #20746 at the University of California, Davis. Recipient cattle were housed and managed at the University of California, Davis Feedlot.

Control Fetal Collections

Control horned and polled fetuses were either collected from a local processing plant or as part of separate ongoing departmental experiments. Time of gestation was estimated based on the crown-rump length calculator (University of Wisconsin-Madison) when an exact gestational age was not known. Phenotype was identified, the fetal heads were separated (sagittal) and the horn bud and frontal skin regions were processed for either histological or RT-qPCR analysis.

DNA was isolated from tail tissue samples by means of Qiagen's DNeasy Blood & Tissue Kit (Valencia, CA), and POLLED genotyping was done by polymerase chain reaction (PCR) to determine if they carried either POLLED (P_C or P_F) alleles (primer sequences in Supplementary Table S4). 100 ng of DNA was amplified using GoTaq® Green Master Mix (Promega, San Luis Obispo, CA) and 400 nM of each primer on a SimpliAmp Thermal Cycler (Applied Biosystems, Waltham, MA) for 5 min at 95°C, 35 cycles of 30 s at 95°C, annealing for 30 s (temperatures are in Supplementary Table S4), and extension at 72°C (times are in Supplementary Table S4), followed by 10 min at 72°C. Products were electrophoresed and visualized using 1% Tris-Acetate Ethylenediamine Tetra-Acetic Acid (TAE) agarose gels. PCR products were gel-extracted using a modified version of the "freeze-squeeze" method[25]. Briefly, filter columns were prepared by cutting the ends (approximately 3-4 mm) of p20 filter tips (Mettler-Toledo) and placing them in 1.5 mL tubes. Bands were excised from the gel, placed into

the filter columns, incubated at -80°C for 5 min and centrifuged at max speed for 3 min. The filter tip containing the agarose was discarded and the filtrate containing the DNA was sent for Sanger sequencing (GENEWIZ, San Francisco, CA).

Guide RNA Design and Construction

The online tools sgRNA Scorer 2.0[26,27] and Cas-OFFinder[28] were used to design guide RNAs targeting the 5' and 3' regions flanking *lincRNA#1* (*LOC100848368*) on chromosome 1 of the UMD3.1.1 bovine reference genome[29]. Guide selection was done with the requirements of no less than three mismatches in the guide sequence for off-target sites in the genome with at least one mismatch in the seed region (8–11 bp upstream of the PAM sequence). The top two guides for each target (Supplementary Table S1) were ordered from Synthego (Menlo Park, CA) with no modifications of the gRNAs. *In vitro* cleavage assays were done to test cleavage efficiency by incubating 80 ng of PCR amplified target sequence, 100 ng of gRNA, 150 ng of Cas9 protein (PNA Bio, Inc., Newbury Park, CA), in 1 x Buffer 3.1 (New England Biolabs, Ipswich, MA) at 37°C for 1 hr. Products were electrophoresed and imaged using a 2% agarose gel.

Embryo Production

Bovine ovaries were obtained from an abattoir and transported to the laboratory in 35–37°C sterile saline. Collection of cumulus-oocyte complexes (COCs) was done via aspiration of follicles and groups of 50 COCs were matured in 4-well dishes containing 500 μL of maturation media (BO-IVM, IVF Bioscience, Falmouth, United Kingdom). COC maturation was done in a humidified 5% CO_2 incubator at 38.5°C for 20-22 hr. Oocytes were fertilized in groups of 25 per drop (60 μL) of SOF-IVF[29] covered with OVOIL (Vitrolife, Sweden). Holstein horned homozygous pp or Angus polled homozygous P_C semen was used to fertilize homozygous pp oocytes to create embryos for the horned and polled embryo groups by IVF. A concentration of 2 × 10^6 sperm per mL was used for an incubation period of 6 hr at 38.5°C in a humidified 5% CO_2

incubator. Light vortexing in SOF-HEPES medium[30] was done for 5 min to denude presumptive zygotes of cumulus cells. No more than 100 zygotes per well were incubated in 400 μL of culture media (BO-IVC, IVF Bioscience) covered with 300 μL of OVOIL at 38.5°C in a humidified atmosphere of 5% CO_2, 5% O_2 and 90% N_2 for 7–8 days.

Guide-RNA Testing

To determine gRNA mutation rates, laser-assisted cytoplasmic microinjection[31] of presumptive zygotes was performed with 6 pL of a mixture of 67 ng/μL of gRNA and 167 ng/μL of Cas9 protein (PNA Bio) incubated at room temperature for 30 min prior to injection. Embryos were incubated for 7–8 days and those that reached the blastocyst stage were lysed in 10 μL of Epicenter DNA extraction buffer (Lucigen, Palo Alto, CA) at 65°C for 6 min then 98°C for 2 min. The target regions were amplified by PCR using primers designed with Primer3 (Supplementary Table S4)[32,33]. A nested PCR approach was undertaken with the first round of PCR containing 10 μL GoTaq® Green Master Mix (Promega), 200 nM of each primer and 9.2 μL of DNA in lysis buffer for 5 min at 95°C, 35 cycles of 30 s at 95°C, 30 s annealing (temperatures in Supplementary Table S4), and 72°C extension (times in Supplementary Table S4) at followed by 5 min at 72°C. The second round of PCR was run on 1 μL of first round PCR reaction using GoTaq® Green Master Mix (Promega) with 200 nM of each primer for 3 min at 95°C, 35 cycles of 30 s at 95°C, 30 s annealing (temperatures in Supplementary Table S4), and extension at 72°C (times in Supplementary Table S4), followed by 5 min at 72°C. Products were electrophoresed and visualized on a 1% agarose gels, excised and purified using the QIAquick Gel Extraction Kit (Qiagen, Valencia, CA). The DNA was then Sanger sequenced (GENEWIZ), and analyzed using CRISP-ID[34] and ICE[35].

Mutation rates for co-injected IVF embryos were determined using the same methods described above utilizing one of the two 5’ gRNAs with the most efficient 3’ gRNA (67 ng/μL of

each guide) alongside 167 ng/μL of Cas9 protein (PNA Bio). Blastocysts were collected as previously described and the target region was amplified using a nested PCR approach with primers designed using Primer3 (Supplementary Table S4)[32,33]. The first round of PCR was performed on 9.5 μL of DNA in lysis buffer using LongAmp® Taq Master Mix (New England Biolabs) and 400 nM of each primer for 3 min at 94°C, 35 cycles of 30 s at 94°C, 30 s at 63°C, and 4 min 30 s at 65°C, followed by 10 min at 65°C. The second round of PCR was run on 1 μL of first round PCR using GoTaq ® Green Master Mix (Promega) and 200 nM of each primer for 3 min at 95°C, 35 cycles of 30 s at 95°C, 30 s at 64°C, and 4 min 15 s at 72°C, followed by 10 min at 72°C. PCR products were electrophoresed and visualized on a 1% TAE agarose gel then excised and purified using the modified "freeze-squeeze" method described above. The DNA was Sanger sequenced (GENEWIZ), and analyzed using CRISP-ID[34] and Mixed Sequences Reader[36].

Embryo Transfers

Recipient cattle estrus synchronization began 16 days preceding the embryo transfer. On day 0, recipients received an intravaginal progesterone releasing device (1.38 g; Eazi-Breed CIDR; Zoetis) and gonadorelin (100 μg; Factrel; Zoetis). The CIDRs were removed and prostaglandin (25 mg; Lutalyse; Zoetis) was administered on day 7, then a second dose of gonadorelin (100 μg; Factrel; Zoetis) was given on day 9 while recipients were monitored for signs of estrus. On day 9 of synchronization, presumptive zygotes were injected with linc 5'g1 and linc 3'g1 RNP complexes as described above. Embryos were injected in groups of 50 – 60, and fresh editing reagents were prepared between each group. Recipient synchronization was confirmed on day 15 via detection of a corpus luteum using a transrectal ultrasound (5.0 MHz linear probe; EVO Ibex, I.E. Medical Imaging). Embryo transfers were performed on day 16. A caudal epidural of 100 mg 2% lidocaine (Xylocaine; Fresenius) was administered to recipients

prior to embryo transfer. Straws (0.25cc) were loaded with three blastocysts each and transferred into the uterine horn ipsilateral to the corpus luteum using a non-surgical transcervical technique. Any remaining blastocysts that were not transferred were analyzed via PCR and Sanger sequencing as described previously to get an editing profile of embryos transferred. On day 28 of embryonic development, recipient cow blood was drawn to diagnose pregnancy via PAG detection, and on days 35 and 75, transrectal ultrasonography was performed for conformation of pregnancy. Recipients were resynchronized for subsequent embryo transfers if they did not become pregnant from prior embryo transfers.

Phenotypic and Genotypic Analysis of Fetuses

At 90 days of gestation, recipient cattle were slaughtered via penetrating captive bolt and subsequent exsanguination. The reproductive tracts were collected, fetuses were recovered from the uterine horns, and horn bud phenotyping was performed. Fetal liver and tail tissue samples were collected for DNA extraction and recipient muscle tissue was harvested for experimental controls. The frontal skin and horn bud regions were collected for histological and RT-qPCR analysis.

Fetal genotypes were determined via DNA extraction from tissue samples using the DNeasy Blood & Tissue Kit (Qiagen). 80 ng of DNA was PCR amplified using GoTaq® Green Master Mix (Promega) and 400 nM of each primer for 3 min at 95°C, 40 cycles of 30 s at 95°C, 30 s at 62°C, and 4 min at 72°C, followed by 10 min at 72°C. PCR products were electrophoresed and visualized on 1% TAE agarose gels. DNA was extracted using the “freeze-squeeze” method previously described. Fetuses were also tested for the P_C and P_F alleles at the POLLED locus utilizing the PCR protocol that was described for control fetal collections.

Histological Analysis of Fetuses

Tissue samples from the horn bud and frontal skin were fixed in 4% paraformaldehyde (Thomas Scientific, LLC, Swedesboro, NJ) for 18 hr at 4°C. Samples were washed in phosphate-buffered saline three times on a rocker for 30 min and placed in 70% ethanol. Tissues were dehydrated in a graded ethanol series and cleared with xylene in a vacuum infiltration processor (Sakura Tissue-Tek VIP 5, Torrance, CA). Samples were then embedded in paraffin blocks, cut in 5 µm sections using a Leica RM2255 microtome (Leica Biosystems, Buffalo Grove, IL) and stained with hematoxylin and eosin. Visualization was done with an Echo Revolve microscope (Discover Echo Inc., San Diego, CA).

Reverse Transcription Quantitative PCR Analysis of Fetuses

Horn bud tissue disruption was done under liquid nitrogen using a mortar and pestle, and RNA was extracted using TRIzol (Invitrogen, Waltham, MA) per the manufacturer's instructions. The RNA (5µg) was treated using RQ1 RNase-free DNase (Promega, San Luis Obispo, CA), and cDNA was synthesized from 2 µg of RNA using SuperScript II Reverse Transcriptase (RT; Invitrogen, Waltham, MA), random hexamers (Invitrogen, Waltham, MA) and oligo dT (Promega, San Luis Obispo, CA) alongside appropriate positive and negative controls. To confirm successful DNase treatment and cDNA synthesis, 40 cycles of PCR was performed on the cDNA alongside RT negative controls (lacking either RT enzyme or RNA) using *RPLP0* and *HPRT1* primers as described above, and products separated on a 1% TAE gel. A standard curve for quantitative PCR (qPCR) was made using a 7-point 5-fold dilution series of either cDNA (for reference genes; 100 ng/reaction) or genomic DNA (for target genes; 100 ng/reaction) and used with every qPCR assay. PowerUp SYBR mix (Applied Biosystems) was used for qPCR of either 20 ng (for reference genes), or 100 ng (for target amplicons) of cDNA, all in triplicate. Primers were either found in the literature[1] or were designed as described above,

spanning exon/exon junctions when possible (Supplementary Table S4). qPCR was performed on the QuantStudio 3 Real-Time PCR System (Applied Biosystems) using the following program: 50°C for 2 min, 95°C for 10 min, followed by 40 cycles of 95°C for 15 s, 60°C for 1 min, followed by a dissociation curve. Three reference genes (*GAPDH*, *HPRT1* and *RPLP0*) were used, and normalization of target gene expression was done using the formula: $Y_i = \frac{Q_{Ti\,x}\,dil_T}{dil_R\ x\ \sqrt[3]{Q_{R1i}\ x\ Q_{R2i}\ x\ Q_{R3i}}}$ where Y_i is the normalized target gene expression for the ith fetus, Q_{Ti} and Q_{Ri} are target and reference gene quantities, respectively, and dil_T and dil_R are the dilution factors used for the cDNA target and reference amplicons[34].

Statistical Analysis

Comparison between blastocyst development, mutation and KO rates were evaluated using a binomial logistic regression model in R with gRNA modeled as a fixed effect. Differences were considered significant when $P < 0.05$.

Acknowledgements

The authors would like to thank Jason Lin for his help in ovary collection and transportation from the processing plant to UC Davis as well as his assistance with fetal collection. They also wish to thank Marissa Fisher and Danny Vickers for their help with managing the animal herds and Drs. Tara Urbano and Celeste Morris for their help during embryo transfers and pregnancy checks. This work was funded by the National Institute for Food and Agriculture National Needs Graduate and Postgraduate Fellowship no. 2017-38420-26790 from the U.S. Department of Agriculture (USDA), the USDA Regional Research Project W4171: Germ Cell and Embryo Development and Manipulation for the Improvement of Livestock, and the Henry A. Jastro Research Fellowship in the College of Agricultural and Environmental Science at UC Davis.

Author's Contributions

S.L.H performed the experiments with additional input from A.L.V. and J.D.M. S.L.H. participated in sample processing and data analysis. B.R.M. was responsible for embryo transfers and monitoring of pregnancies. J.F.T. assisted with qPCR analysis. S.L.H. and J.D.M. wrote the manuscript with suggestions from all co-authors. All authors read and approved the final version.

Competing Interests

The authors declare no competing interests.

Data Availability

Data produced and evaluated in this study are included in this published article and its corresponding Supplementary Information file.

REFERENCES

1 Allais-Bonnet, A. *et al.* Novel insights into the bovine polled phenotype and horn ontogenesis in Bovidae. *PLoS One* **8**, e63512. https://doi.org/10.1371/journal.pone.0063512 (2013).

2 Rothammer, S. *et al.* The 80-kb DNA duplication on BTA1 is the only remaining candidate mutation for the polled phenotype of Friesian origin. *Genet. Sel. Evol.* **46**, 1-5. https://doi.org/10.1186/1297-9686-46-44 (2014).

3 Medugorac, I. *et al.* Whole-genome analysis of introgressive hybridization and characterization of the bovine legacy of Mongolian yaks. *Nat. Genet.* **49**, 470-475. https://doi.org/10.1038/ng.3775 (2017).

4 Medugorac, I. *et al.* Bovine polledness--an autosomal dominant trait with allelic heterogeneity. *PLoS One* **7**, e39477. https://doi.org/10.1371/journal.pone.0039477 (2012).

5 Utsunomiya, Y. T. *et al.* Hornless Nellore cattle (Bos indicus) carrying a novel 110 kbp duplication variant of the polled locus. *Anim. Genet.* **50**, 187-188. https://doi.org/10.1111/age.12764 (2019).

6 Carlson, D. F. *et al.* Production of hornless dairy cattle from genome-edited cell lines. *Nat. Biotechnol.* **34**, 479-481. https://doi.org/10.1038/nbt.3560 (2016).

7 Young, A. E. *et al.* Genomic and phenotypic analyses of six offspring of a genome-edited hornless bull. *Nat. Biotechnol.* **38**, 225-232. https://doi.org/10.1038/s41587-019-0266-0 (2020).

8 Guttman, M. *et al.* Chromatin signature reveals over a thousand highly conserved large non-coding RNAs in mammals. *Nature* **458**, 223-227. https://doi.org/10.1038/nature07672 (2009).
9 Ulitsky, I., Shkumatava, A., Jan, C. H., Sive, H. & Bartel, D. P. Conserved function of lincRNAs in vertebrate embryonic development despite rapid sequence evolution. *Cell* **147**, 1537-1550. https://doi.org/10.1016/j.cell.2011.11.055 (2011).
10 Khalil, A. M. *et al.* Many human large intergenic noncoding RNAs associate with chromatin-modifying complexes and affect gene expression. *Proc. Natl. Acad. Sci. USA* **106**, 11667-11672. https://doi.org/10.1073/pnas.0904715106 (2009).
11 Gil, N. & Ulitsky, I. Regulation of gene expression by cis-acting long non-coding RNAs. *Nat. Rev. Genet.* **21**, 102-117. https://doi.org/10.1038/s41576-019-0184-5 (2020).
12 Zhang, B. *et al.* The lncRNA Malat1 is dispensable for mouse development but its transcription plays a cis-regulatory role in the adult. *Cell Rep.* **2**, 111-123. https://doi.org/10.1016/j.celrep.2012.06.003 (2012).
13 Goudarzi, M., Berg, K., Pieper, L. M. & Schier, A. F. Individual long non-coding RNAs have no overt functions in zebrafish embryogenesis, viability and fertility. *Elife* **8**, e40815. https://doi.org/10.7554/eLife.40815 (2019).
14 Betancur, P., Bronner-Fraser, M. & Sauka-Spengler, T. Assembling neural crest regulatory circuits into a gene regulatory network. *Annu. Rev. Cell. Dev. Biol.* **26**, 581-603. https://doi.org/10.1146/annurev.cellbio.042308.113245 (2010).
15 Wiedemar, N. *et al.* Independent polled mutations leading to complex gene expression differences in cattle. *PLoS One* **9**, e93435. https://doi.org/10.1371/journal.pone.0093435 (2014).
16 Wang, Y. *et al.* Genetic basis of ruminant headgear and rapid antler regeneration. *Science* **364**, eaav6335. https://doi.org/10.1126/science.aav6335 (2019).
17 Xiao, A. *et al.* Chromosomal deletions and inversions mediated by TALENs and CRISPR/Cas in zebrafish. *Nucleic Acids Res.* **41**, e141. https://doi.org/10.1093/nar/gkt464 (2013).
18 Fujii, W., Onuma, A., Sugiura, K. & Naito, K. Efficient generation of genome-modified mice via offset-nicking by CRISPR/Cas system. *Biochem. Biophys. Res. Commun.* **445**, 791-794. https://doi.org/10.1016/j.bbrc.2014.01.141 (2014).
19 Hennig, S. L. *et al.* Evaluation of mutation rates, mosaicism and off target mutations when injecting Cas9 mRNA or protein for genome editing of bovine embryos. *Scientific Reports* **10**, 22309. https://doi.org/10.1038/s41598-020-78264-8 (2020).
20 Wiener, D. J., Wiedemar, N., Welle, M. M. & Drogemuller, C. Novel features of the prenatal horn bud development in cattle (Bos taurus). *PLoS One* **10**, e0127691. https://doi.org/10.1371/journal.pone.0127691 (2015).
21 Pauli, A. *et al.* Systematic identification of long noncoding RNAs expressed during zebrafish embryogenesis. *Genome Res.* **22**, 577-591. https://doi.org/10.1101/gr.133009.111 (2012).
22 Han, X. *et al.* Mouse knockout models reveal largely dispensable but context-dependent functions of lncRNAs during development. *J. Mol. Cell. Biol.* **10**, 175-178. https://doi.org/10.1093/jmcb/mjy003 (2018).
23 Hennig, S. L. *et al.* A deletion at the polled P_C locus alone is not sufficient to cause a polled phenotype in cattle. *Sci. Rep.* (*Submitted*).

24 Lin, J. C. & Van Eenennaam, A. L. Electroporation-mediated genome editing of livestock zygotes. *Front. Genet.* **12**, 648482. https://doi.org/10.3389/fgene.2021.648482 (2021).
25 Polman, J. K. & Larkin, J. M. Purification of DNA from agarose gels. *Biotechnol. Tech.* **3**, 329-332. https://doi.org/10.1007/BF01875631 (1989).
26 Aach, J., Mali, P. & Church, G. M. CasFinder: Flexible algorithm for identifying specific Cas9 targets in genomes. *bioRxiv*. https://doi.org/10.1101/005074 (2014).
27 Chari, R., Yeo, N. C., Chavez, A. & Church, G. M. sgRNA Scorer 2.0: A species-independent model to predict CRISPR/Cas9 activity. *ACS Synth. Biol.* **6**, 902-904. https://doi.org/10.1021/acssynbio.6b00343 (2017).
28 Bae, S., Park, J. & Kim, J. S. Cas-OFFinder: a fast and versatile algorithm that searches for potential off-target sites of Cas9 RNA-guided endonucleases. *Bioinformatics* **30**, 1473-1475. https://doi.org/10.1093/bioinformatics/btu048 (2014).
29 Elsik, C. G. *et al.* The genome sequence of taurine cattle: a window to ruminant biology and evolution. *Science* **324**, 522-528. https://doi.org/10.1126/science.1169588 (2009).
30 Bakhtari, A. & Ross, P. J. DPPA3 prevents cytosine hydroxymethylation of the maternal pronucleus and is required for normal development in bovine embryos. *Epigenetics* **9**, 1271-1279. https://doi.org/10.4161/epi.32087 (2014).
31 Bogliotti, Y. S., Vilarino, M. & Ross, P. J. Laser-assisted cytoplasmic microinjection in livestock zygotes. *J. Vis. Exp.* https://doi.org/10.3791/54465 (2016).
32 Koressaar, T. & Remm, M. Enhancements and modifications of primer design program Primer3. *Bioinformatics* **23**, 1289-1291. https://doi.org/10.1093/bioinformatics/btm091 (2007).
33 Untergasser, A. *et al.* Primer3--new capabilities and interfaces. *Nucleic Acids Res.* **40**, e115. https://doi.org/10.1093/nar/gks596 (2012).
34 Dehairs, J., Talebi, A., Cherifi, Y. & Swinnen, J. V. CRISP-ID: decoding CRISPR mediated indels by Sanger sequencing. *Sci. Rep.* **6**, 28973. https://doi.org/10.1038/srep28973 (2016).
35 Hsiau, T. *et al.* Inference of CRISPR edits from Sanger trace data. *BioRxiv*. https://doi.org/10.1101/251082 (2019).
36 Chang, C. T. *et al.* Mixed sequence reader: a program for analyzing DNA sequences with heterozygous base calling. *ScientificWorldJournal* **2012**, 365104. https://doi.org/10.1100/2012/365104 (2012).

TABLES AND FIGURES

Table 1. Embryo transfer (ET) results from zygotes injected 6 hours post insemination with Cas9 protein and gRNAs linc 5'g1 and linc 3'g1. Three blastocysts were transferred per recipient. Conformation of pregnancies was performed on day 35 of gestation and fetal viability at 75 days of gestation. Nonviable fetuses were harvested immediately, and viable fetuses were harvested at 90 days of gestation.

ET	Genotype at the POLLED loci	Blastocysts Transferred	Recipients	35 Days of Gestation		75 Days of Gestation		Viable Fetuses (%)	Fetuses Harvested (%)
				Pregnant (%)	Fetuses Detected (%)	Pregnant (%)	Fetuses Detected (%)		
1	pp	9	3	2 (67)	5 (56)	2 (67)	5 (56)	0 (0)	5 (56)
	P_CP	15	5	1 (20)	2 (13)	0 (0)	0 (0)	-	-
2	P_CP	15	5	4 (80)	5 (33)	4 (80)	5 (33)	5 (33)	5 (33)
Total	**pp**	**9**	**3**	**2 (67)**	**5 (56)**	**2 (67)**	**5 (56)**	**0 (0)**	**5 (56)**
	P_CP	**30**	**10**	**5 (50)**	**7 (23)**	**4 (40)**	**5 (17)**	**5 (17)**	**5 (17)**

Table 2. Fetal genotypes at the target *lincRNA#1* locus from embryo transfers (ETs) of zygotes injected 6 hours post insemination with Cas9 protein and gRNAs linc 5'g1 and linc 3'g1. A fetus was considered mutated if a mutation was found at one or both gRNA target sites. Knockout rates are further classified in subsets of monoallelic (mono), biallelic (bi) and mosaic. Regarding ET1 where fetal demise occurred, days of gestation refers to how far along the fetuses were in development before they expired, not the days in which they were harvested.

ET	Days of Gestation	Total Fetuses	Total Mutation (%)	Total Knockout (%)	Subset of Knockout Fetuses		
					Non-Mosaic		Mosaic (%)
					Mono (%)	Bi (%)	
1	35-50	5	5 (100)	5 (100)	0 (0)	5 (100)	0 (0)
2	90	5	5 (100)	5 (100)	0 (0)	3 (60)	2 (40)
Total	**-**	**10**	**10 (100)**	**10 (100)**	**0 (0)**	**8 (80)**	**2 (20)**

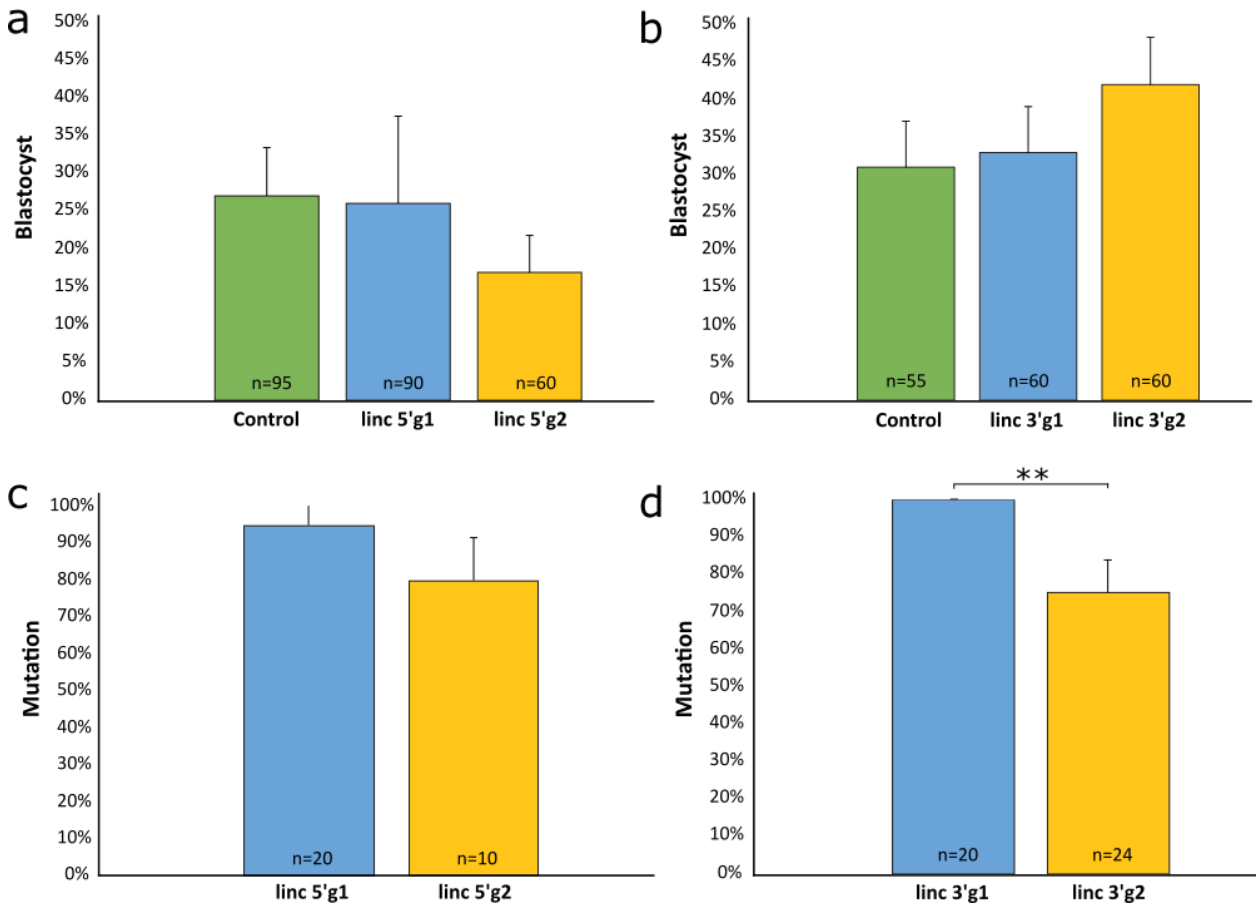

Figure 1. Comparison of uninjected and microinjected zygote development rates and mutation efficiencies. Zygotes were microinjected with gRNA/Cas9 ribonucleoproteins targeting the 5' and 3' regions surrounding *lincRNA#1* at 6 hours post insemination. Blastocyst development rate of uninjected control (green) and microinjected embryos when targeting the (**a**) 5' and (**b**) 3' regions surrounding *lincRNA#1*. Percentage of Cas9-induced mutations in blastocysts when injected with ribonucleoproteins targeting the (**c**) 5' and (**d**) 3' regions surrounding *lincRNA#1*. Error bars = SEM. $^{**}P < 0.01$.

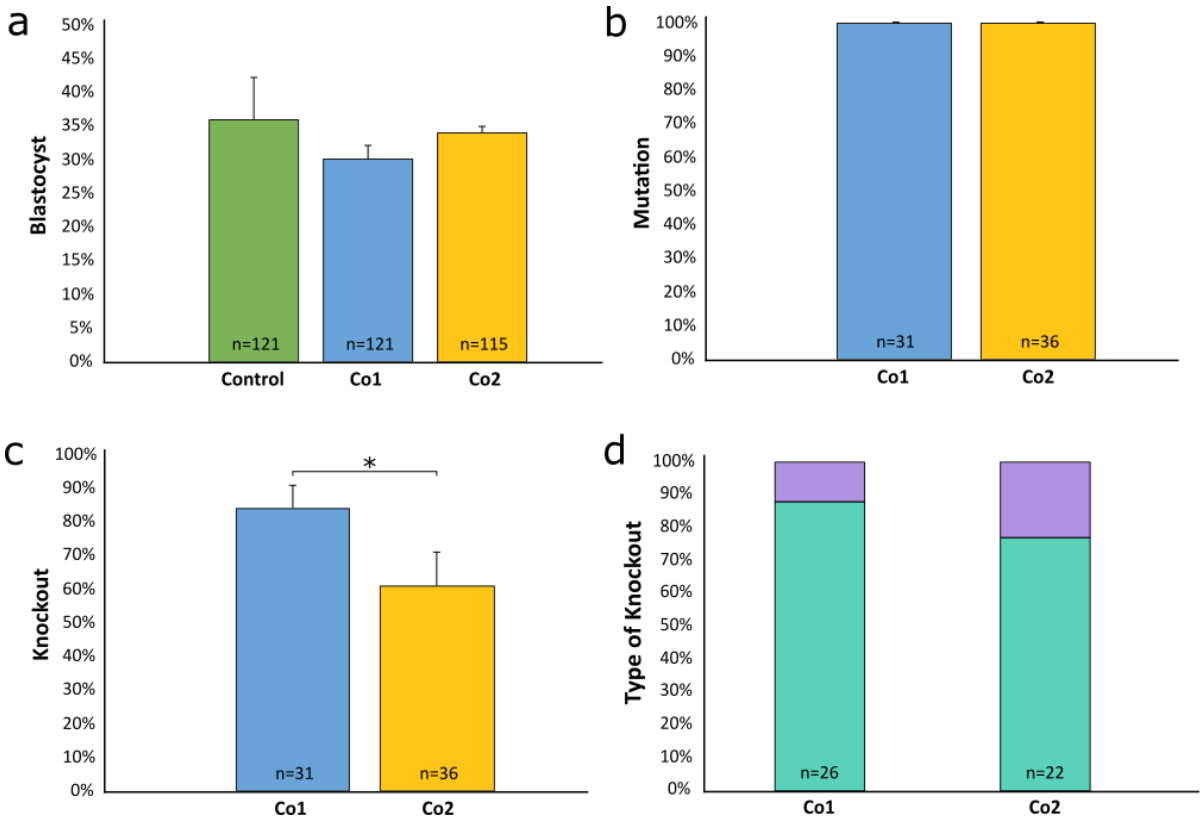

Figure 2. Comparison of uninjected and microinjected zygote development rates and mutation and knockout efficiencies. Zygotes were microinjected with Cas9 protein and either linc 5'g1 and linc 3'g1 (Co1), or linc 5'g2 and linc 3'g1 (Co2), at 6 hours post insemination. (**a**) Percentage of uninjected control (green) and microinjected zygotes that reached the blastocyst stage of development. (**b**) Mutation rates and (**c**) knockout rates in embryos injected with gRNA/Cas9 ribonucleoproteins for Co1 (blue) and Co2 (yellow) injection groups. Blastocysts were classified as mutated if a mutation occurred in at least one target site. (**d**) Type of *lincRNA#1* knockout (%) in injected embryos. Bi = biallelic (aqua); Mosaic (purple). Error bars = SEM. **P* < 0.05.

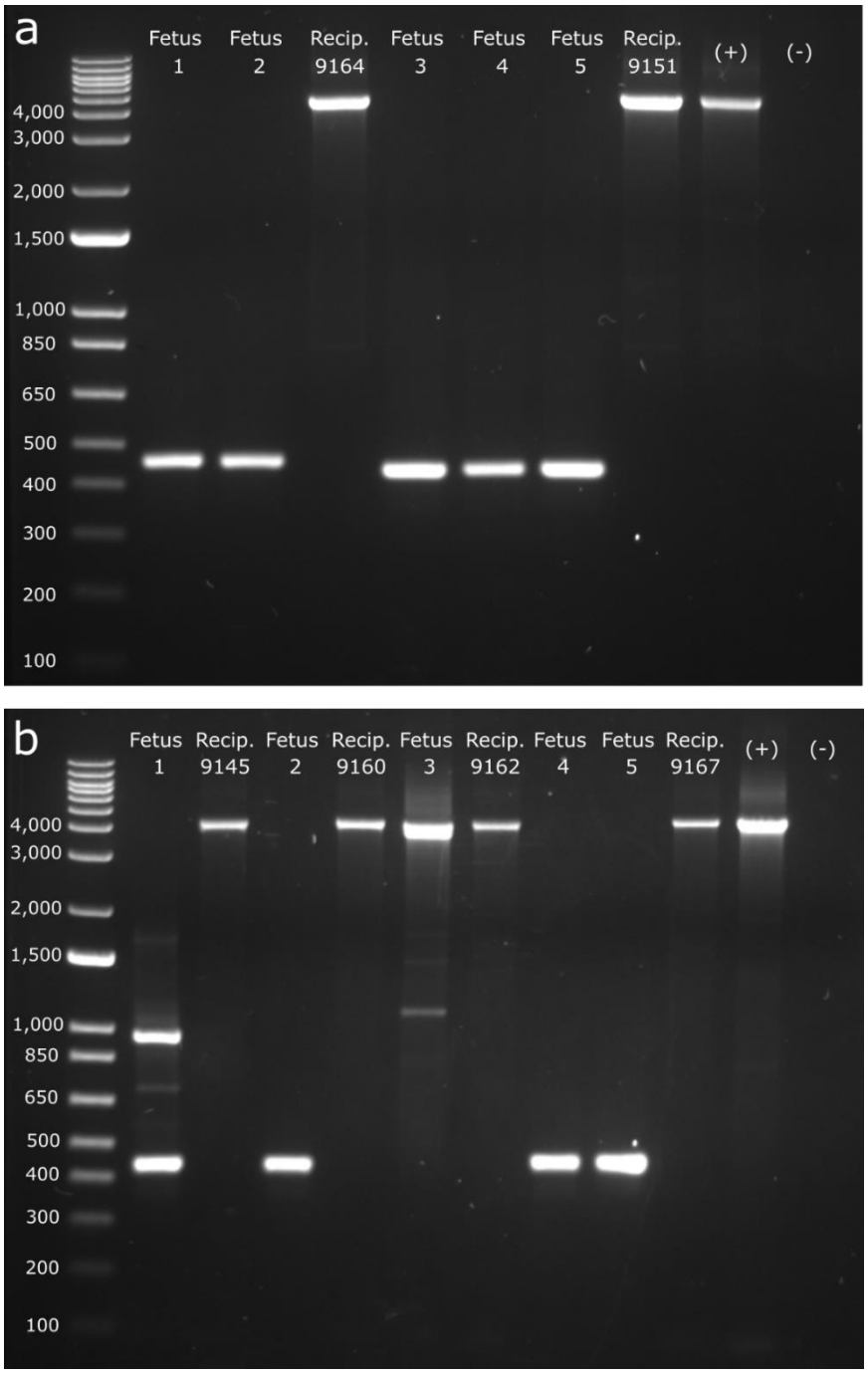

Figure 3. Fetal genotypic analysis from embryo transfers (ETs) and their corresponding recipients (recip.). Gels visualizing the genotypes of fetuses from (**a**) ET1 and (**b**) ET2. DNA was extracted from fetal and recipient tissue and PCR amplified. Gel electrophoresis was done to visualize the *lincRNA#1* targeted deletion. *lincRNA#1* amplicon is 4,189 bp and expected knockout size is 456 bp. Recipient DNA follows the respective fetuses they carried.

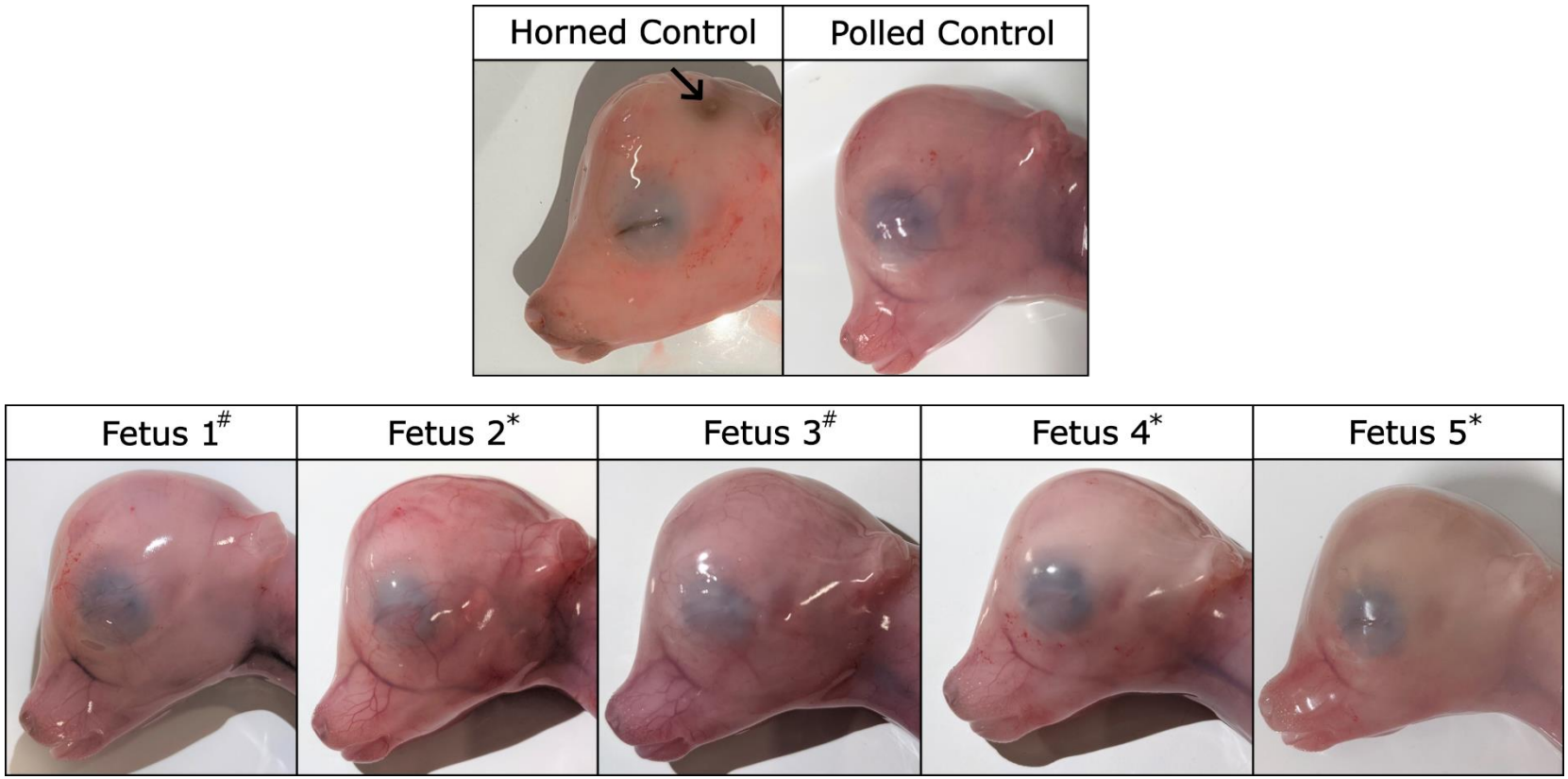

Figure 4. Phenotypic analysis of horn bud development in edited P_CP fetuses and age-matched unedited horned (pp) and polled (P_CP) controls. Fetuses were harvested at 90 days of gestation. Black arrow indicates cranial indent indicative of horn bud development. Edited fetuses were #mosaic or *biallelic *lincRNA#1* knockout.

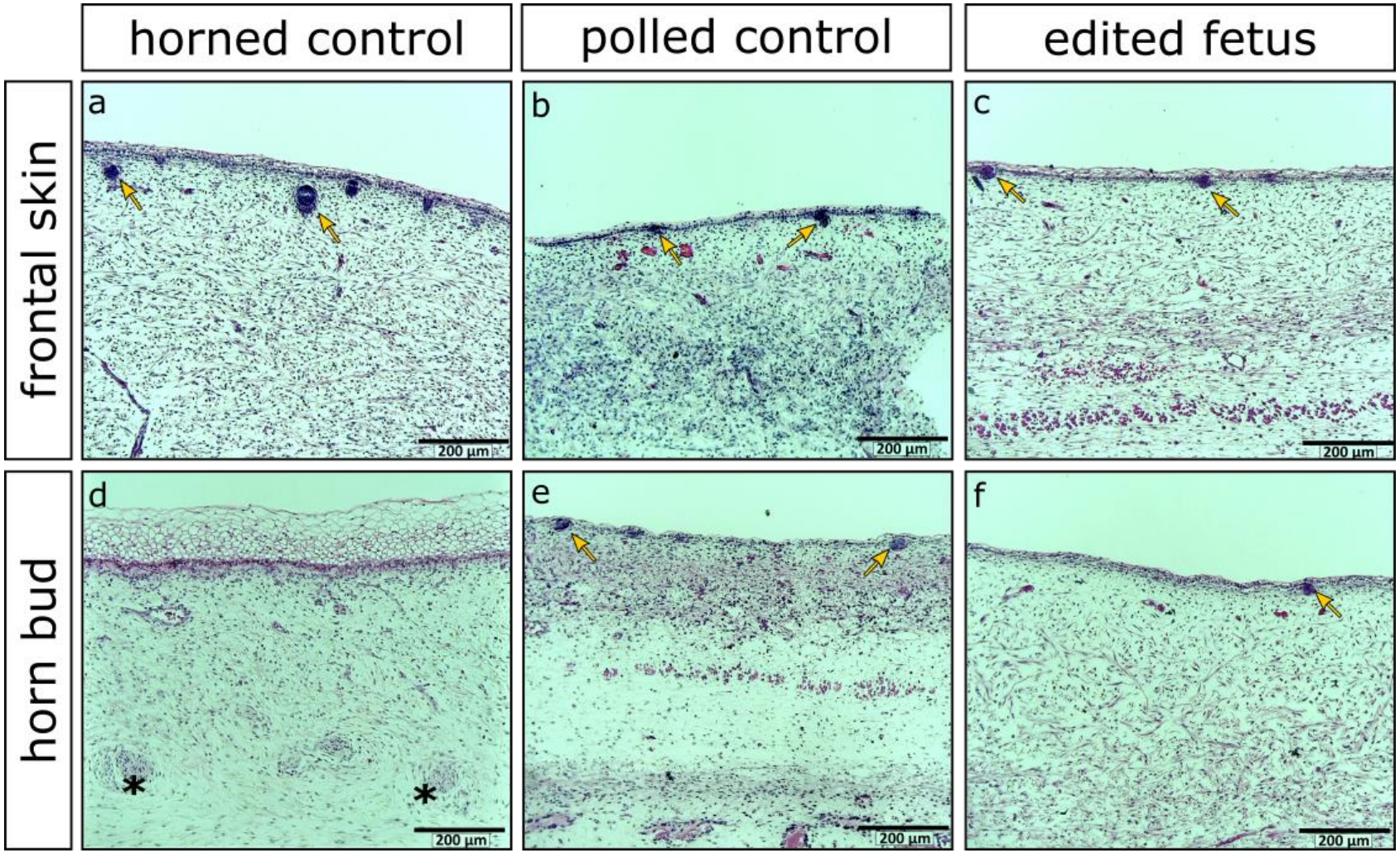

Figure 5. Histological analysis of a representative fetus harvested from embryo transfer (ET) 2 alongside horned and polled controls. (**a-c**) Fontal skin and (**d-f**) horn bud region of age matched horned and polled control fetuses alongside fetus 2, a representative biallelic *lincRNA#1* knockout fetus from ET2, at 90 days of gestation. Multiple layers of vacuolated keratinocytes and nerve bundles (black stars) can be seen in the horn bud region of the horned control fetus, and hair follicles can be seen in the frontal skin of all fetuses as well as the horn bud regions of the polled control and the knockout fetus (yellow arrows).

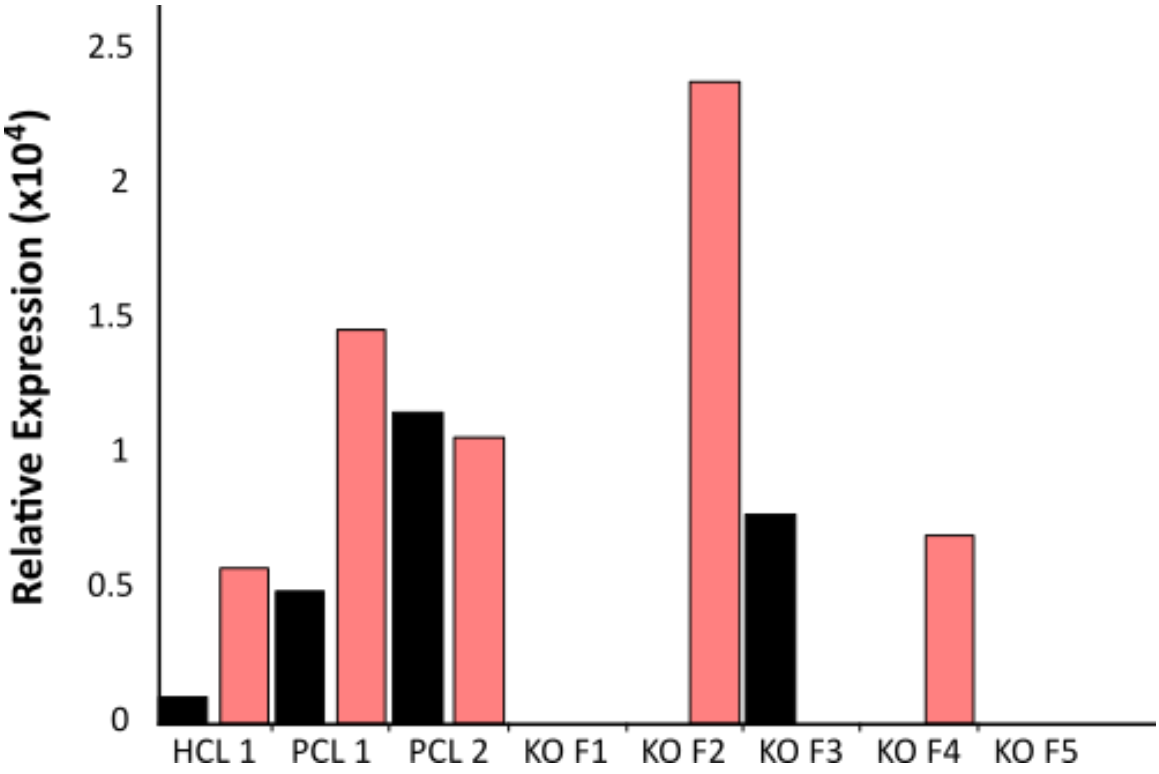

Figure 6. Relative expression of *lincRNA#1* and *OLIG1* in the horn bud region of *lincRNA#1* knockout fetuses (KO F1-5), and one horned (HCL1) and two polled (PCL1 & PCL2) age matched controls. *lincRNA#1* (black) and *OLIG1* (salmon) were normalized relative to three reference genes (*GAPDH*, *RPLP0* and *HPRT1*). *lincRNA#1* KO genotypes are as follows: mosaic KO (F1), biallelic KO (F2), mosaic KO (F3), biallelic KO (F4) and biallelic KO (F5).

SUPPLEMENTARY DATA

Supplementary Table S1. Guide RNAs targeted the 5’ and 3’ flanking sequence of *lincRNA#1*.

Target Region	Name	Sequence
5’ of *lincRNA#1*	linc 5'g1	TGCGGGCAGATGTCTTGCCG
	linc 5'g2	TCTGAGCTGCTGAAGTGTGC
3’ of *lincRNA#1*	linc 3'g1	GTTGCTTGAACGCTCTGCGA
	linc 3'g2	TCTGCCTAAAATTCGGTTAA

Supplementary Table S2. Rate of blastocyst development and mutations in zygotes after microinjection of gRNA/Cas9 ribonucleoproteins targeting the 5' and 3' regions of *lincRNA#1*. *In vitro* fertilized bovine embryos were microinjected 6 hours post insemination. On day 8, blastocysts were counted, and Sanger sequencing was done to determine mutations. ^{A,B,a,b}Letters that differ in the same column are significantly different; $^{A,B}P < 0.01$; $^{a,b}P < 0.05$.

Target Region	gRNA	Total Embryos	Total Blastocysts (%)	Total Analyzed	Total Mutations (%)
5'	Non-Injected Control	95	26 (27)^{a}	-	-
	linc 5'g1	90	23 (26)^{a}	20	19 (95)^{a}
	linc 5'g2	60	10 (17)^{a}	10	8 (80)^{a}
3'	Non-Injected Control	55	17 (31)^{A}	-	-
	linc 3'g1	60	20 (33)^{A}	20	20 (100)^{A}
	linc 3'g2	60	25 (42)^{A}	24	18 (75)^{B}

Supplementary Table S3. Blastocyst, mutation, and targeted knockout rates of zygotes following microinjection of Cas9 protein, linc 3'g1 and linc 5'g1 (Co1) or linc 5'g2 (Co2). *In vitro* fertilized bovine embryos were microinjected 6 hours post insemination. On day 8, blastocysts were counted, and Sanger sequencing was done to determine mutations. Blastocysts were categorized as mutated if a mutation occurred in at least one target site. [a,b]Letters that differ in the same column are significantly different ($P < 0.05$).

Time of Injection	Total Embryos	Total Blastocysts (%)	Total Analyzed	Total Mutation (%)	Total Deletion (%)	Subset of Deletion Embryos		
						Non-Mosaic		Mosaic (%)
						Mono (%)	Bi (%)	
Non-Injected Control	121	44 (36)[a]	-	-	-	-	-	-
Co1	121	36 (30)[a]	31	31 (100)[a]	26 (84)[a]	0 (0)[a]	23 (88)[a]	3 (12)[a]
Co2	115	39 (34)[a]	36	36 (100)[a]	22 (61)[b]	0 (0)[a]	17 (77)[a]	5 (23)[a]

Supplementary Table S4. PCR primers used for amplification of *lincRNA#1* target regions and P_C and P_F alleles. Quantitative PCR (qPCR) primers used for quantification of *lincRNA#1* and *OLIG1* transcripts and reference genes. BLs = blastocysts; KO = knockout.

Target	PCR Round	Forward	Reverse	Tm (°C)	Extension Time
linc 5'guides	1st	ACACGACTGAGCAGCTAACT	ACTCTCTGTGACCGCATGAA	60	1 min
	2nd	GACAGGGTGGAAAGACAAGC	GGTCTTTTCCAATGAGCCCC	62	30 s
linc 3' guides	1st	AGGGAGTGCAAGTTGATCCA	TATGGCCAGAATCGCTCACA	60	1 min 30 s
	2nd	TGTCTGACTCCTTGCAACCA	CCTTTGAAACGTTTGGCTCC	60	1 min 15 s
lincRNA#1 KO in BLs	1st	CGTGTGGATACCTCTCAGCT	CTGGCTGTTTTAGTCTGGGC	63	4 min 30 s
	2nd	AGGGAGTGCAAGTTGATCCA	GGTCTTTTCCAATGAGCCCC	64	4 min 15 s
lincRNA#1 KO in fetuses	1st	TGGACACGTGTGGATACCTC	GCCATCCCAGTGGTGAGAAC	62	4 min
P_C allele	1st	GAAGTGTGGCCGGTAGAAAA	TCCGCATGGTTTAGCAGGATTCA	60	1 min
P_F allele	1st	CCATCTTGGGTACAGCGTTT	TGTTCTGTGTGGGTTTGAGG	60	30 s
lincRNA#1 (qPCR)	1st	ACCAGGAGGGGAGAAAGAAA	TTCGGGAGAGGAAGGAGGT	60	30 s
OLIG1 (qPCR)	1st	CATCATCGCGACAAAACATC	AATTCCCAGGTCGATGAGTG	60	30 s
GAPDH (qPCR)	1st	TTCAACGGCACAGTCAAGG	ACATACTCAGCACCAGCATCAC	60	30 s
RPLP0 (qPCR)	1st	TCTCCTTCGGGCTGGTCAT	AGGAAGCGGGAATGCAGAGT	60	30 s
HPRT1 (qPCR)	1st	GAACGGCTGGCTCGA	TCCAACAGGTCGGCAAAGAA	60	30 s

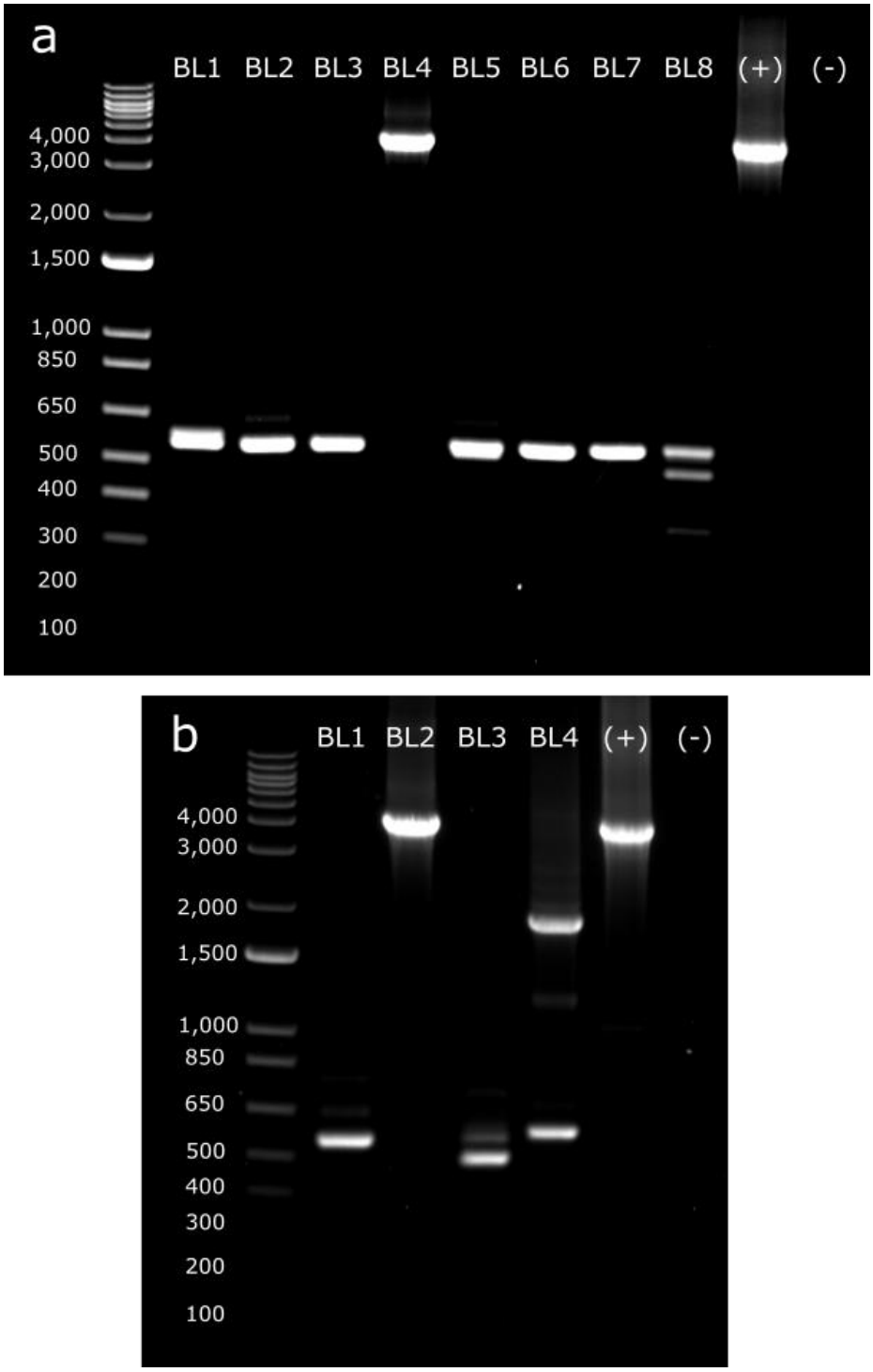

Supplementary Figure S1. Knockout detection at the *lincRNA#1* locus of remaining embryos not transferred for embryo transfer 2. (**a**) Remaining embryos co-injected with Cas9 protein and linc 5'g1 and linc 3'g1 in the first injection group (group 1) and (**b**) second injection group (group 2). Following culture to day-8 blastocysts (BLs), DNA was extracted, PCR amplified and gel electrophoresis was done. Wild type *lincRNA#1* amplicon is 4,287 bp and expected size with deletion is 554 bp.

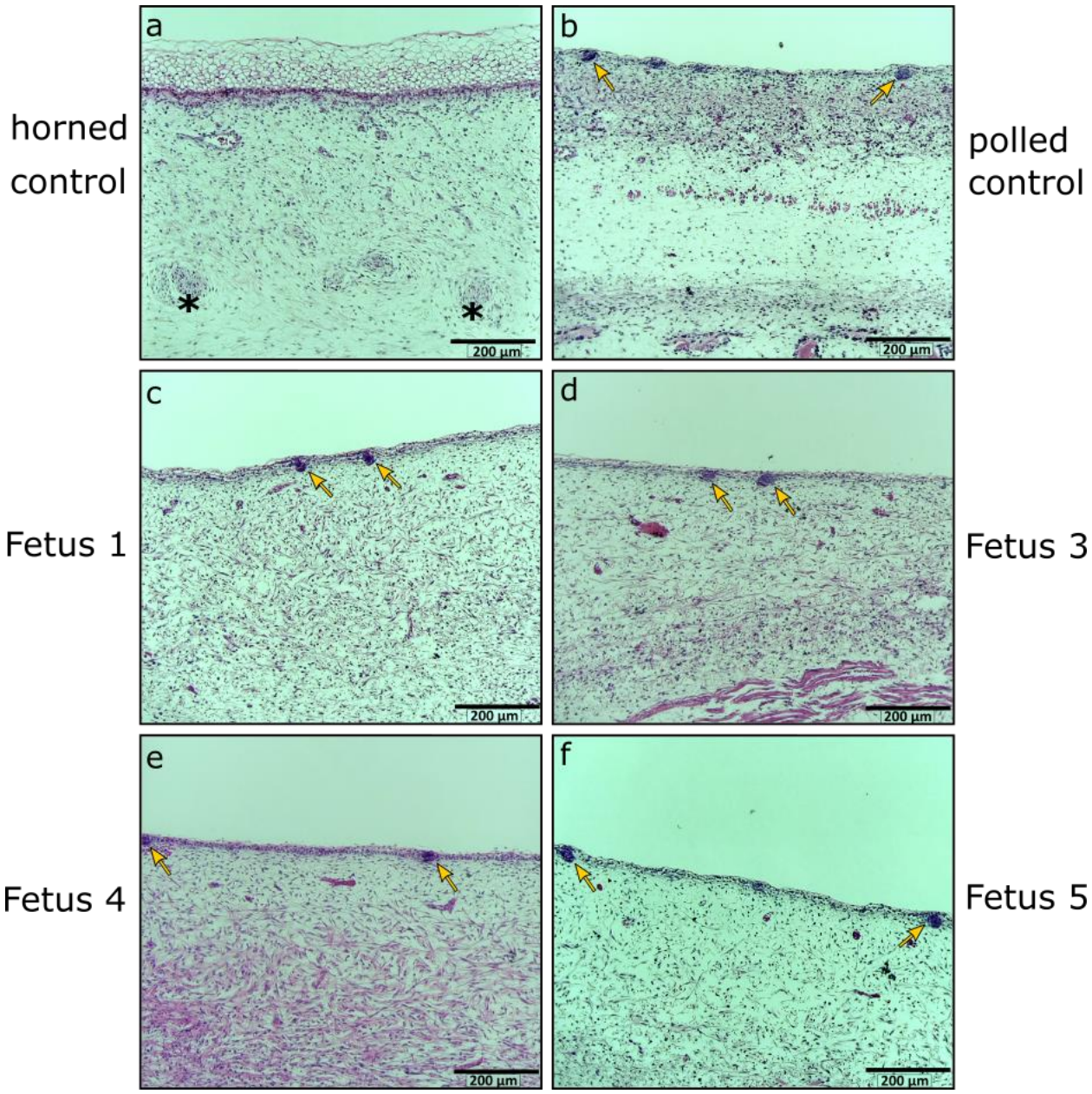

Supplementary Figure S2. Horn bud histological analysis of 90-day fetuses harvested from embryo transfer (ET) 2 alongside horned and polled controls. (**a**) Horn bud of horned and (b) polled age matched control fetuses alongside (c-f) the horn bud regions of *lincRNA#1* knockout (KO) fetuses at 90 days of gestation. Multiple layers of vacuolated keratinocytes and nerve bundles (black stars) can be seen in the horn bud region of the horned control fetus, and hair follicles can be seen in the horn bud regions of the polled control and edited fetus (black arrows). Stained with hematoxylin and eosin. Fetal genotypes are as follows: fetus 1, mosaic KO; fetus 3, mosaic KO; fetus 4, biallelic KO; fetus 5, biallelic KO.

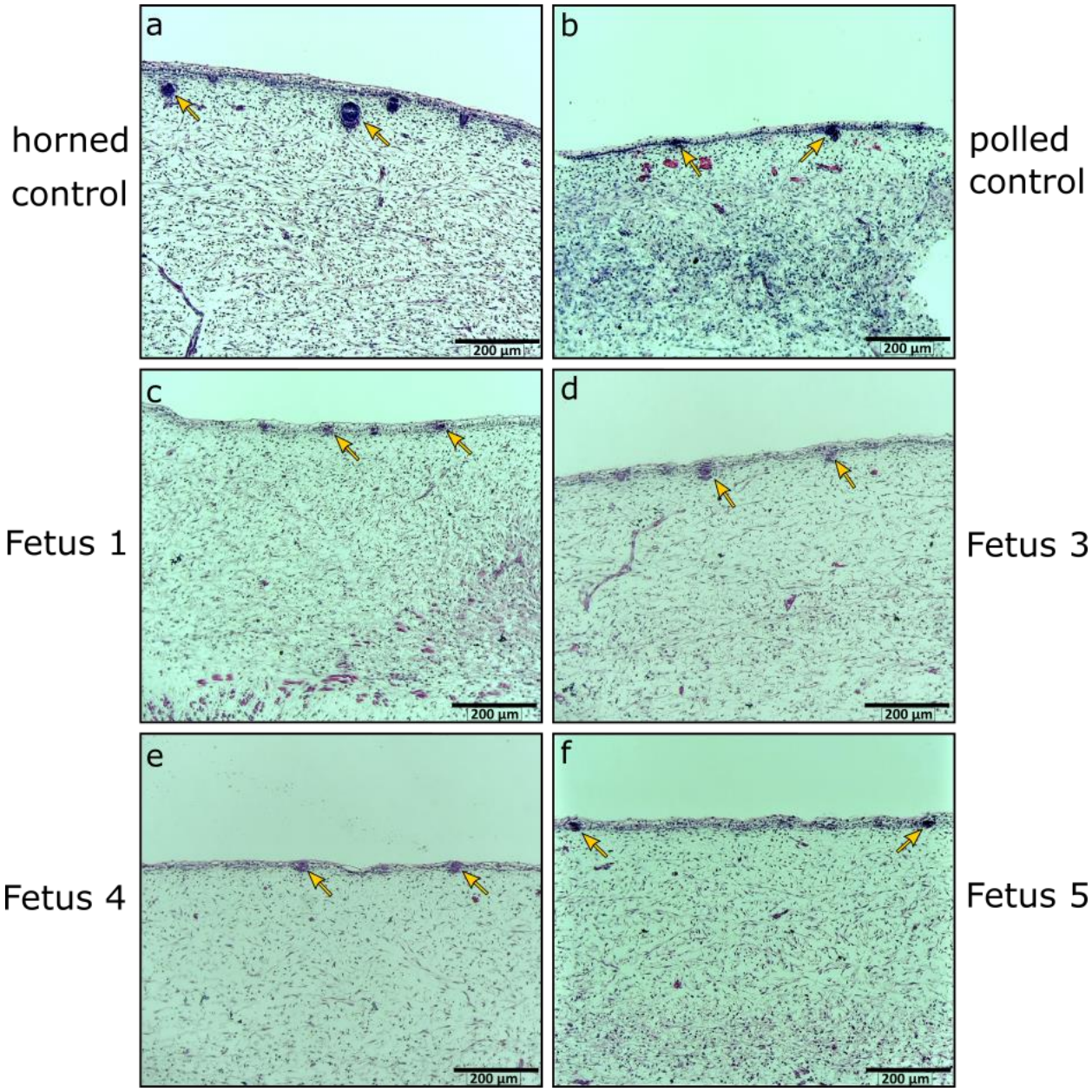

Supplementary Figure S3. Frontal skin histological analysis of 90-day fetuses harvested from embryo transfer (ET) 2 alongside horned and polled controls. (**a**) Fontal skin of horned and (b) polled age matched control fetuses alongside (c-f) the frontal skin of lincRNA#1 knockout (KO) fetuses at 90 days of gestation. Hair follicles can be seen in the frontal skin of all fetuses (yellow arrows). Stained with hematoxylin and eosin. Fetal genotypes are as follows: fetus 1, mosaic KO; fetus 3, mosaic KO; fetus 4, biallelic KO; fetus 5, biallelic KO.

Chapter 5: Future Directions

In these studies, we have developed a CRISPR-Cas9 direct cytoplasmic injection (CPI) protocol for bovine embryos. We optimized gRNA design, selecting guides with no less than three mismatches in the guide sequence for off-target sites using the UMD3.1.1 bovine reference genome[1] with at least one mismatch in the seed region (8-11 bp upstream of the PAM sequence) to minimize off-target effects. We also found the use of Cas9 protein to be superior to Cas9 mRNA with respect to the induction of higher mutation rates and lower mosaicism rates. Although we experienced high rates of mosaicism in our fist experiment, we aimed to address this in the following experiment by optimizing timing of CPI as well as comparing *in vitro* transcribed (IVT) and synthetic gRNAs to improved deletion efficiencies in our dual guide approach. We were then able to utilize our dual guide approach to knockout regions of the bovine genome thought to play a role in causing the polled phenotype: the missing 10 bp at the P_C allele and a long intergenic non-coding RNA, *lincRNA#1*. Although we were successful at creating biallelic knockout fetuses for analysis, future studies should be undertaken on several fronts including improvement of the current protocol involving embryo transfers to more efficiently obtain genome edited fetuses, further investigation of lincRNA#1, a transcriptome comparison of horned and polled fetuses, and the creation of P_C knock-in fetuses to address the animal welfare concern of disbudding/dehorning.

Embryo Transfers of Genome Edited Embryos

We have demonstrated our ability to create biallelic knockout embryos with our efficient CRISPR-Cas9 dual guide approach, however we encountered struggles obtaining knockout fetuses due to embryo transfer issues. The transfer of genome edited embryos is a relatively recent protocol at our facilities, so it is not unexpected to encounter difficulties. We have greatly

improved our protocol, obtained useful equipment for aiding in transfers and optimized many techniques that have helped increase our pregnancy rates. For example, we were able to obtain an incubator to transport the transfer straws containing our genome edited embryos and discovered the optimum incubator temperature is 36°C. One trend we did notice was the importance of speed. Oftentimes, the embryo transfers were used as a teaching moment for veterinary students, thus slowing down the process. We noticed a great dip in pregnancy rates for embryo transfers conducted when veterinary students were performing procedures. For future experiments involving the transfer of genome edited embryos, it is recommended the transfers be performed as quickly as possible by a trained veterinarian.

The Future of *lincRNA#1*

Although we have demonstrated *lincRNA#1* does not play a role in the polled phenotype, it's function still remains unclear. Many studies have shown that lncRNAs play cis-regulatory roles[2-5], typically over genes within a 10 kb proximity[2]. This led us to question the potential regulatory role *lincRNA#1* had over *OLIG1*, a nearby gene involved in neural crest cell differentiation[6] and proven to play a role in horn growth[7]. When we attempted to investigate this potential relationship, we saw great variability of *OLIG1* expression amongst our edited and non-edited control 90 day old fetuses. Because *OLIG1* is typically expressed later in development[8], future studies should be done to create *lincRNA#1* knockout fetuses and time of harvest should be delayed. Collection of fetuses at 120 and 150 days of gestation rather than 90 days would provide better insight into the potential regulatory role *lincRNA#1* plays over *OLIG1* and give a much clearer answer of whether a regulatory effect is occurring at all.

Quantifying lincRNA#1 expression in 90 day old fetuses proved to be quite challenging. Although Allais-Bonnet et al. were able to easily detect *lincRNA#1*[9], Wiedemar et al.[8], like us,

struggled to find expression. It's possible that this overexpression could be breed specific, or the time of its overexpression could vary by breed. Future studies should be performed to analyze *lincRNA#1* expression across a range of gestational ages in fetuses collected from a processing plant. This would help determine when, if at all, *lincRNA#1* overexpression consistently occurs in polled fetuses.

One study that would provide great insight into the mechanism behind the polled phenotype would be the analysis of horned and polled fetuses across differing gestational ages using RNA sequencing (RNA-seq). Wiedemar et al. were able to perform RNA-seq on one horned and one polled fetus at 150 days of gestation[8]. Although they were able to gain insight on the genes involved in horn bud development at that point in gestation, more gestational ages are needed to get a clearer picture on the full mechanism behind polled. Additionally, investigations of another discovered lincRNA (*LOC100848215)* which is expressed only in horned ruminants, and has decreased or even absent expression in the presence of one or two copies of the P_C polled allele[8], would be another interesting candidate to knockout to determine if is its expression is required for horn bud formation in cattle.

Polled for Production

Since we discovered the deletion of a region containing the 10 bp missing in the P_C allele is not sufficient to induce the polled phenotype, the best approach to create polled cattle would be to use the CRISPR-Cas9 system to introduce the P_C allele into genetically horned embryos. Rather than using somatic cell nuclear transfer (SCNT) of an edited cell line like the study by Carlson et al.[10], our optimized CPI system could be used to test a variety of P_C knock-in approaches in embryos, thus avoiding the inefficiencies and complications associated with SCNT[11,12]. Our previously described method demonstrating successful knock-ins using

homology-mediated end joining[13,14] could be used, however we did encounter plasmid integration into the genome with this method[14]. To avoid this, various forms of repair template could be tested including double- and single-strand DNA templates as well as a circularized repair template that only contains the knock-in cassette of interest (minicircle), leaving out the plasmid backbone and thus the risk of plasmid integration into the genome[15].

Overall, we have developed an efficient CRISPR-Cas9 CPI protocol for the production of biallelic knockout bovine embryos. With this protocol, we were able to disprove both of our hypotheses: (1) deleting the 10 bp sequence from both p alleles at the *POLLED* locus using genome editing would result in animals with a polled phenotype, and (2) knocking out both copies of *lincRNA#1* in both pp and P_Cp embryos using genome editing would always result in animals with a horned phenotype. Although we have optimized production for obtaining biallelic knockout embryos, further embryo transfer protocol optimization needs to be done to achieve higher pregnancy rates. The mystery behind *lincRNA#1* still remains. Future studies need to be performed to determine if it is present in a variety of cattle breeds, as well as analyze its variability across different gestational time points using RNA-seq to help uncover a possible regulatory role. Finally, using our optimized CPI protocol in combination with various forms of repair templates is the best approach to achieve introgression of the P_C allele at the *POLLED* locus in horned breeds of cattle. This method would be a rapid approach to acquiring polled cattle while preserving elite genetic merit and addressing a major welfare concern.

References

1 Elsik, C. G. *et al.* The genome sequence of taurine cattle: a window to ruminant biology and evolution. *Science* **324**, 522-528. https://doi.org/10.1126/science.1169588 (2009).

2 Cabili, M. N. *et al.* Integrative annotation of human large intergenic noncoding RNAs reveals global properties and specific subclasses. *Genes Dev.* **25**, 1915-1927, https://doi.org/10.1101/gad.17446611 (2011).

3 Wang, K. C. & Chang, H. Y. Molecular mechanisms of long noncoding RNAs. *Mol. Cell* **43**, 904-914, https://doi.org/10.1016/j.molcel.2011.08.018 (2011).

4 Martens, J. A., Laprade, L. & Winston, F. Intergenic transcription is required to repress the *Saccharomyces cerevisiae SER3* gene. *Nature* **429**, 571-574, https://doi.org/10.1038/nature02538 (2004).

5 Maenner, S. *et al.* 2-D structure of the A region of Xist RNA and its implication for PRC2 association. *PLoS Biol.* **8**, e1000276, https://doi.org/10.1371/journal.pbio.1000276 (2010).

6 Betancur, P., Bronner-Fraser, M. & Sauka-Spengler, T. Assembling neural crest regulatory circuits into a gene regulatory network. *Annu. Rev. Cell. Dev. Biol.* **26**, 581-603, https://doi.org/10.1146/annurev.cellbio.042308.113245 (2010).

7 Wang, Y. *et al.* Genetic basis of ruminant headgear and rapid antler regeneration. *Science* **364**, https://doi.org/10.1126/science.aav6335 (2019).

8 Wiedemar, N. *et al.* Independent polled mutations leading to complex gene expression differences in cattle. *PLoS One* **9**, e93435, https://doi.org/10.1371/journal.pone.0093435 (2014).

9 Allais-Bonnet, A. *et al.* Novel insights into the bovine polled phenotype and horn ontogenesis in Bovidae. *PLoS One* **8**, e63512, https://doi.org/10.1371/journal.pone.0063512 (2013).

10 Carlson, D. F. *et al.* Production of hornless dairy cattle from genome-edited cell lines. *Nat. Biotechnol.* **34**, 479-481, https://doi.org/10.1038/nbt.3560 (2016).

11 Akagi, S., Geshi, M. & Nagai, T. Recent progress in bovine somatic cell nuclear transfer. *Anim. Sci. J.* **84**, 191-199, https://doi.org/10.1111/asj.12035 (2013).

12 Wang, Z. Genome engineering in cattle: recent technological advancements. *Chromosome Res.* **23**, 17-29, https://doi.org/10.1007/s10577-014-9452-6 (2015).

13 Owen, J. R. *et al.* Harnessing endogenous repair mechanisms for targeted gene knock-in of bovine embryos. *Sci. Rep.* **10**, 16031, https://doi.org/10.1038/s41598-020-72902-x (2020).

14 Owen, J. R. *et al.* One-step generation of a targeted knock-in calf using the CRISPR-Cas9 system in bovine zygotes. *BMC Genom.* **22**, 118, https://doi.org/10.1186/s12864-021-07418-3 (2021).

15 Alves, C. P. A., Prazeres, D. M. F. & Monteiro, G. A. Minicircle Biopharmaceuticals–An Overview of Purification Strategies. *Front. Chem. Eng.* **2**, https://doi.org/10.3389/fceng.2020.612594 (2021).